

A Delayed Neutron Counting System for the Analysis of Special Nuclear Materials

Un système de comptage de neutrons retardés pour l'analyse de matériaux nucléaires spéciaux

A Thesis Submitted to the
Division of Graduate Studies of the Royal Military College of Canada

By

Madison Theresa Sellers

In Partial Fulfillment of the Requirements for the Degree of
Masters of Applied Science in Nuclear Engineering

June 2011

© This thesis may be used within the Department of National Defence,
but copyright for open publication remains the property of the author.

Acknowledgements

I would like to thank my supervisors Dr. David Kelly and Dr. Emily Corcoran for their guidance and advice throughout this project. I appreciate all the time and resources devoted and the numerous opportunities provided to present this work. The technical assistance of John Shaw, Steve White, Clarence McEwen and Matthew MacKay for the development of the delayed neutron counting system is gratefully acknowledged. The time dedicated by SLOWPOKE-2 staff Kathy Nielsen and Kristine Mattson is appreciated as it allowed me extensive experimentation time with the reactor. The experimentation process was also greatly aided by Dave Ferguson, who spent many hours troubleshooting the DNC system with me.

I am grateful for the initial opportunity to work with RMC's nuclear group provided by Dr. Bennett who also encouraged me to apply for graduate studies. The staff and students in nuclear engineering are most supportive and it has been a pleasure working with this group. I would also like to thank my friends and family who have encouraged me in my studies. This study was made possible through funding provided by the Director General of Nuclear Safety.

Finally, thank you Steve for all of your support and encouragement.

Abstract

Nuclear forensic analysis is a modern science that uses numerous analytical techniques to identify and attribute nuclear materials in the event of a nuclear explosion, radiological terrorist attack or the interception of illicit nuclear material smuggling. The Canadian Department of National Defence has participated in recent international exercises that have highlighted the Nation's requirement to develop nuclear forensics expertise, protocol and capabilities, specifically pertaining to the analysis of special nuclear materials (SNM). A delayed neutron counting (DNC) system has been designed and established at the Royal Military College of Canada (RMC) to enhance the Government's SNM analysis capabilities. This analytical technique complements those already at RMC by providing a rapid and non-destructive method for the analysis of the fissile isotopes of both uranium (U) and plutonium (Pu).

The SLOWPOKE-2 reactor at RMC produces a predominately thermal neutron flux. These neutrons induce fission in the SNM isotopes ^{233}U , ^{235}U and ^{239}Pu releasing prompt fast neutrons, energy and radioactive fission fragments. Some of these fission fragments undergo β^- decay and subsequently emit neutrons, which can be recorded by an array of sensitive ^3He detectors. The significant time period between the fission process and the release of these neutrons results in their identification as 'delayed neutrons'. The recorded neutron spectrum varies with time and the count rate curve is unique to each fissile isotope. In-house software, developed by this project, can analyze this delayed neutron curve and provides the fissile mass in the sample. Extensive characterization of the DNC system has been performed with natural U samples with ^{235}U content ranging from 2 – 7 μg . The system efficiency and dead time behaviour determined by the natural uranium sample analyses were validated by depleted uranium samples with similar quantities of ^{235}U resulting in a typical relative error of 3.6%. The system has accurately determined ^{235}U content over three orders of magnitude with ^{235}U amounts as low as 10 ng. The results have also been proven to be independent of small variations in total analyte volume and geometry, indicating that it is an ideal technique for the analysis of samples containing SNM in a variety of different matrices. The

Analytical Sciences Group at RMC plans to continue DNC system development to include ^{233}U and ^{239}Pu analysis and mixtures of SNM isotopes.

Keywords: *delayed neutron counting, special nuclear materials, nuclear forensics*

Résumé

L'analyse nucléaire légale est une science moderne qui utilise plusieurs techniques d'analyse pour identifier et attribuer des matériaux nucléaires dans le cas d'explosion nucléaire, d'attaque terroriste radiologique ou de la découverte de contrebande illicite de matériaux nucléaires. Le Ministère de la défense nationale du Canada a participé récemment à des exercices internationaux qui ont mis en lumière le besoin de notre pays de développer le savoir-faire en analyse nucléaire légale, ainsi que les protocoles et les capacités, plus spécifiquement pertinents à l'analyse de matériaux nucléaires spéciaux (MNS). Un système de comptage de neutrons retardés (CNR) a été conçu et mis en œuvre au Collège militaire royal du Canada (CMR) pour augmenter les capacités du gouvernement en analyse de MNS. Cette technique analytique complète celles déjà utilisées au CMR en fournissant une méthode rapide et non-destructrice pour l'analyse d'isotopes fissiles tels que l'uranium (U) et le plutonium (Pu).

Le réacteur SLOWPOKE-2 du CMR produit en prédominance un flux de neutrons thermiques. Ces neutrons provoquent la fission des isotopes de MNS tels que ^{233}U , ^{235}U et ^{239}Pu qui relâche des neutrons rapides prompts, de l'énergie et des fragments de fission radioactifs. Certains de ces fragments de fission se désintègrent par émission β^- et, par la suite, émettent des neutrons retardés, qui peuvent être détectés au moyen d'une batterie de détecteurs sensibles à l'hélium-3. Le spectre des neutrons retardés enregistrés change avec le temps et la courbe du taux de comptage est unique à chaque isotope fissile. Une partie de ce projet consistait à développer un logiciel-maison destiné à l'analyse de la courbe de neutrons retardés et à la détermination de la masse fissile dans l'échantillon. Le système CNR a été caractérisé de façon extensive à l'aide d'échantillons d'uranium naturel avec des teneurs en ^{235}U variant de 2 à 7 μg . L'efficacité du système et le comportement du temps mort tels que déterminés par les analyses d'échantillons d'uranium naturel ont été validés par des analyses semblables faites avec des échantillons d'uranium appauvri avec des teneurs en ^{235}U comparables, ce qui a permis d'établir une erreur relative typique de 3.6%. Le système a déterminé avec précision la teneur en ^{235}U sur trois ordres de grandeur avec des quantités de ^{235}U aussi faibles

que 10 ng. Les résultats ont aussi démontré qu'ils sont indépendants des petites variations du volume et de la géométrie des échantillons analytiques, indiquant que cette technique est idéale pour l'analyse d'échantillons contenant des MNS selon une variété de différentes matrices. Le Groupe de sciences analytiques du CMR prévoit continuer le développement du système CNR pour y inclure l'analyse du ^{233}U et ^{239}Pu , ainsi que des mélanges d'isotopes de MNS.

Mots-clefs: *comptage de neutrons retardés, matériaux nucléaires spéciaux, analyse nucléaire légale.*

Contents

Acknowledgements	v
Abstract	vii
Résumé	ix
Contents	xi
List of Figures	xiii
List of Tables	xv
Nomenclature	xvi
Chapter 1 Introduction	1
Chapter 2 Literature Review	5
2.1 Special Nuclear Materials	5
2.2 Nuclear Forensic Analysis	7
2.3 Delayed Neutron Counting	8
2.4 A Summary of Selected DNC Systems	12
Chapter 3 Theory & Background	15
3.1 The Physics of Fissile Materials	15
3.2 The Production of Delayed Neutrons	19
3.3 Neutron Detection	25
3.4 Delayed Neutron Count Rate Behaviour	34

Chapter 4	Experimental	37
4.1	Delayed Neutron Counting System Overview	37
4.2	Data Analysis Software	41
4.3	Consumables	43
4.4	Delayed Neutron Counting Procedure	44
Chapter 5	Results & Discussion	49
5.1	Neutron Detector Optimization	50
5.2	Additional Contributions to Overall Count Rate	52
5.3	Characterizing the DNC System	64
5.4	Validating the Fissile Analysis Program and DNC System	70
5.5	The Experimental Determination of ^{235}U Content	76
Chapter 6	Conclusions & Recommendations	81
6.1	Conclusions	81
6.2	Recommendations	82
References		85

List of Figures

Figure 2-1: A Record of Nuclear and Radioactive Material Trafficking [7]	6
Figure 3-1: Binding Energy per Nucleon as a Function of A [32]	16
Figure 3-2: Fission Cross Sections of Special Nuclear Materials [32]	18
Figure 3-3: Fission Product Yield as a Function of Product Mass [32]	19
Figure 3-4: The Decay Scheme for Delayed Neutron Production [37]	20
Figure 3-5: Individual DN Group Contribution to Overall Count Rate for ^{235}U	22
Figure 3-6: A Comparison of SNM Count Rate Curves	23
Figure 3-7: A Comparison of SNM Count Rate Curves	24
Figure 3-8: Delayed Neutron Activity Saturation	25
Figure 3-9: Typical Count Curve for BF_3 and ^3He Neutron Detectors [11]	27
Figure 3-10: Thermal Neutron Intrinsic Efficiency of Proportional Counters [11]	29
Figure 3-11: The Cross Sections of ^3He and ^{10}B [32]	30
Figure 3-12: Paralyzable and Non-Paralyzable Dead Time Comparison [43]	32
Figure 4-1: Delayed Neutron Counting Graphical User Interface	38
Figure 4-2: The SLOWPOKE-2 Reactor Schematic [49]	39
Figure 4-4: DNC System Counter Geometry	41
Figure 4-5: Fissile Analysis Program Structure	43
Figure 4-6: Possible Sample Pathways and Pressure Signals in the DNC System	45
Figure 5-1: Helium-3 Detector Count Plateaux for Six Detectors used in Counter	51
Figure 5-2: System Background in the Absence of Vials at SLOWPOKE-2 Site 5	53
Figure 5-3: System Background Independence of Count Time	54
Figure 5-4: Consistency of Vial Counts, $B(t)$, Over Several Runs	55
Figure 5-5: Selected Data Showing $B(t)$ Independence of Total Vial Mass	56
Figure 5-6: $B(t)$ Site Dependence	57
Figure 5-7: $B(t)$ Comparison to ^{235}U Experiments	58

Figure 5-8: The Effects of Irradiation Time on $B(t)$	59
Figure 5-9: The Fissile Analysis Program Least Squares (LSQR) Fit to $B(t)$	60
Figure 5-10: Comparison of $2.92 \mu\text{g } ^{235}\text{U}$ in Site 5 before and After Cleaning	62
Figure 5-11: Comparison of Contamination in Site 5 before and After Cleaning	63
Figure 5-12: Recorded Count Rates and Dead Time for Non-paralyzable System	65
Figure 5-13: Efficiency Independence of ^{235}U Mass with 2σ Uncertainties	67
Figure 5-14: A Comparison of Analytical ($40 \mu\text{s}$, non-paralyzable), Empirical and No Dead Time Models	68
Figure 5-15: A Semi-log plot comparing dead time corrections.	69
Figure 5-16: The Ratio of Empirical Fit to True Count Rate for Nat. U Samples	70
Figure 5-17: The Fissile Analysis Program Least Squares fit to Experimental Data	71
Figure 5-18: Comparison of Count Consistency for Eight Sets	72
Figure 5-19: Detailed Comparison of Count Consistency for Eight Sets	73
Figure 5-20: A Comparison of Displacement and Default Position Runs	76
Figure 5-21: A Comparison of DNC Output for Natural and Depleted U Samples	77
Figure 5-22: A Comparison of DNC Output μg Quantities of ^{235}U	78
Figure 5-23: A Comparison of DU and Nat U in nanogram quantities	79
Figure A-1: A Comparison of ^{238}U σ_f to SNM [32]	96
Figure B-1: Retrieving Data in the Matlab Command Prompt	104
Figure B-2: Calling the Fissile Analysis Program	105
Figure B-3: The Fissile Analysis Program Display of ^{235}U amounts	105
Figure B-4: The Fissile Analysis Program Curve Fit to Experimental Data	106
Figure B-5: Fissile Analysis Curve Fitting to Improperly Functioning Electronics	106
Figure C-1: An Example of the Q-Test for Data Rejection [63]	112
Figure D-2: The DNC System at RMC Schematic [64]	116

List of Tables

Table 2-1: A Brief Description of Recent Events Involving HEU or Pu [8]	6
Table 2.2: A Summary of Selected DNC Systems	13
Table 3-1: Critical Energies for Fission [29, 30]	17
Table 3-2: Delayed Neutron Data for Thermal Fission in ^{235}U [29]	21
Table 3-3: Thermal Neutron Detector Efficiencies in Current Literature [52]	29
Table 5-1: Moderator Thickness Effects on Neutron Count	52
Table 5-2: Sample Results for Dead Time Determination (2σ uncertainties)	65
Table 5-3: Consistency of DNC System Output	73
Table 5-4: Challenging DNC Calibration with Depleted Uranium (2σ Uncertainty)	74
Table 5-5: Solution Volume Effects on ^{235}U Determination (2σ uncertainties)	75
Table A-1: Delayed Neutron Data for Thermal Fission in ^{233}U [29]	95
Table A-2: Delayed Neutron Data for Thermal Fission in ^{239}Pu [29]	96
Table A-3: A List of Delayed Neutron Precursors [38]	97
Table B-1: Raw DNC System Data for Sample Q1	101
Table C-1: Blank Signal Counts, Mean and Standard Deviation	113
Table C-2: Standard Counts & Detection Limit Determination	114

Nomenclature

Symbol	Name	Units
A	Atomic Mass	[amu]
$B(t)$	Transport Vial Contribution	[counts s ⁻¹]
$C(t)$	Count Rate Recorded by DNC System	[counts s ⁻¹]
D	Detected Count Rate	[counts s ⁻¹]
E	Energy	[MeV]
M_i	Molar Mass of isotope i	[amu]
N_A	Avogadro's Number	[g mol ⁻¹]
Q	Charge of Secondary Particles in Detector Reactions	[MeV]
R	Real (True) Count Rate	[counts s ⁻¹]
$S(t)$	Total Count Rate Contribution from all isotopes	[counts s ⁻¹]
$S(t)_i$	Count Rate Contribution from isotope i	[counts s ⁻¹]
AZ	Isotope Z with atomic Mass A	
m_i	Mass of isotope i	[g]
n	Total number of fissile isotopes present in sample	
s_i	Neutron Source	
t	Time Since Decay Time has Elapsed	[s]
t_d	Decay Time	[s]
t_{irr}	Irradiation Time	[s]
$t_{1/2}$	Half-life	[s]

1_0n	Neutron	
1_1p	Proton	
β^-	Beta Particle	
Γ	Gamma Ray	
a_i	Delayed Neutron Group i Production over all Neutrons	
β_j	Production Ratio of Delayed Neutron Group j	
ε_g	Geometric Detector Efficiency	
ε_{abs}	Absolute Efficiency	
ε_{int}	Intrinsic Efficiency	
Σ	Interaction Cross Section	[b]
σ_f	Fission Cross Section	[b]
Λ	Lifetime	[s ⁻¹]
Φ_{th}	Thermal Neutron Flux	[neutrons cm ⁻² s ⁻¹]
ν_d	Total Delayed Neutrons Per Fission for Isotope i	
ν_i	Total Neutrons Per Fission for Isotope i	
T	Dead Time	[s]
X	Number of quanta produced by the source	

Acronyms

BF	Boron Trifluoride
CNSC	Canadian Nuclear Safety Commission
CPS	Counts Per Second
CRM	Certified Reference Material
DNC	Delayed Neutron Counting
DRDC	Defence Research and Development Canada
DU	Depleted Uranium
ENDF	Evaluated Nuclear Data Files
HEU	Highly Enriched Uranium
IAEA	International Atomic Energy Agency
ITWG	International Technical Working Group
LSQR	Least Squares Fit
NFA	Nuclear Forensic Analysis
NPT	Non-Proliferation Treaty
PE	Polyethylene
RDD	Radiological Dispersal Device
RMC	Royal Military College of Canada
SLOWPOKE	Safe LOW POver K(c)ritical Experiment
SNM	Special Nuclear Materials

Chapter 1

Introduction

Nuclear forensic analysis (NFA) is a new and developing science that involves the investigation and attribution of nuclear materials. In the event of a radiological/nuclear terrorist or state attack this discipline would work alongside law enforcement and other governmental agencies to provide the information required for the identification and prosecution of those responsible [1]. NFA is also an effective instrument in the event of the interception of illicit nuclear materials as the origin of many materials may be traced through their assay. Other areas that would benefit from NFA techniques include the examination of radiological dispersal devices (RDDs) and the investigation of nuclear weapons detonation [2].

NFA can determine important characteristics of a nuclear material including its age, isotopic composition and place of origin. This technique is often applied alongside radiological protection dosimetry, traditional forensics and intelligence work. NFA can aid responders in reconstructing key features of a nuclear device or material. A country's capability to trace effectively nuclear materials could also discourage those planning to use these materials for malicious purposes [2]. It is important that laboratories employ some non-destructive techniques so as to preserve traditional evidence or at least to consume negligible quantities of the material.

The fissile isotopes of uranium (U) and plutonium (Pu) are classified as *special nuclear materials* (SNM) and the analysis and detection of these materials is an area of great importance in NFA. The fissile SNM ^{233}U , ^{235}U and ^{239}Pu can be used in high yield nuclear weapons, radiological dispersal devices (RDDs) or for the malicious contamination of public food or water. The international community led by the International Atomic Energy Agency (IAEA) has emphasized the requirement

to develop nuclear forensic capabilities, expertise and protocols for the effective safeguarding of nuclear material [3]. The requirements for nations to develop their individual capabilities to detect, intercept and respond to trafficking and the malicious use of nuclear materials have also been underscored in recent years.

As a signatory of the Non-Proliferation Treaty (NPT), Canada is required to properly safeguard its special nuclear materials [4]. All uranium and plutonium materials are accounted for in Canada and verified by the IAEA safeguards committee. Recent international exercises administered by the International Technical Working Group (ITWG) have highlighted the requirement for national governments to develop their own sophisticated NFA capabilities and protocols. A report published by Defence Research and Development Canada (DRDC) [5] evaluated Canada's nuclear forensics capabilities and deficiencies during an ITWG exercise. In this exercise a nuclear material sample of unknown isotopic composition was delivered to several Canadian laboratories for analysis and data interpretation. The report [5] recommended that protocols should be defined for handling radioactive evidence to ensure that analysis is conducted in an efficient manner. It was also emphasized that the analysis be completed in a few select laboratories to minimize sample transport time.

The ITWG-DRDC report identified the Royal Military College of Canada (RMC) as a laboratory capable of the analysis of SNMs, as it is licensed to hold such materials and already has some of the required instrumentation. Through this Master's thesis, RMC has continued to enhance its nuclear forensics capabilities by the installation and validation of a delayed neutron counting (DNC) system for SNM analysis. The DNC system aims to use the SLOWPOKE-2 reactor as a source of neutrons and to provide a quick and non-destructive capability to determine accurately SNM isotopic concentrations and differentiate between various fissile isotopes. This system could also be applied commercially to provide rapid elemental analysis for natural U in geological samples, a process that takes significantly longer when other analytical techniques are employed.

This document provides an introduction to the field of nuclear forensics analysis, specifically pertaining to special nuclear material analysis. The requirements and current Canadian nuclear forensic capabilities will be discussed and the technique of delayed neutron counting introduced. The DNC system at RMC constructed for this project is discussed in Chapter 4 following a review

of the necessary theory and background. Chapter 5 presents and discusses all the results obtained when validating this system for ^{235}U analysis. The future direction of this project is outlined in the final chapter of this document.

Chapter 2

Literature Review

2.1 Special Nuclear Materials

Nuclear materials are required to produce both high yield nuclear weapons and radiological dispersal devices (RDDs). Materials originating from industrial and medical applications can be used in an RDD or for the contamination of public areas. Very specific nuclear materials are required to produce high yield nuclear explosive devices and are termed *special nuclear materials* (SNM). The Atomic Energy Act of 1954 defines special nuclear materials as plutonium, or uranium enriched in ^{233}U or ^{235}U [6]. These materials are of great interest as they are the essential components in the production of nuclear weapons [1]. The acquisition of these materials is one of the most difficult tasks when constructing a nuclear weapon or RDD and the primary form of proliferation prevention is through the stringent safeguarding of these materials. Obtaining SNM is of great interest to those attempting to construct such weapons as it eliminates the need to enrich uranium isotopes or produce synthetic nuclear materials, arguably one of the most difficult tasks in producing nuclear weapons.

SNM are tracked by international and national regulatory agencies including the International Atomic Energy Agency (IAEA) and the Canadian Nuclear Safety Commission (CNSC). The IAEA also monitors incidents involving the trafficking of nuclear materials as depicted in Figure 2-1 [7]. Figure 2-1 indicates there are a significant number of nuclear material interceptions, some of which involved SNM and are briefly described in Table 2-1. Since the early 1990s, nuclear material smuggling interceptions have been on the rise, and have included cases involving highly enriched

uranium (HEU) and plutonium [7], five of which occurred between July 2009 and June 2010 [8]. The significant number of incidents involving the trafficking of nuclear materials has highlighted the requirement for the international community to develop the capabilities to handle the possibly of nuclear weapon or RDD construction and detonations.

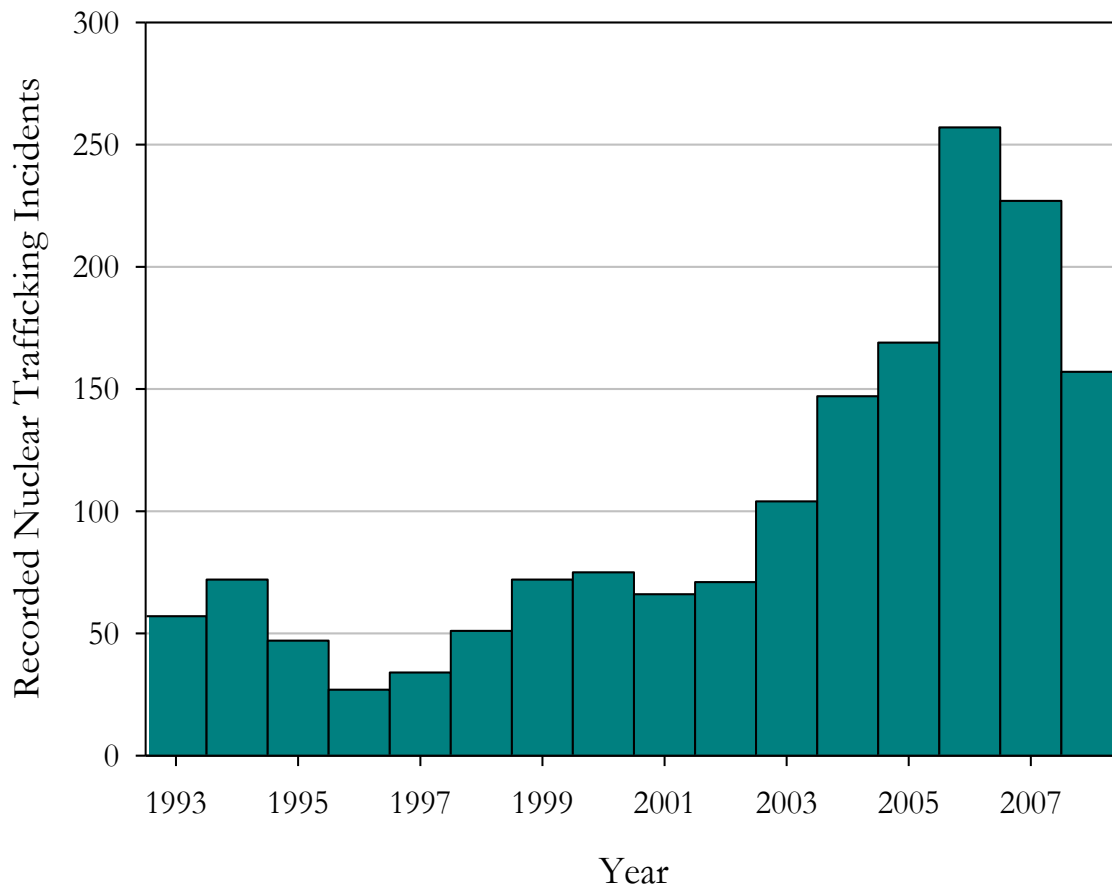


Figure 2-1: A Record of Nuclear and Radioactive Material Trafficking [7]

Table 2-1: A Brief Description of Recent Events Involving HEU or Pu [8]

Date	Description
2009 – 2010	Variable enrichment levels of U found in scrap metal yards throughout Europe
February 2009	Cs-137 source (74 GBq) stolen at gunpoint from a storage facility is recovered
March 2010	The sale of 14 g of HEU is intercepted in Georgia
July 2010	~1400 g of depleted uranium is confiscated in Moldova

2.2 Nuclear Forensic Analysis

It is imperative to determine the material's origin in the event of the interception of nuclear material trafficking. The assay of this material and that of material remaining pre- or post-detonation of an RDD or high-yield nuclear explosive can lead to its characterization and attribution. Nuclear forensics analysis is a relatively new field of science which analyses nuclear materials recovered from the interception of unused materials or the radioactive debris following a nuclear explosion or other form of dispersion. Important characteristics of the nuclear material can be determined; these include its isotopic composition, origin and the time it was produced. Nuclear forensics works most effectively when applied alongside law enforcement, radiological protection dosimetry, traditional forensics and intelligence work; it can allow government agencies to construct key features of a nuclear device. A country's capability to trace a material could also discourage those planning to use nuclear technology for malicious purposes. Laboratories using nuclear forensic analysis should try to employ non-destructive techniques in order to preserve traditional evidence or at least consume negligible quantities of material.

Canada's Nuclear Forensics Analysis Development

Recent round robin exercises involving several nations and administered by the International Technical Working Group (ITWG) have emphasized Canada's current nuclear forensic capabilities. A report published by Defence Research and Development Canada (DRDC) [5] evaluated Canada's nuclear forensic capabilities and its deficiencies. In this exercise a nuclear material sample of unknown isotopic composition was delivered to several Canadian laboratories for analysis.

In the ITWG exercise three government agencies in Ottawa (Royal Canadian Mounted Police, Defence Research and Development Canada and Health Canada) acquired traditional and nuclear forensic evidence before delivering the sample to other laboratories across the country, which included RMC. The data collected were compared and cross referenced with the results from other countries, which performed similar evaluations on separate allotments of the same SNM sample. For the ITWG exercise, RMC performed neutron activation analysis but did not provide an

interpretation of the results. Techniques employed by other laboratories included inductively coupled plasma-mass spectroscopy, gamma ray spectrometry and alpha spectroscopy, all of which are available at RMC. When the results from the Canadian laboratories and agencies were compared with other countries, the errors in isotopic concentrations were considerably higher in Canada. In addition, Canada was not as accurate when dating the sample, and many laboratories in Canada were found to lack a proper description of their analysis procedure [5].

The report [5] recommends that protocols be defined for handling radioactive evidence and the analysis is completed in a more efficient manner. Also, it was suggested that in order to minimize shipping requirements, which resulted in significant delays in the analysis and reporting for this exercise, the analysis be completed at one or two laboratories. The report concluded that DRDC Ottawa and Health Canada could perform most of the forensic analysis and should contract RMC to perform additional analyses.

2.3 Delayed Neutron Counting

Delayed neutron counting (DNC) is a technique capable of determining the amount of fissile content in an unknown sample. In this form of analysis samples containing fissile material are exposed to a neutron source (typically a neutron emitter such as ^{252}Cf or the neutron flux of a nuclear reactor). After the samples have been exposed to neutrons for a sufficient time, they are transferred to a neutron detection site where the delayed neutrons produced as a result of fission are recorded. The neutron counts are compared to that of standards to determine the amount of fissile materials present. DNC is a technique with many advantages as it is rapid and capable of determining fissile content over a large range of concentrations.

The Uses of DNC

The most common use of DNC is the determination of uranium content in geological samples. Environmental and geological samples are also analyzed for their uranium and thorium

content in reactors with fast neutrons [9]. The possible applications of this technique have been expanded to include defective fuel monitoring in nuclear generating stations, safeguards analysis, and health and safety analysis. Delayed neutron monitoring is employed in several commercial reactors as a means of detecting failed fuel elements [10]. In the case of fuel defects, fission products will escape into the coolant resulting in delayed neutron signatures, which can be recorded through DNC. Other industrial applications include the monitoring of fissile materials to prevent nuclear worker and public over exposure [11]. ^{239}Pu is a particularly hazardous SNM as it has a high specific alpha activity and long biological residence time. It is thus an extremely toxic material [12]. DNC has been employed to measure nuclear workers' exposure levels by analyzing urine for uranium content [13]. This analysis could be extended to include the bioassay of ^{235}U and ^{239}Pu in urine. The most recent developments of the DNC technique have seen their applications in safeguards. The capability of the method to detect rapidly the fissile isotopes ^{239}Pu , ^{233}U and ^{235}U has stimulated new developments in the technique. Current research has seen the development of large and handheld DNC systems used for the detection of smuggled fissile material.

Neutron Sources

Common neutron sources used for DNC include the neutron flux of a nuclear reactor (thermal or fast) or the neutrons produced through spontaneous decay or fission. Most systems use reactors with wide variations in neutron flux to irradiate the sample for a set duration, after which the fissile mass is transferred to a counter arrangement. A nuclear reactor provides a large neutron flux and typically a high degree of timing and flux precision. However, many nuclear detection departments and facilities do not have a reactor and instead use a spontaneous fission source, usually ^{252}Cf . The spontaneous fission of the ^{252}Cf source produces fast neutrons, which irradiate the samples [14]. Many “shuffler” DNC systems incorporate ^{235}Cf sources. In a shuffler, the sample may be transferred from an irradiation to a counter site, as is the case with nuclear reactor DNC; however, some systems move the neutron source itself. Many shufflers keep the fissile sample to be analyzed stationary while they move the neutron source in and out. While the use of a ^{252}Cf is inexpensive, when compared to the operating and construction costs of a nuclear reactor, it usually has a lower neutron flux and greater uncertainties in irradiation fluxes and timings. The new

generation of DNC as a safeguards technique has seen the use of portable neutron sources. These systems produce and record the neutrons resultant from the fission of SNM. A system was developed by Rosenstock *et al.* and has been used to irradiate (through a handheld neutron generator) and record the delayed neutron count rates from fissile samples contained in shielded briefcases [15].

DNC System Neutron Detection

As previously mentioned most DNC systems employ BF_3 or ^3He detectors. The number and type of detectors used is usually dependent on the budget of the system being designed and the availability of the desired fill gas. ^3He detectors can be pressurized upwards of 40 atm, which produces a highly efficient detector when compared to its BF_3 counterpart that is usually maintained at atmospheric pressures [11]. In most systems the neutron detectors are imbedded in a neutron moderator, typically polyethylene, paraffin or oil, which thermalizes the neutrons. The majority of DNC systems connect the detectors in parallel so the counts of all detectors are summed as they are processed by the electrical equipment. Typical nuclear instrumentation consists of several detectors, which are connected to a high voltage source. The signals recorded by the detectors are combined and delivered to an amplifier, single channel analyzer, and counter. For delayed neutron counting, the energy of the delayed neutrons is typically not recorded and energy discrimination levels are set to avoid recording large energy gamma pulses.

System Background Concerns

Several distinct sources contribute to time-dependant and time-independent background signals. Background radiation, that is to say radiation from sources that are external to the detector, typically results in few counts per time unit in a well-shielded counter apparatus. However, it is important to both characterize and minimize this contribution. Most systems incorporate some degree of shielding, which surrounds the counter arrangement. These shielding materials should have a high thermal neutron absorption cross section and ideal materials include cadmium and boron [43]. As these materials can be expensive many systems incorporate thin layers of neutron absorption liner surrounded by other shielding materials including concrete [16].

Fast neutron interactions can contribute to background, particularly the $^{17}\text{O}(n,p)^{17}\text{N}$ and $^{18}\text{O}(n,d)^{17}\text{N}$ neutron reactions, which will produce delayed neutrons with half-lives of 4.14s through the decay of ^{17}N [17]. The principal sources of oxygen and nitrogen sources are the air and water contained in the irradiated sample capsules. Many DNC systems with a considerable fast neutron flux have incorporated a delay of $\sim 20\text{s}$ before the delayed neutrons are recorded, which allows the ^{17}N delayed neutron contribution to decay through several half-lives [18]. In addition, sample capsules or containers themselves may also contain delayed neutron producing impurities including oxygen or uranium. Also, it is possible in some systems that capsules may pick up contaminant from the inner linings of the DNC system as they travel through the system [19].

Inherent sample radioactivity or sample activation has the potential to produce gamma radiation, which may also contribute to background. These contributions can be minimized by increasing the lower limit on the energy discriminator of the channel analyzer. This may result in partial lower energy neutron losses and a reduction in system efficiency. However, it is advantageous as this discrimination results in a significant reduction in gamma background. Several DNC systems have also incorporated some form of gamma shielding material in between the sample and detector locations in the counting arrangement [20].

Finally, some DNC systems are sensitive to slight vibrations resulting as the capsules travel into the counter arrangement, which may result in additional counts. These contributions can be minimized by lowering pneumatic pressures and thus reducing the speed at which the sample capsules travel to/from the count arrangement. These non-nuclear effects can be quantified by operating the DNC system under normal operation conditions with the neutron source absent and recording the counts. These effects are rarely mentioned in literature so it is reasonable to assume they are minimal.

Fissile Content Determination Methods

Most DNC systems, particularly the older models, determine fissile content through the analysis of the cumulative neutron counts recorded in the designated counting time. This method is sufficient for the analysis of samples containing one fissile isotope. Geological and environmental

DNC sample analysis typically use this technique as the man-made isotopes ^{233}U and ^{239}Pu are not expected to be found in natural samples [21]. In the cumulative method the total neutron count is recorded for a standard of known fissile content in addition to the background, which is usually determined by analyzing an empty sample capsule under identical experimental conditions. Samples containing unknown fissile content are then run through the DNC system and their cumulative count recorded. The background count is then subtracted from each the standard and unknown and the resulting ratios are simply compared to determine the fissile content.

In samples containing unknown fissile isotopes the cumulative count method is not sufficient to determine the isotope and quantities present. If the total count for a set duration were solely recorded, the system would be unable to differentiate between individual fissile isotopes. Many new DNC systems, particularly those with safeguard applications record the count rate as a function of time. This allows for the unique signature of each fissile isotope to be displayed and analyzed. Recent work by Li *et al* [20] has seen the employment of the DNC technique to discern the isotopic signals from ^{239}Pu and ^{235}U mixtures. These samples were irradiated for 60s after which the delayed neutron count rate curve was analyzed to separate the individual fissile isotope contributions and determine the mass of SNM isotopes present.

2.4 A Summary of Selected DNC Systems

Table 2.2 contains a summary of other DNC systems reported in the literature. Important characteristics including the number and type of neutron detectors, moderator material, efficiency/sensitivity, method of fissile determination and applications are included.

Table 2.2: A Summary of Selected DNC Systems

Author	Year	Neutron Source	Timings $t_{ir}-t_d-t_c$ (s)	Detection	Moderator	Dead Time Correction	Method of Determination	Efficiency/ Sensitivity	Use
Rosenburg [22]	1977	Thermal neutron ϕ 4×10^{12} neutrons $\text{cm}^{-2}\text{s}^{-1}$	60-20-50	$6 \text{ }^{10}\text{BF}_3$	Polyethylene	NR	Cumulative	10% Efficiency / 110 cts per $1 \mu\text{g U}$	Geological sample analysis
Kunzendorf [23]	1980	Thermal neutron ϕ 2×10^{13} neutrons $\text{cm}^{-2}\text{s}^{-1}$	20-5-10	9 BF_3	Water free Oil	Empirical (Polynomial)	Cumulative Counts	817 ± 22 counts per 1 $\mu\text{g U}$	Used for U determination in geological samples
Minor [24]	1981	Thermal neutron ϕ 6×10^{12} neutrons $\text{cm}^{-2}\text{s}^{-1}$	20-11-30	$2 \text{ }^3\text{He}$	Polyethylene	Gross counts are corrected	Cumulative Counts	27%	Stream Sediment analysis
Ernst [25]	1982	Thermal neutron ϕ $\sim 5 \times 10^{12}$ neutrons $\text{cm}^{-2}\text{s}^{-1}$		8 BF_3	Polyethylene	NR		Sensitivity levels of 0.01 μg	Geochemical analysis
Duke [21]	1983	SLOWPOKE-2 ϕ $\sim 1 \times 10^{12}$ neutrons $\text{cm}^{-2}\text{s}^{-1}$	20-10-20	6 BF_3	Paraffin	NR	Cumulative	Sensitivity 50.1 ± 0.1 ct μg^{-1}	Geochemistry
Benzing [16]	1999	Thermal neutron ϕ $\sim 1 \times 10^{16}$ neutrons $\text{cm}^{-2}\text{s}^{-1}$		18 BF_3	Polyethylene	NR	Cumulative		Environmental Sample analysis

Li [20]	2004	Thermal neutron ϕ 6×10^{12} neutrons $\text{cm}^{-2}\text{s}^{-1}$	60 – 0.2 - 60	5 ^3He	Polyethylene	NR	Count Rate Analysis	7.3 %	Determination of ^{235}U and ^{239}Pu content in mixtures
Lindstorm [26]	2006	Thermal neutron ϕ 3×10^{13} neutrons $\text{cm}^{-2}\text{s}^{-1}$	60-3-60	10 ^3He	Polyethylene	NR	Cumulative & Decay Curve	29%	Nuclear device detection & nuclear forensics
Glasgow [27]	2008	Thermal neutron ϕ 4×10^{13} neutrons $\text{cm}^{-2}\text{s}^{-1}$	60-25-60	18 BF_3		NR		Detection limit of 20 $\text{pg } ^{235}\text{U}$	Safeguards
Moon [18]	2009	Thermal neutron ϕ 3×10^{13} neutrons $\text{cm}^{-2}\text{s}^{-1}$	60-20-60	18 ^3He	Polyethylene	NR	Net Counts	Estimated up to 30% / 5.06 counts per ng U	U determination in Geological Samples
Rosenstock [15]	2009	14 MeV neutrons handheld device	Varied	6 ^3He	Polyethylene	NR	Decay Curve Analysis	-	Detection of Concealed Fissionable Materials

*NR = not reported

Chapter 3

Theory & Background

3.1 The Physics of Fissile Materials

Nuclei are formed through the different combinations of nucleons; for example, the combination of a neutron and proton forms the nucleus of deuterium. Energy is released in the form of a 2.2 MeV γ ray in the process of deuterium nucleus formation [28]. This energy release results in a deuteron with a mass less than the sum of its individual constituents. The energy released in the formation of nucleus is known as *binding energy* and the binding energy per nucleon is a measure of the stability of that nucleus [29]. The higher a binding energy, the more stable a radionuclide, as it would require larger amounts of energy to break the nucleus into its constituents. Figure 3-1 shows the average binding energy per nucleon of some isotopes as a function of atomic mass, A , showing an increase in stability until $A \approx 50$, followed by a decrease in heavier isotopes including ^{235}U as indicated. It is important to note that the binding energy varies for individual nucleons and Figure 3-1 presents the average binding energy for per nucleon in each isotope [33].

A compound nucleus is formed when a nucleus absorbs a neutron. This compound nucleus has energy equal to the sum of that incident neutron's kinetic energy and the binding energy, E_b , of that neutron to that compound nucleus. Some compound nuclei with high atomic mass numbers will fission into two smaller nuclei, releasing large amounts of energy and producing a more stable nucleon configuration [30]. Induced fission may occur when an isotope $^A Z$ absorbs a neutron and the binding energy of the last neutron in $^A Z$ and its kinetic energy is greater than the energy required

to fission that isotope [30]. The SNM isotopes ^{235}U , ^{233}U and ^{239}Pu are able to undergo the process of fission upon interaction with low energy neutrons as the binding energy of that neutron alone is sufficient for fission. These isotopes are thus defined as fissile materials [30]. The differences between fissile materials (^{235}U , ^{233}U and ^{239}Pu) and fissionable isotopes (^{238}U , ^{232}Th) can be explained using Table 3-1.

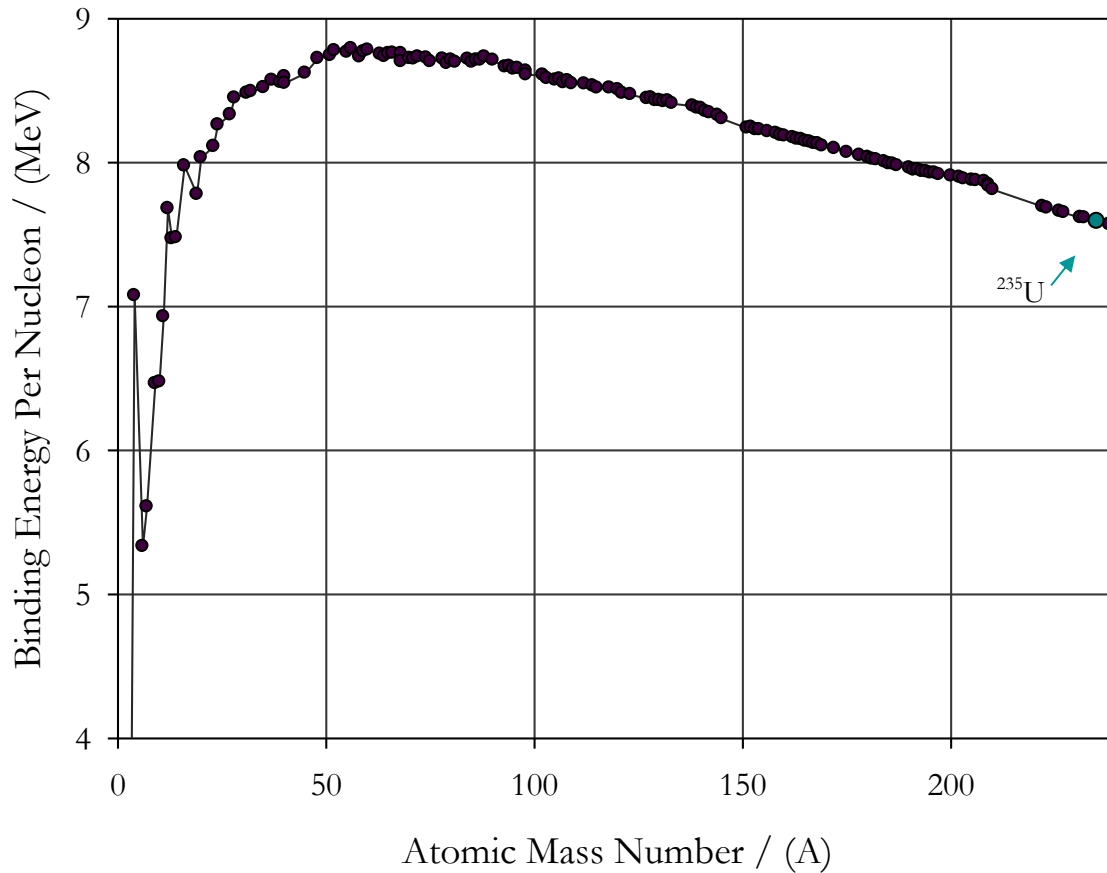


Figure 3-1: Binding Energy per Nucleon as a Function of A [33]

When ^{235}U absorbs a non-energetic neutron it becomes the compound nucleus ^{236}U and the binding energy of the last neutron to the compound nucleus is 6.4 MeV as shown in Table 3-1 [30,31]. This is 1.1 MeV more than the energy required for the fission of ^{236}U , therefore the compound nucleus will divide into more favourable nucleon configurations by fission. If the critical energy required for fission is higher than the binding energy of the last neutron in the compound nucleus (as is the case when ^{238}U absorbs a neutron and becomes ^{239}U) fission is not possible without the kinetic energy of the incident neutron or additional photon. These isotopes are termed

fissionable isotopes as they form a compound that requires energetic neutrons in order to undergo induced fission. Many fissionable isotopes, particularly ^{232}Th and ^{238}U can be converted into fissile isotopes through the absorption of a neutron and subsequent β^- decay; these isotopes are also termed *fertile*.

Table 3-1: Critical Energies for Fission [30, 31]

Target Nucleus A_Z	Compound Nucleus	Fission Activation Energy ${}^{A+1}_Z$ (MeV)	E_B of last n in ${}^{A+1}_Z$ (MeV)	Classification
^{233}U	^{234}U	4.6	6.6	Fissile
^{235}U	^{236}U	5.3	6.4	Fissile
^{238}U	^{239}U	5.5	4.9	Fissionable/Fertile
^{232}Th	^{233}Th	6.5	5.1	Fissionable/Fertile
^{239}Pu	^{240}Pu	4.0	6.4	Fissile

The cross section term, σ , is used to describe the probability of a particular collision process, for example fission, σ_f [32]. The probabilities of a fission reaction upon an interaction with energetic neutrons are displayed as cross sections for the SNM isotopes ^{235}U , ^{233}U and ^{239}Pu in Figure 3-2 [33]. The cross sections for these isotopes decreases with increasing neutron kinetic energy with the exception of the resonance region that occurs at higher neutrons energies [34]. Fissionable or fertile isotopes including ^{238}U have significantly lower fission cross sections in the lower neutron energy range, which is shown in Appendix A.

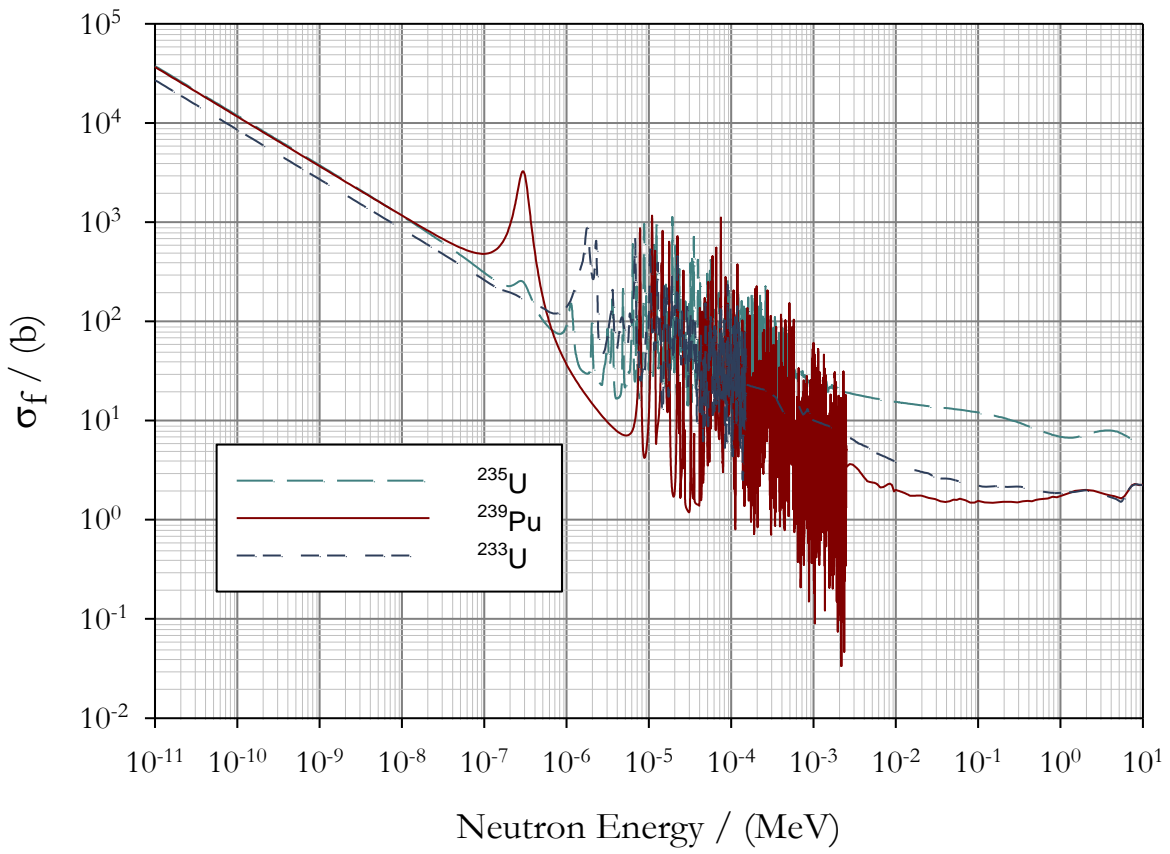


Figure 3-2: Fission Cross Sections of Special Nuclear Materials [33]

3.2 The Production of Delayed Neutrons

When an isotope undergoes fission it splits usually into two unequal fission fragments with a wide range of atomic masses and releases an average energy of 1.98 MeV for ^{235}U [35]. An average between 2 or 3 prompt neutrons are released less than 10^{-14}s after the fission of ^{235}U , ^{233}U and ^{239}Pu [36]. Figure 3-3 shows the fission product yield for SNM upon thermal neutron induced fission. The fission product yield is not distributed evenly over atomic mass and is dependent on the fissile isotopes as evident in Figure 3-3.

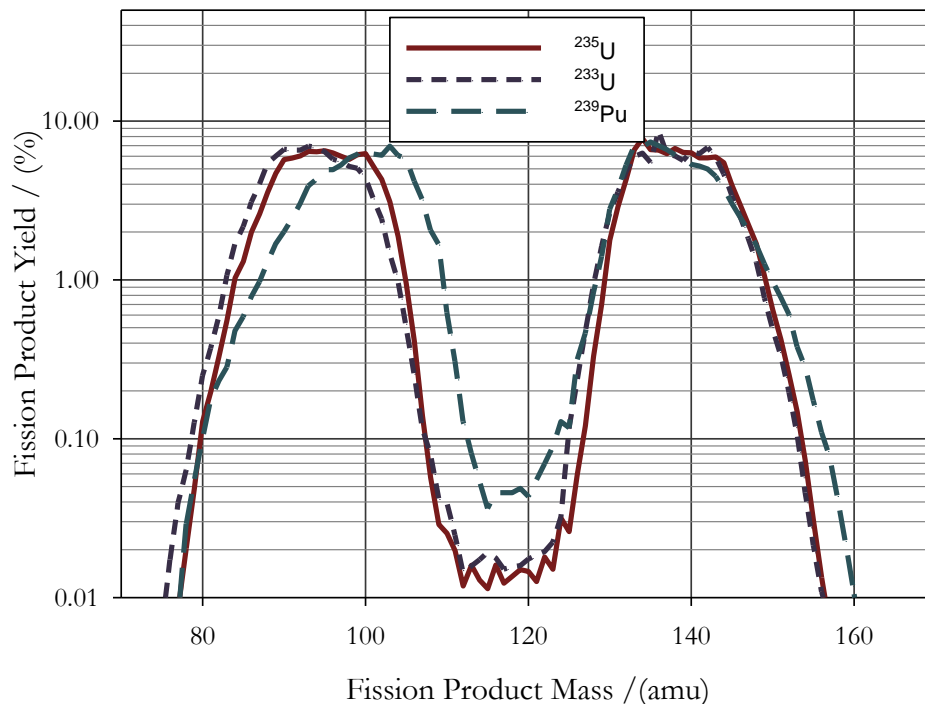


Figure 3-3: Fission Product Yield as a Function of Product Mass [33]

Some fission products are unstable and will decay to excited states, and a few of them will emit neutrons at times greater than 10^{-14}s after fission. For example, the fission fragment ^{87}Br undergoes beta decay to either an excited or ground state of ^{87}Kr as shown in Figure 3-4. One neutron in the excited state of ^{87}Kr is not bound and will be released immediately from the nucleus with a kinetic energy of 0.3 MeV. The fission product ^{87}Br is therefore referred to as a *delayed neutron precursor*. The half-life of this delayed neutron precursor is 55s as this is the half-life of ^{87}Br β^- decay

[37,38]. There have been over 60 delayed neutron precursors identified, the most prominent being ^{89}Br , ^{87}Br , ^{94}Rb , ^{137}I and ^{135}Sb [35], a more detailed list can be found in Appendix A [39].

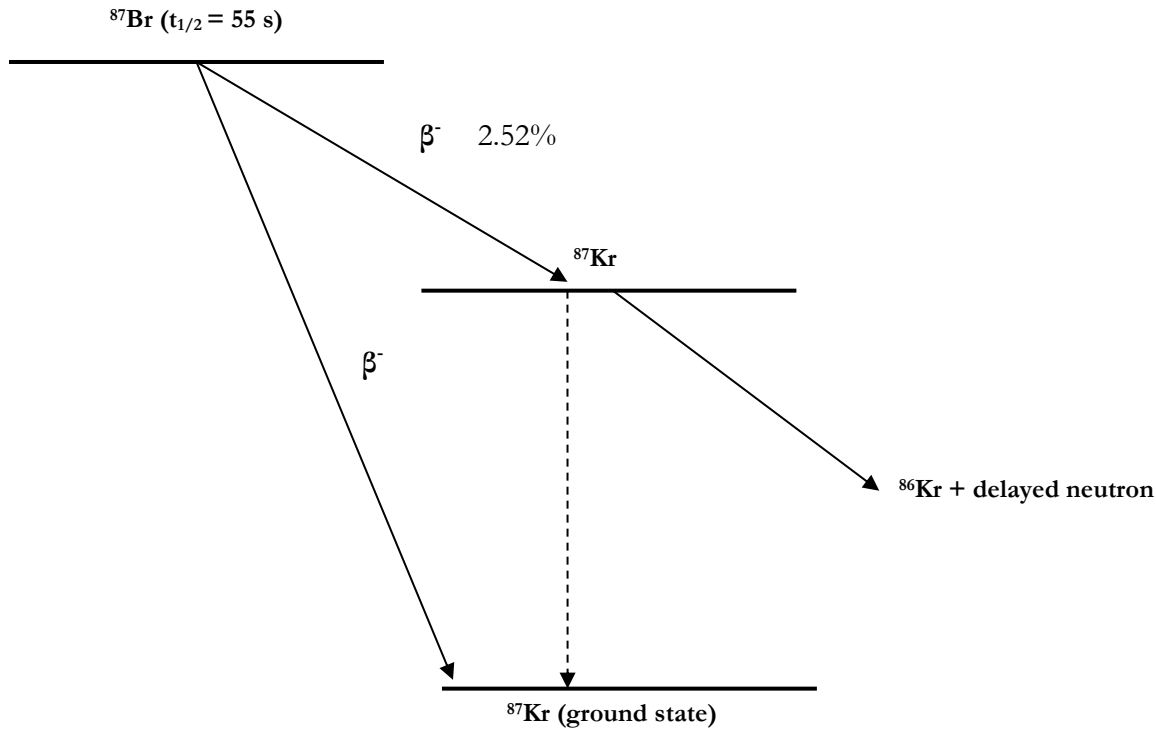


Figure 3-4: The Decay Scheme for Delayed Neutron Production [38]

Delayed neutron precursors are often grouped by average half-life and production ratios as shown in Table 3-2 for the thermal fission of ^{235}U . Most recent data from the IAEA [40] divides the many delayed neutron precursors into eight groups with half-lives ($t_{1/2}$) ranging from 0.198 to 55.6s. The decay constant is also noted in Table 3-2 and is related to the group half-life as outlined in Eq.(3-1). Table 3-2 also contains the production ratios a_i and β_i that represent the ratio of delayed neutrons, ν_d , from group i over the sum of all delayed neutrons ν_d , and total neutrons released in fission, ν_f , respectively. The total delayed neutron count rate curve recorded after the irradiation of fissile materials will be a superposition of the 8 individual groups, most of which are shown in Figure 3-5, the final group is not shown as the half-life is so short. The delayed neutron data tables and figures for ^{233}U and ^{239}Pu can be found in Appendix A.

Table A-1 and Table A-2.

$$\lambda = \frac{\ln(2)}{t_{1/2}} \quad (3-1)$$

Table 3-2: Delayed Neutron Data for Thermal Fission in ^{235}U [30]

Group	$t_{1/2}$ [s]	λ [s^{-1}]	$\beta_i = \nu_i/\nu_d$	$\alpha_i = \nu_i/\nu_t$
1	55.6	0.014267	0.0328 ± 0.0042	0.0218 ± 0.0029
2	24.5	0.028292	0.1539 ± 0.0068	0.1023 ± 0.0036
3	16.3	0.042524	0.091 ± 0.009	0.0605 ± 0.0063
4	5.21	0.133042	0.197 ± 0.023	0.131 ± 0.016
5	2.37	0.292467	0.3308 ± 0.0066	0.2200 ± 0.0083
6	1.04	0.666488	0.0906 ± 0.0046	0.0600 ± 0.0036
7	0.424	1.634781	0.0812 ± 0.0016	0.0540 ± 0.0021
8	0.198	3.554600	0.0229 ± 0.0095	0.0152 ± 0.0064

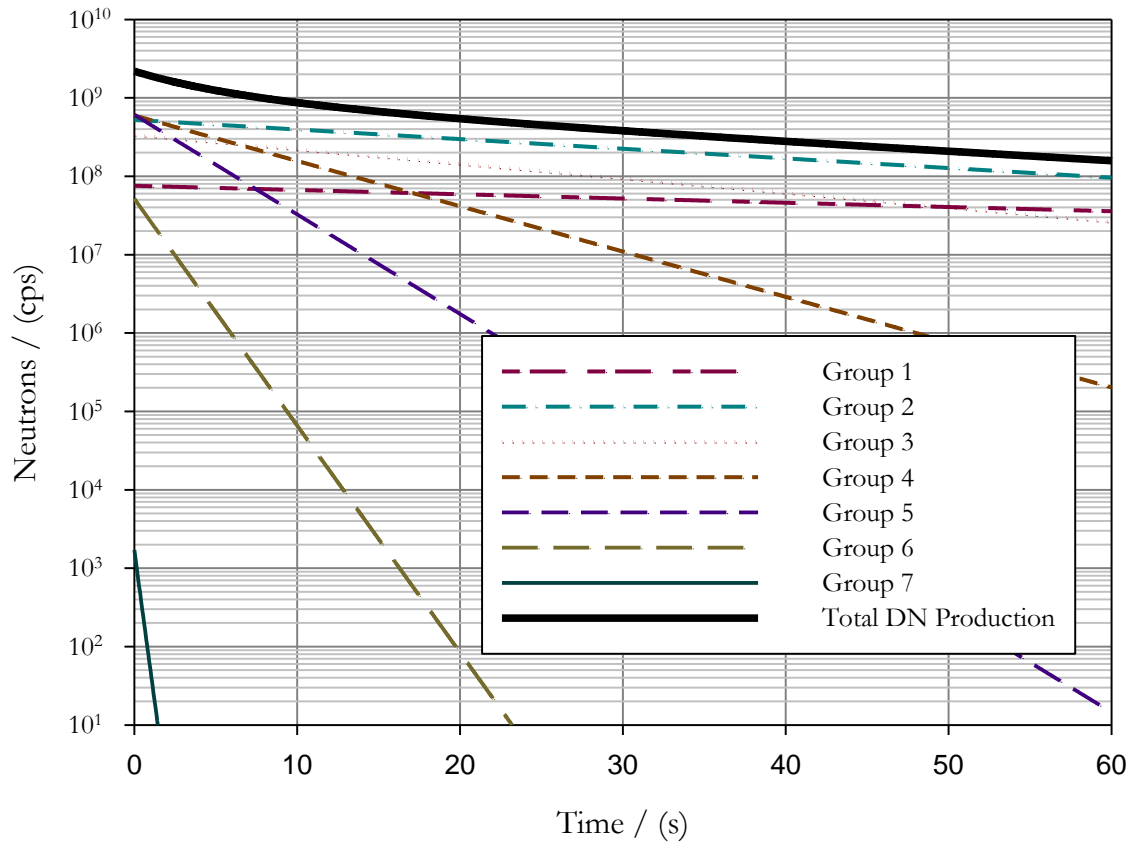


Figure 3-5: Individual DN Group Contribution to Overall Count Rate for ^{235}U

As previously depicted in Figure 3-3 the fission fragment yields vary between individual fissile materials. As a direct consequence, the delayed neutron production ratio also varies for each SNM as the delayed neutrons produced are dependent on the fission fragment yields. The differences in both total delayed neutron yield and individual group production ratios result in signature delayed neutron count rate curves for each of ^{235}U , ^{233}U and ^{239}Pu . Figure 3-6 shows a comparison of the delayed neutron count rate curves under the same experimental conditions for 1 g of each ^{235}U , ^{233}U and ^{239}Pu . The slight variation in the curve's shape makes it possible to identify the fissile isotope present through an analysis of the signature of the delayed neutron curve produced and this is shown in Figure 3-7. Figure 3-7 shows the same data as the previous Figure, however the data has been normalized to an identical starting point to emphasize the different delayed neutron behaviour of each isotope.

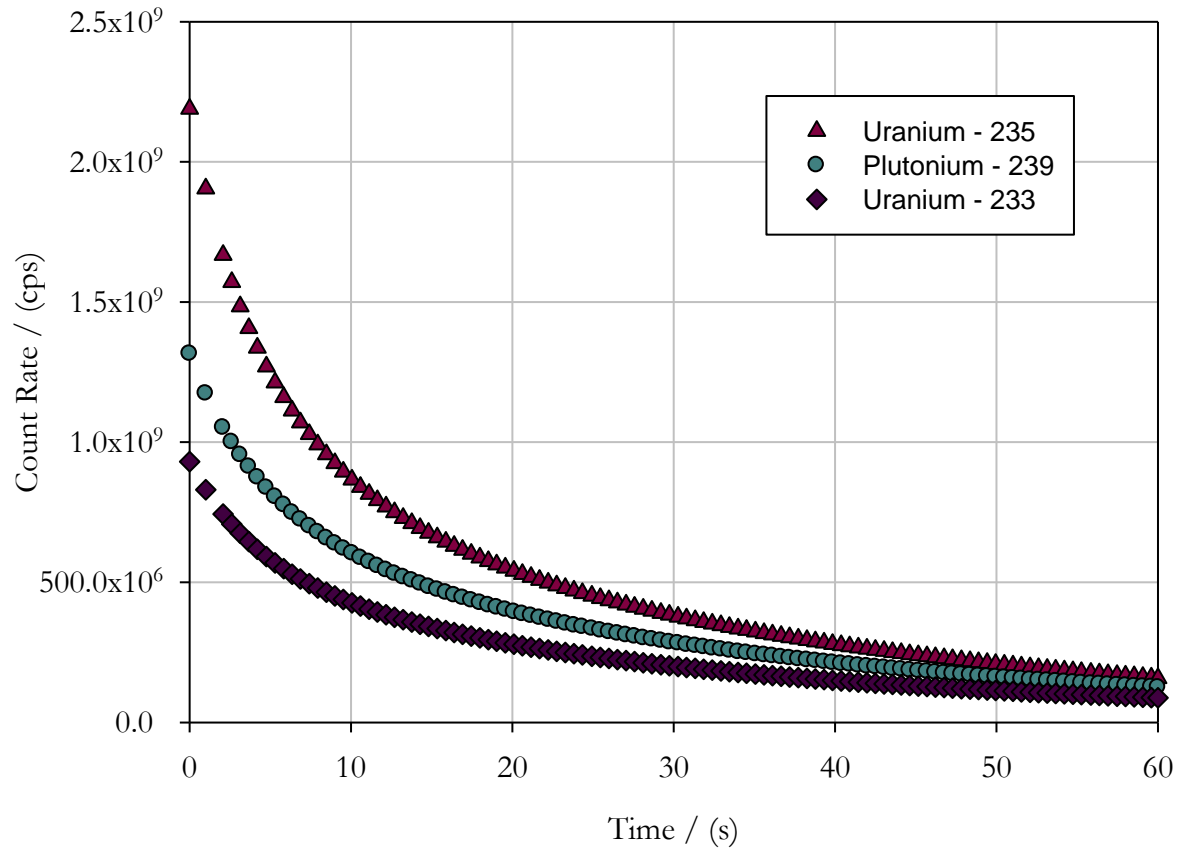


Figure 3-6: A Comparison of SNM Count Rate Curves

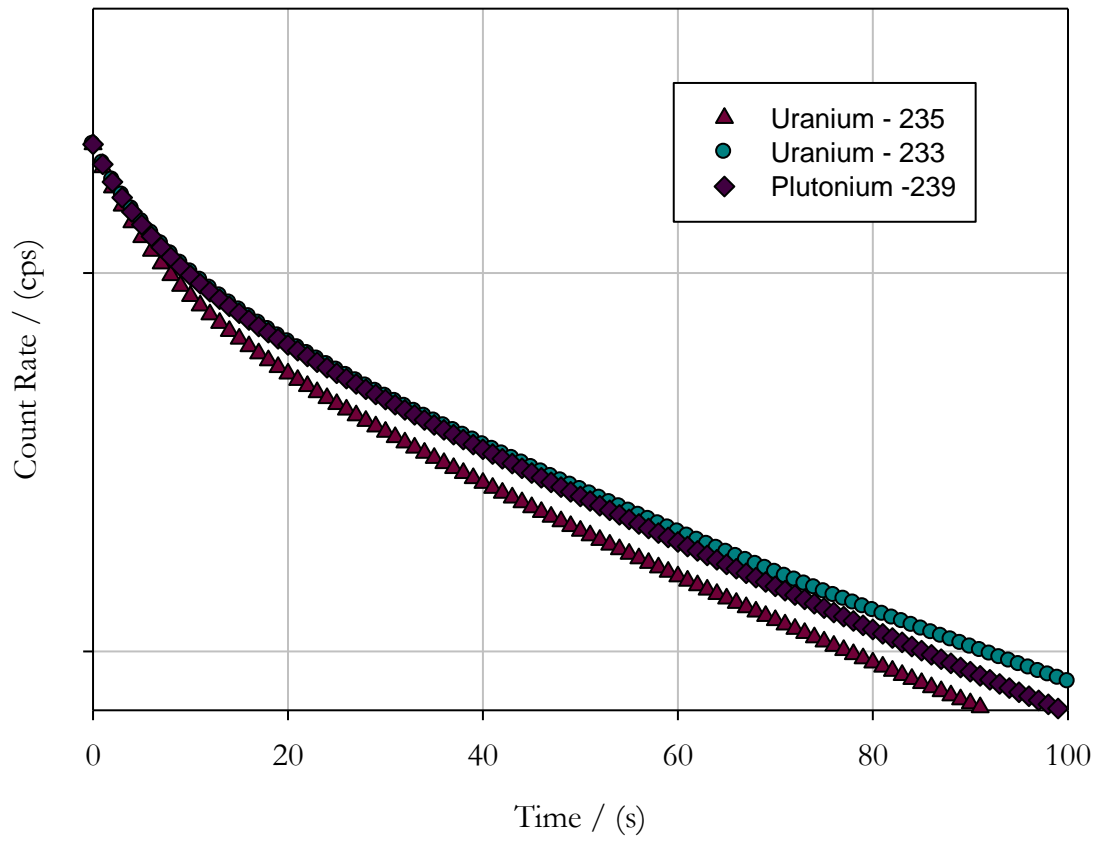


Figure 3-7: A Comparison of SNM Count Rate Curves

The delayed neutron production of a sample containing fissile isotopes is dependent on the time that the sample is exposed to a neutron flux. The delayed neutron activity of fissile isotopes are saturated quickly as shown in Figure 3-8 and sample exposure times greater than two minutes are uncommon as they result in a minimal increase in delayed neutron activity.

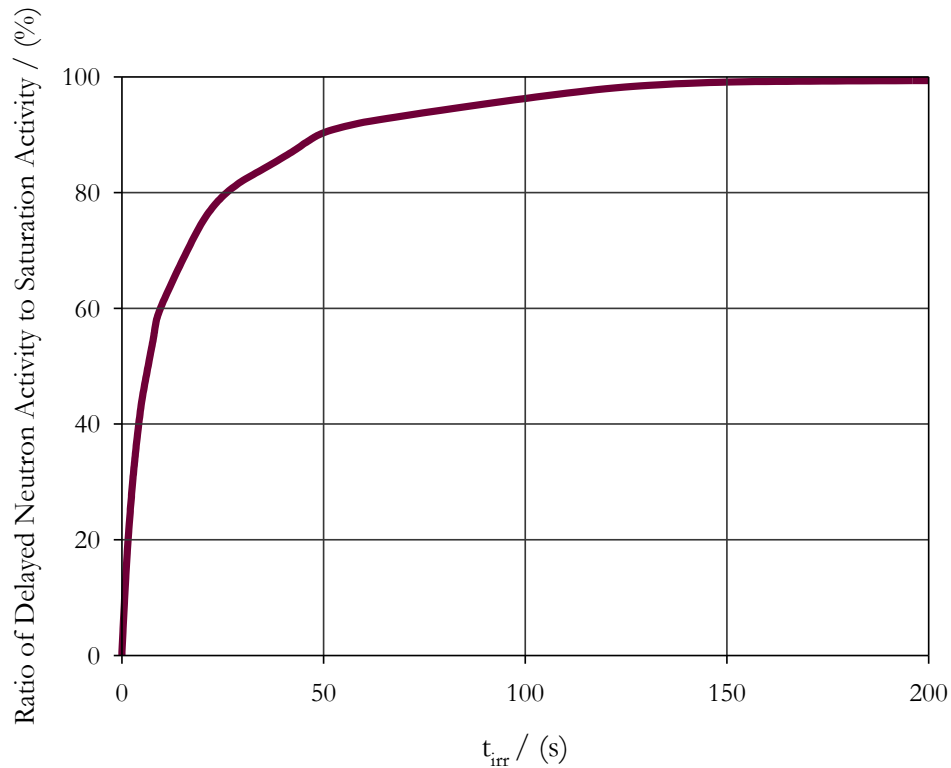
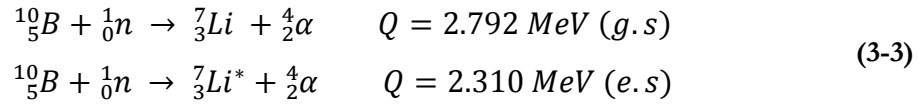
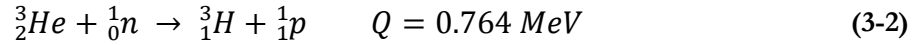


Figure 3-8: Delayed Neutron Activity Saturation

3.3 Neutron Detection

A Comparison of ^3He and BF_3 Detectors

There are two commonly used gas proportional counters used for neutron detection, ^3He and BF_3 . The BF_3 counters are usually enriched in ^{10}B . ^3He and ^{10}B each have a high thermal neutron absorption cross section of 5330 b and 3840 b, respectively [41]. The reactions involving neutrons in the ^3He and BF_3 detectors are shown in Eqs.(3-2) and (3-3) [11].



where Q is the energy liberated in the reaction (MeV). The ground state and excited states are denoted by *g.s.* and *e.s.* respectively. ${}^7\text{Li}^*$ is an excited state of ${}^7\text{Li}$.

In both the boron and helium-3 detectors the energetic and charged particles produced interact with the atoms of the gas filling the volume of the proportional counter. These interactions strip electrons and produce ion and electron pairs that are collected by the electrodes in the detector. In each detector the charge of the secondary particles are amplified, read by the instrumentation and recorded as neutron counts. Typical nuclear instrumentation has fixed energy discrimination levels and all charges above and below these levels are disregarded by the recording apparatus [44]. It is expected that applied instrumental voltages will experience slight fluctuations, which may effect the signals recorded by the apparatus. If the amplified signal is affected enough to be below or above the discriminator levels these counts will not be recorded and this will negatively affect counting consistencies.

The counts recorded by the apparatus can be stabilized by applying a voltage to the detectors, which lies in the plateau illustrated in Figure 3-9. By setting the applied voltage somewhere in the range of the counting plateau the recorded counts will be independent of minor fluctuations in voltage. Both BF_3 and ${}^3\text{He}$ detectors are insensitive to small variations in temperatures and applied detector voltage if this voltage lies in the counting plateau. An example of a neutron detector's counting plateau is shown in Figure 3-9 [11].

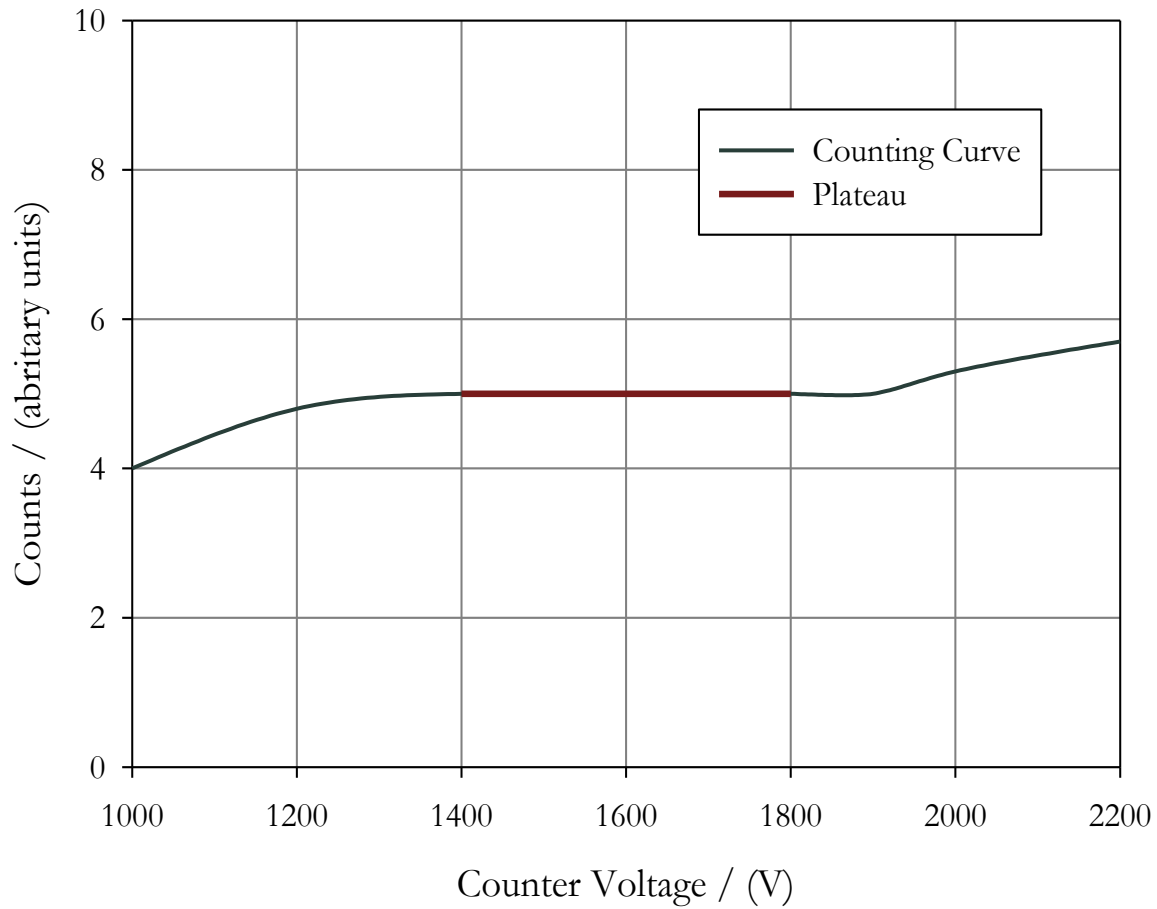


Figure 3-9: Typical Count Curve for BF₃ and ³He Neutron Detectors [11]

Detection Efficiency

The efficiency of radiation detection systems is shown in Eq. (3-4) [44].

$$\varepsilon = \frac{C}{\chi} \quad (3-4)$$

where ε is the absolute efficiency of the system, C the number of counts recorded by the system and χ the number of quanta produced by the source. The absolute efficiency is itself a function of two efficiencies as shown in Eq. (3-5) [11].

$$\varepsilon = \varepsilon_g \varepsilon_{int} \quad (3-5)$$

where ε_g is the geometric efficiency and ε_{int} is the intrinsic efficiency defined in Eq. (3-6).

The geometric efficiency is the probability that the particle emitted from the source will penetrate the sensitive volume of the detector, it is dependent on many physical parameters including the distance and angle between the source and detectors. The geometric efficiency is also dependent on the behaviour of the particle during its travel through the medium separating the source from the detectors; for example, some particles will be scattered away or absorbed before they contact the detector's surface.

The intrinsic efficiency is the probability that once the particle comes into contact with a detector it will actually be recorded by the system as a count. This depends on the energy of the incoming radiation and the operating characteristics of the system. BF_3 and ^3He detectors can have almost any intrinsic efficiency as it is dependent on how much gas is used in the detector as shown in Figure 3-10 and on the incident neutron's energy [11]. Table 3-3 contains additional examples of ^3He and BF_3 intrinsic values found in current literature.

^3He detectors can be filled to pressures exceeding 40 atm which increases their intrinsic efficiency significantly as shown in Figure 3-10. However BF_3 counters are usually produced at 1 atm as to avoid the accidental release of the toxic boron gas. Figure 3-10 shows a comparison the efficiency of some ^3He and BF_3 detectors as a function of tube diameter and internal pressure [11] for a particular manufacturer. The efficiency in Figure 3-10 is the *intrinsic efficiency* defined in Eq. (3-6).

$$\varepsilon_{int} = \frac{\text{number of pulses recorded}}{\text{number of radiation quanta incident on detector}} \quad (3-6)$$

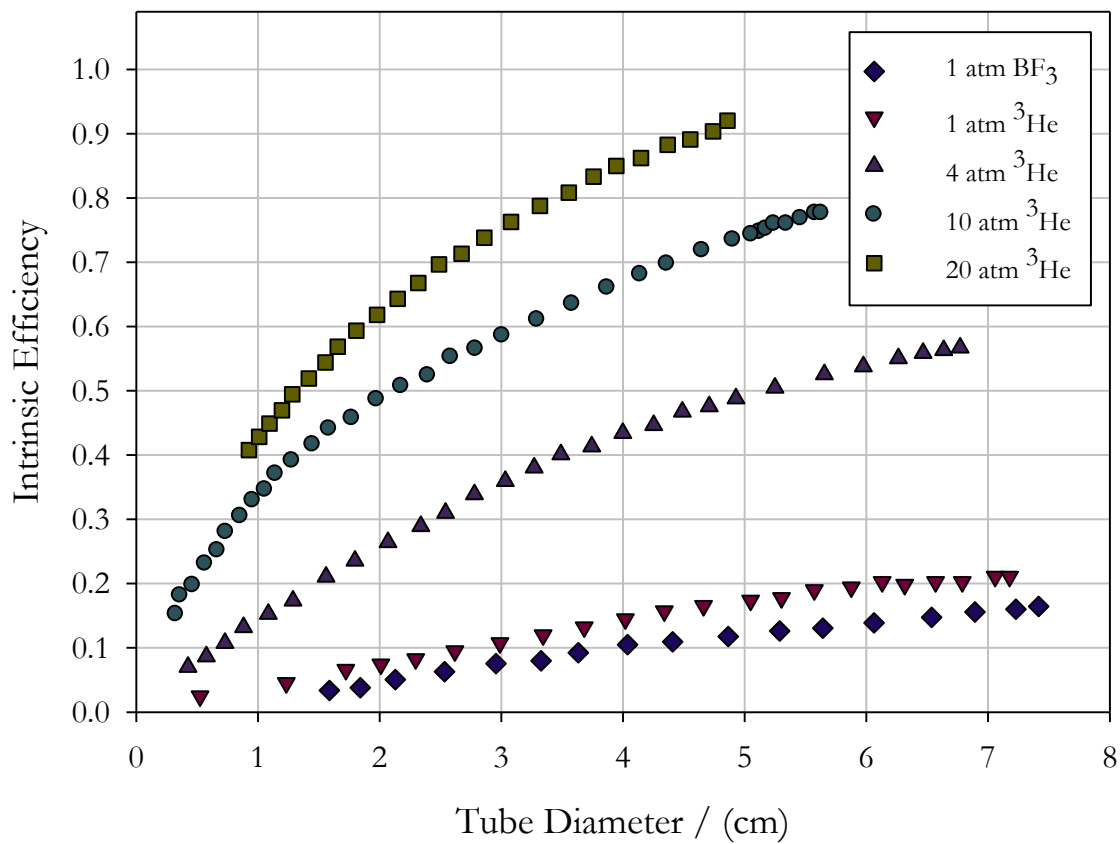


Figure 3-10: Thermal Neutron Intrinsic Efficiency of Proportional Counters [11]

Table 3-3: Thermal Neutron Detector Efficiencies in Current Literature [52]

Type	Size	Neutron Active Material	Neutron Detection Efficiency
³ He (4 atm), Ar (2atm)	2.5 cm diam.	³ He	77%
³ He (4 atm), Ar (2 atm)	2.5 cm diam.	³ He	77%
BF ₃ (0.66 atm)	5 cm diam.	¹⁰ B	29%
BF ₃ (1.18 atm)	5 cm diam.	¹⁰ B	46%
¹⁰ B-lined	0.2 mg/cm ²	¹⁰ B	10%

Figure 3-11 shows that both ^3He and BF_3 are most sensitive to thermal neutrons as their sensitivity is directly proportional to the neutron absorption cross sections. Thermal neutrons therefore dominate the counts recorded in the presence of a mixed neutron energy field. Both detector types are typically separated from neutron sources by moderator material, which thermalizes the neutrons and results in higher detection efficiency. Common neutron moderating materials include the hydrocarbon polyethylene and paraffin [42] and also water and graphite [43]. The large differences in pulse sizes recorded from incident gamma and neutrons are large enough in each detector type to allow effective discrimination between these different types of radiation. Therefore, both detectors can operate effectively in a gamma background up to $10 \text{ R}\cdot\text{h}^{-1}$ [11].

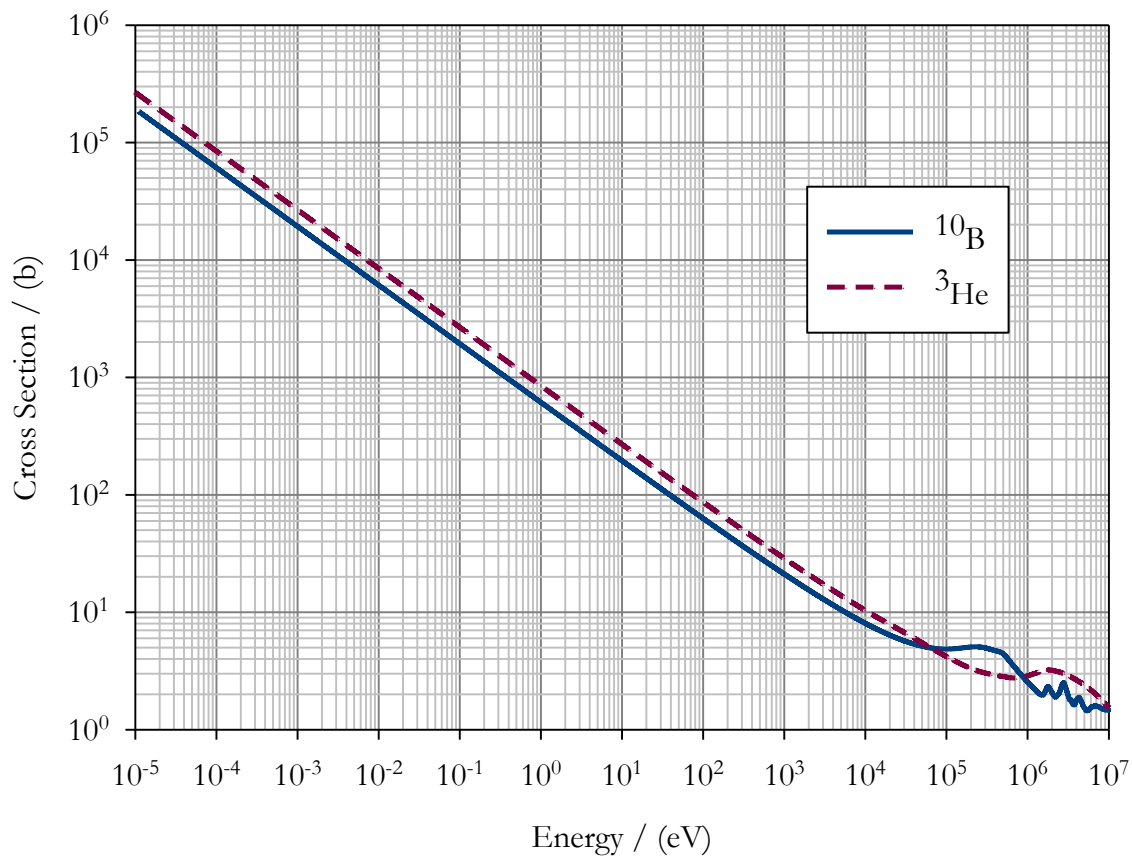


Figure 3-11: The Cross Sections of ^3He and ^{10}B [33]

Electrical Dead Time

Paralyzable and Non-Paralyzable Detection Systems

There is always a delay between the time when a neutron enters a BF_3 or ^3He tube and the time when that event is recorded. Any additional detector interactions during this delay will not be recorded by the system electronics. This effect, known as system *dead time*, is resultant from delays in the detector, wiring and recording system processing. Figure 3-12 shows the effect system dead time has on the number of events recorded by the system. In Figure 3-12 each system will not record the third and fifth true counts as it is still occupied with processing the previous counts.

There are two common types of dead time, non-paralyzable and paralyzable. In paralyzable dead time models, shown in Figure 3-12, counts are lost if they occur within τ of any preceding event, where τ is the dead time of the system. In a non-paralyzable system the sixth true count would be recorded by the system as the fifth would not add to the delay in the system processing time.

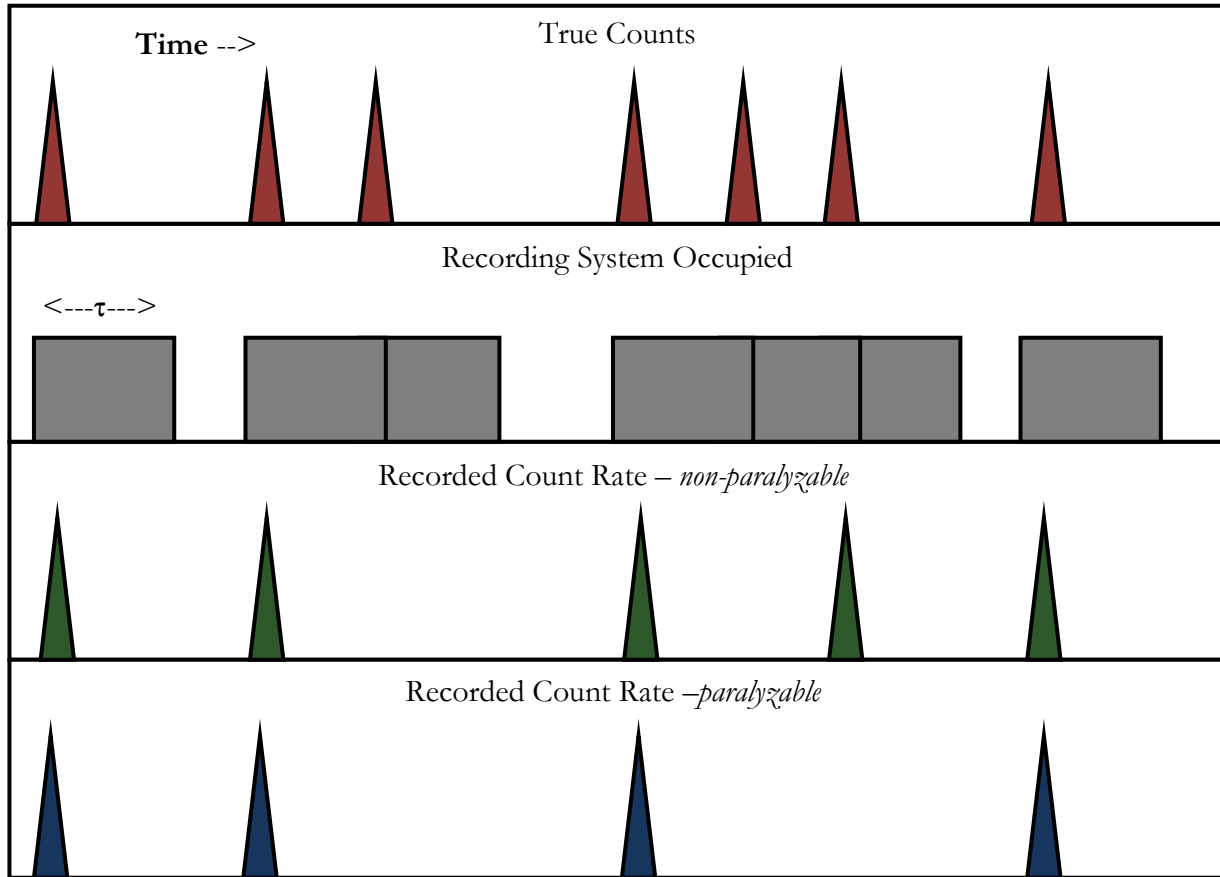


Figure 3-12: Paralyzable and Non-Paralyzable Dead Time Comparison [44]

The models for non-paralyzable and paralyzable dead time are shown in Eqs. (3-7) and (3-8), respectively [44].

$$R = \frac{D}{1-D\tau} \text{ (non-paralyzable)} \quad (3-7)$$

$$D = R e^{-R\tau} \text{ (paralyzable)} \quad (3-8)$$

where R is the true count and D is the count recorded with dead time effects. Once the system has finished processing a count in time, τ , it is immediately able to process additional counts in a non-paralyzable system. In a paralyzable system, the processing time is interrupted by any additional counts and these counts will prolong the processing time resulting in even less counts as shown in Figure 3-12.

Determining the Dead Time Constant

The two source method is a common way of determining dead time in a system and consists of comparing the count rates from two measured sources individually and their combined count rate [35]. The count rate of the source combination will be lower than the summation of the two individual sources in a system with significant dead time effects. For systems with a background count rate, D_b , the dead time (τ) can be determined as shown in Eq. (3-9) [35], the derivation of which can be found in Appendix A.

$$\tau \approx \frac{D_1 + D_2 - D_{12} - D_b}{D_{12}^2 - D_1^2 - D_2^2} \quad (3-9)$$

where D_1 is the recorded count rate from source 1, D_2 the recorded count rate from source 2, and D_{12} the recorded count rate from the combination of source 1 and source 2 and D_b is the background count rate. Eq. (3-9) is valid for $D_1\tau \ll 1$ and $D_2\tau \ll 1$, as is typically the case.

If it is not practical to reanalyze samples and the counts are solely dependent on one isotope's mass, two separate sources s_x and s_y can be used where the mass of s_x was approximately equal to half of the mass of s_y . Thus, s_x can be treated as the two individual sources and s_y as the combination of those two sources. Therefore D_1 and D_2 are equal and are the count rate from s_x , and D_{12} the count rate from s_y (as the mass of $s_x = 0.5s_y$) and Eq. (3-9) is simplified.

$$\tau \approx \frac{D_x + D_x - D_y - D_b}{D_y^2 - D_x^2 - D_x^2} \quad (3-10)$$

$$\tau \approx \frac{2D_x - D_y - D_b}{D_y^2 - 2D_x^2} \quad (3-11)$$

3.4 Delayed Neutron Count Rate Behaviour

As mentioned in Section 3.2 the fissile isotopes ^{233}U , ^{235}U and ^{239}Pu require the absorption of neutron to undergo fission and produce delayed neutrons. The probability of the fission process is dependent on the energy of the neutron as shown in Figure 3-2 and is characterized by the fission cross section σ_{fj} for isotope j at that neutron energy. The number of interactions per unit of time is dependent on both the flux of neutrons the isotope is exposed to and the number of fissile atoms present.

The behaviour of the delayed neutrons produced is dependent on the duration the samples are exposed to the neutron flux and the amount of time the activated sample undergoes decay. The shape of the delayed neutron count rate curve produced from each isotope is unique and dependent on the delayed neutron production ratios resultant from the fission product yields shown in Figure 3-3. The delayed neutron count rate from one isotope “ j ”, $S(t)_j$ (counts s^{-1}), is therefore dependent on many experimental and system conditions as outlined in Eq. (3-12) for the case of thermal neutrons [20].

$$S(t)_j = \frac{\varepsilon v_j N_A \sigma_{fj} \Phi m_j}{M_j} \sum_{i=1}^k \beta_{ij} (1 - e^{-\lambda_i t_{irr}}) (e^{-\lambda_i t_d}) (e^{-\lambda_i t}) \quad (3-12)$$

where ε is the absolute neutron detection efficiency of the system, v_j is the average delayed neutrons produced in the fissioning of the SNM isotope “ j ” at that neutron energy, N_A is Avogadro’s number (mol^{-1}), σ_{fj} is the neutron energy dependent fission cross section for isotope “ j ” (b), Φ is the experimental neutron flux ($\text{neutrons cm}^{-2}\text{s}^{-1}$), m_j the mass of the fissile isotope “ j ” (g), M_j the molar mass of that isotope “ j ” (g mol^{-1}), β_{ij} the production ratio for group i for the fission of isotope “ j ”, k is the total number of delayed neutron groups used in the model, λ_i is the half-life associated to that particular delayed neutron group (s^{-1}), t_{irr} is the irradiation time (s), t_d is the time between irradiation time elapses and counting begins, during which the sample decays (s), and t is the time during which neutron counts are recorded (s), t begins after t_{irr} and t_d have elapsed.

For a sample containing a mixture of ^{235}U and ^{239}Pu or any other combination of fissile materials, the total count rate, $S(t)$ (counts s^{-1}), is given by Eq. (3-13).

$$S(t) = \sum_{j=1}^n S(t)_j \quad (3-13)$$

Where n is the total number of delayed neutron producers in a particular sample and j is the isotope number (eg. $j=1$ for ^{235}U , $j=2$ for ^{239}Pu and $j=3$ for ^{233}U).

The total count rate, $C(t)$, recorded by a delayed neutron counting system is a superposition of all the delayed neutron producing isotopes as shown in Eq. (3-13) and any contribution of system background to the overall count as shown in Eq. (3-14).

$$C(t) = S(t) + \textit{Background} \quad (3-14)$$

Background contributions to the overall count rate recorded by such systems are typical and resultant from background radiation and possible sample contamination with delayed neutron producers or other neutron emitters such as ^{252}Cf

If a DNC system is properly characterized such that the background contributions and dead time effects are accurately quantified, the system is capable of determining the fissile isotopes present based on the delayed neutron count rate curve. Determining the overall efficiency of the system allows for the mass or concentration of fissile isotopes present in the sample to be deduced. The consistent behaviour of the delayed neutron production of fissile samples allows the irradiation, counting and analysis process to be automated for rapid fissile content determination.

Chapter 4

Experimental

4.1 Delayed Neutron Counting System Overview

Custom-made executable software controls the pneumatic valves and electronics in the DNC system built at RMC. The SLOWPOKE-2 reactor facility at RMC is used as a neutron source to irradiate the fissile samples. Once the samples have been irradiated for a defined time, they are sent to the counter arrangement, which contains six ^3He detectors connected in parallel. These detectors record the time-dependent delayed neutron count rate, which is saved as an excel file by the executable. This file can be read by an in-house developed fissile analysis program, which determines the fissile isotope mass based on experimental parameters (including corrections for dead time and system background).

System Hardware Control

The DNC system hardware is controlled by an in-house developed code written using the platform LabVIEWTM [45]. This code has two primary functions; hardware and electrical control of the system and user-defined experiment control. The graphic user interface (GUI) shown in Figure 4-1 allows the user two operation options, one manual and one automated. The automated option allows the user to define experimental parameters including the number of samples to be analyzed, the irradiation, decay and count times, and the number and style of replicate analysis. Once the

experimental parameters have been selected and the samples are loaded, the program controls all electrical and hardware aspects of the system as described in Appendix B.



Figure 4-1: Delayed Neutron Counting Graphical User Interface

Each neutron recorded by the system is displayed in real-time on a second tab in the GUI as shown in Appendix B. The neutron counts are recorded in variable time intervals which can range from 0.25s to minutes and are set to a default value of 0.5s. The two column display shows each time interval that has elapsed and the total delayed neutron counts recorded in that interval. This recording of neutron counts can be used to confirm the presence of the sample in the counter arrangement.

SLOWPOKE-2 Nuclear Reactor

The Safe LOW Power K(c)ritical Experiment reactor is a thermal nuclear reactor with a nominal power of 18 kW [46]. The core of the SLOWPOKE-2 at RMC is shown in Figure 4-2 and

contains 198 zircaloy fuel pins each containing uranium-dioxide enriched to 19.89 wt% ^{235}U [47]. The core of the reactor is submerged below 4.4 m of water in the reactor room at RMC [48]. Figure 4-2 shows a schematic of the SLOWPOKE-2 reactor [49]. The flux of the reactor is monitored and read by RMC's SLOWPOKE Integrated Reactor Control and Instrumentation System SIRCIS 2001 software [50], which positions the control rod to maintain power and neutron flux stability. The core is surrounded on all sides by a beryllium annulus and beryllium slabs are placed on the top and bottom, which serves as a neutron reflector. Imbedded in this beryllium reflector are five irradiation sites including the current DNC system irradiation site. Samples are sent via pneumatic air to these irradiation sites where they are exposed to high neutron fluxes for the designated irradiation times.

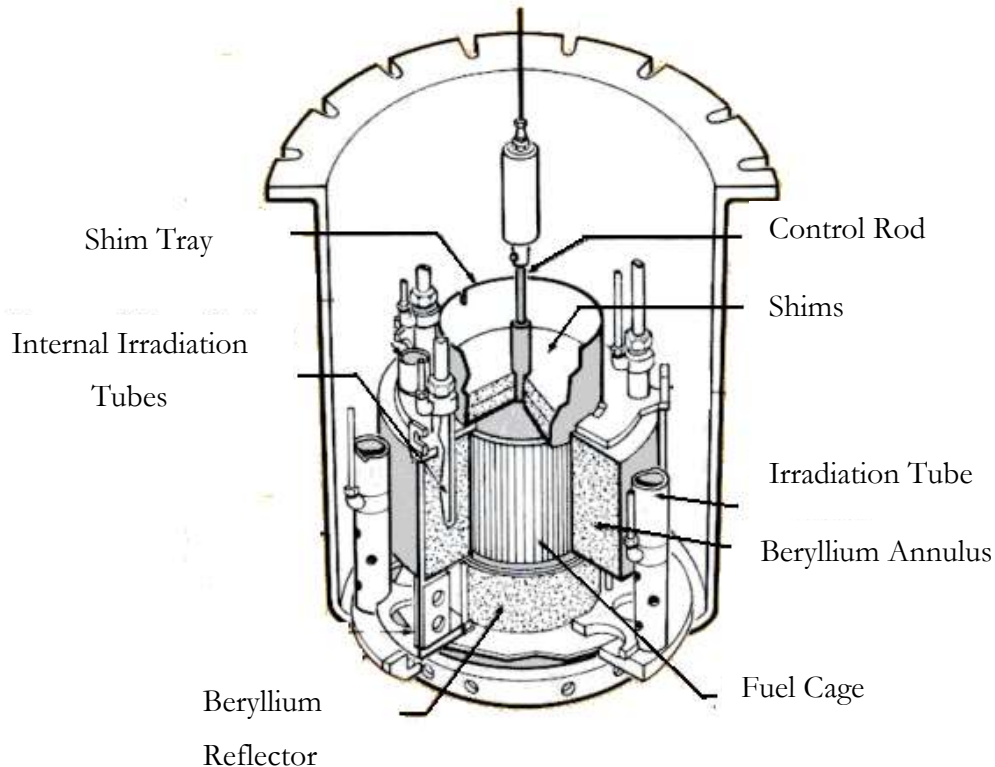


Figure 4-2: The SLOWPOKE-2 Reactor Schematic [49]

When the SLOWPOKE-2 reactor is operating at half power the nominal thermal neutron flux of these inner sites (SLOWPOKE sites 1 through 5) ranges from 5.3 to 5.8×10^{11} ($\pm 5\%$) neutrons $\text{cm}^{-2}\text{s}^{-1}$ [51]. There are also four outer sites in the SLOWPOKE-2, which have a significantly lower thermal neutron flux of 2.6 - 2.8×10^{11} neutrons $\text{cm}^{-2}\text{s}^{-1}$ at half power. The current irradiation site designated for the DNC system at RMC is site 5, an inner with a nominal flux of 5.5×10^{11} neutrons $\text{cm}^{-2}\text{s}^{-1}$ when operating at half power [51].

DNC System Neutron Detection

A photograph of the delayed neutron detection arrangement is shown in Figure 4-3 and consists of six ^3He detectors embedded in paraffin. The detectors were produced by Reuter-Stokes (RS-P4-1613-202, GE Energy, Twinsburg, OH) and are 5 cm in diameter and are pressurized to 4.15 atm. The history of use of these detectors is unknown and current literature discussing similar detectors implies an approximate intrinsic efficiency ranging from 50% to almost 80% [52]. As shown in Figure 4-3, the detectors are arranged concentrically around the sample's position in the counter. Each detector centre is 8 cm from the centre of the sample and the sample rests halfway along the detector's length.

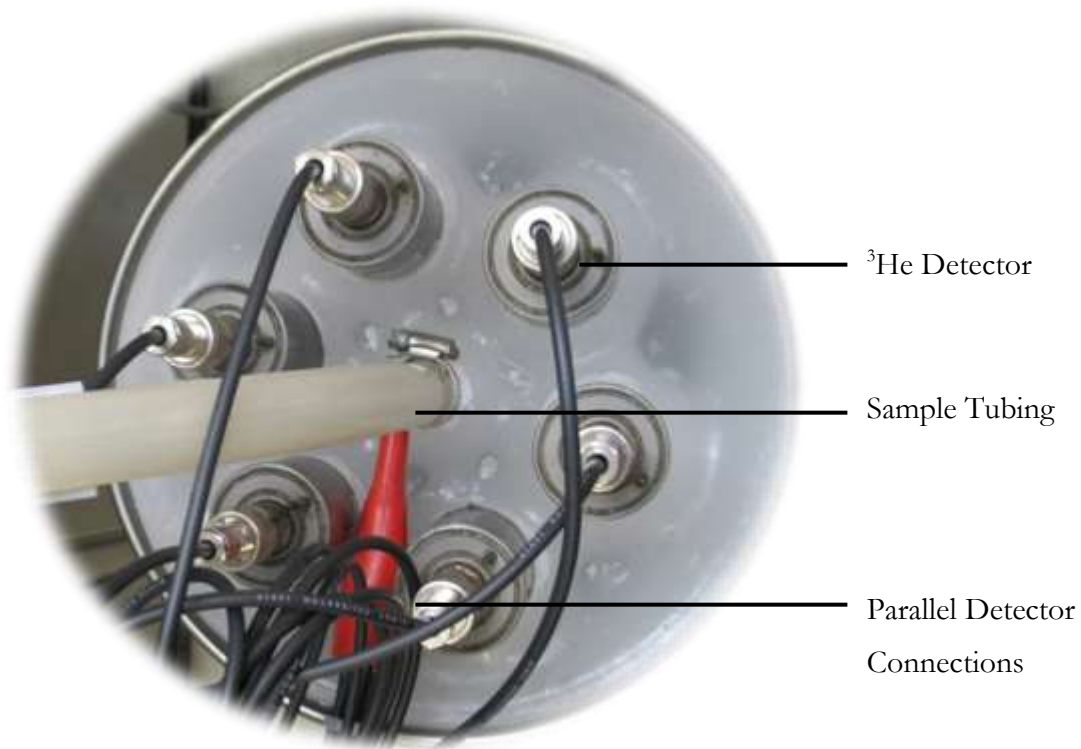


Figure 4-3: DNC System Counter Geometry

The pulses produced in the detectors by the $^3\text{He}(n,p)^3\text{H}$ are too small to analyze so they are sent through a preamplifier, which amplifies the pulses before they are read by the multi-channel analyzer. The multi-channel analyzer (MCA) records the number of pulses as a function of energy. The upper and lower discrimination levels can be set using the discriminator windows attached to the MCA. All of the pulses collected within the discriminator window are recorded by the DNC system software.

4.2 Data Analysis Software

The output file produced by the operations software can be analyzed in the fissile analysis program written in MatlabTM [53], which is capable of outputting the amount of ^{235}U determined by the DNC system for each sample. The output of the executable software contains the time and date when the analysis was conducted, and the delayed neutron counts recorded in segmented time intervals. The raw data associated with each sample consist of five columns containing sample number, corresponding run number, segmented time intervals, the corresponding counts for each time

segment and the sum of all recorded counts for count time duration, an example is shown in Appendix B. The fissile analysis program begins by reading the output file and determining how many samples have been analyzed (and how many cycles they have undergone) and then produces a time and count vector for each sample run.

The DNC system parameters defined through calibration are used alongside Eq. (3-12) to produce the expected count rate for 1 μg of ^{235}U for the unique DNC system characteristics. Experimental parameters including irradiation time, decay time, efficiency and neutron flux can be user defined, however, an additional version of the analysis code is available with these values hard coded for simplicity as shown in Appendix B. The curve for 1 μg of ^{235}U for each experimental time interval is stored for comparison purposes to the modified raw count data.

Once the 1 μg count rate has been produced, the raw data obtained by the fissile analysis code are modified so that the two can be compared. An empirical dead time correction function converts the measured counts to true counts rates and is discussed in more detail in Section 5.3. The true and theoretical count rates for each time interval are then compared and a least squares solution (LSQR) for the mass of ^{235}U present in the sample, which is then displayed for the user in μg .

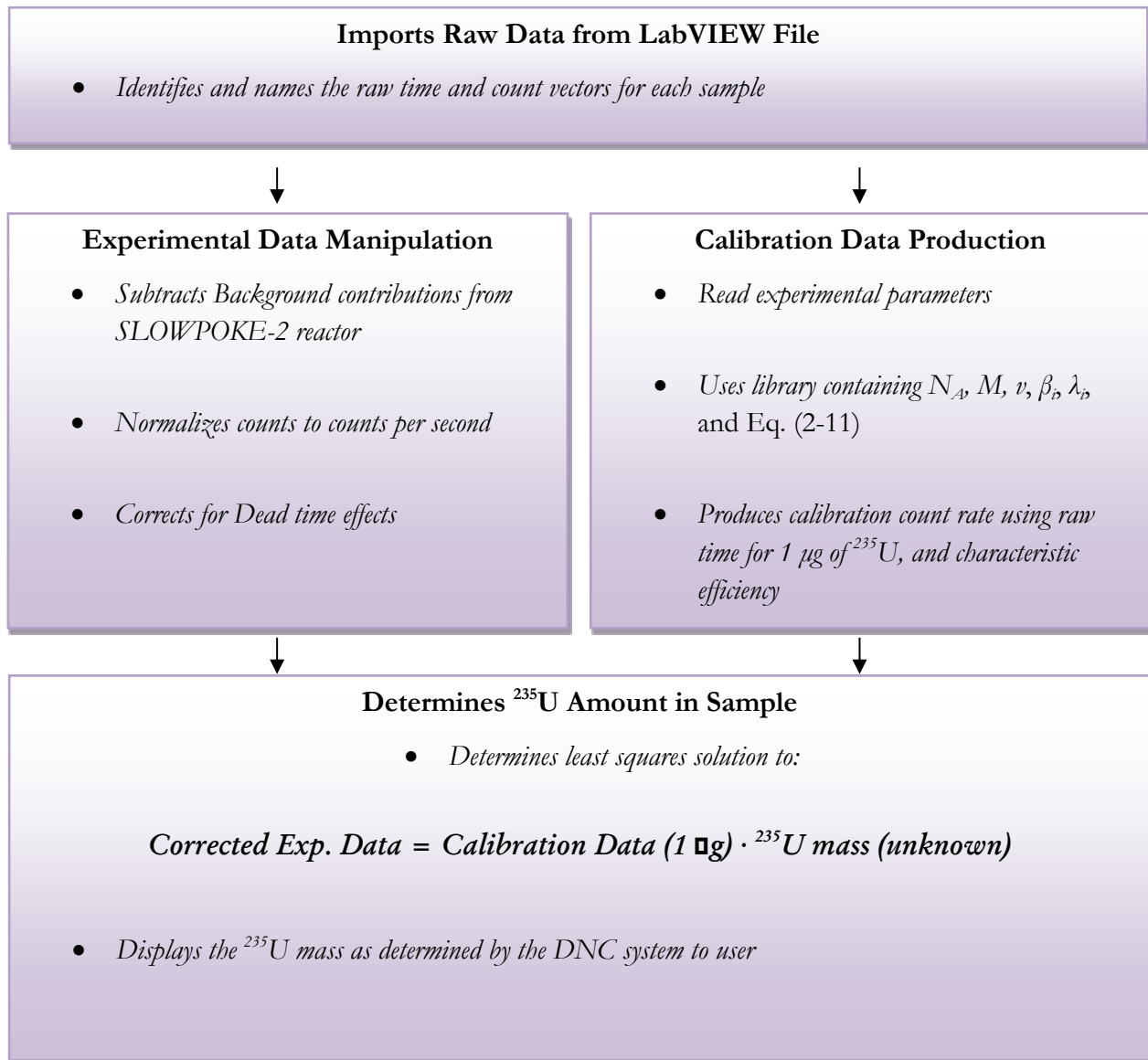


Figure 4-4: Fissile Analysis Program Structure

4.3 Consumables

The fissile consumables used for experimentation consisted of natural uranium (CRM 4321C, NIST, Gaithersburg, MD) and depleted uranium (CRM U005A with 0.5064 ± 0.0003 atom percent ^{235}U). The polyethylene vials (1.5 and 7.0 mL) used to transport the system were obtained from LA Packaging, Yorba Linda, CA. Optima nitric acid and sucrose (Optima, ThermoFisher Scientific,

Ottawa, Ont.) were used to validate the robustness of the system and obtain counts for background and possible delayed neutron interferences. The de-ionised ultra filtered water was prepared at RMC (E-pure, Bamstead, Dubugue, IA). A 37 kBq NIST-traceable multi-element radionuclide source containing ^{210}Pb , ^{241}Am , ^{109}Cd , ^{57}Co , ^{139}Ce , ^{203}Hg , ^{113}Sn , ^{85}Sr , ^{137}Cs , ^{88}Y , and ^{60}Co was (Eckert and Ziegler, Valencia, CA) was used as a source of gamma rays.

The 4321C solution was diluted with 2% nitric acid and used to prepare a 7.32 ppm ^{235}U calibration stock [54]. The depleted uranium control sample was digested in *aqua regia* and also diluted with 2% nitric acid to prepare another 5.39 ppm ^{235}U stock solution [55]. Each of samples was further diluted with 2% nitric acid and distilled water to nominal values of 1 mL with varying amounts of ^{235}U and concentrations.

4.4 Delayed Neutron Counting Procedure

Sample Preparation

Fissile, sucrose and nitric acid solutions were all heat sealed in 1.5 mL vials before being placed in a 7.0 mL vial containing an empty, secondary 1.5 mL vial prior to sample irradiation and analysis. Vials contain Al, V, Na, S, Mg, Br, Cl, Mn, I, K and Co impurities all at concentrations less than 2 ppb [56]. None of the identified impurities are known to produce delayed neutrons upon irradiation in a thermal neutron flux. A fissile pre-test consisting of a comparison of the gamma radiation emitted by the samples to the gamma emission from 10 mg of uranium-235 was conducted prior to sending the sample in the SLOWPOKE-2. This test ensured that the uranium in the sample did not exceed Canadian Nuclear Safety Commission (CNSC) regulatory limits for fissile content additions to the SLOWPOKE-2 reactor at RMC [57].

Analysis Overview

After each sample is sealed in the polyethylene capsules they are placed in the manual loader shown in Figure 4-5. Once the samples are loaded, the experimental parameters: irradiation time, decay time and count time, are selected on the GUI. Figure 4-5 shows all possible paths the samples could take depending on the preference of the user and whether they would like cyclic or pseudo cyclic sample analysis. In the case of this work, all samples were analyzed one at a time with no pseudo cyclic irradiation/counting. Samples that were re-analyzed for further data collection were done so days apart to allow for significant reductions in sample radiation levels.

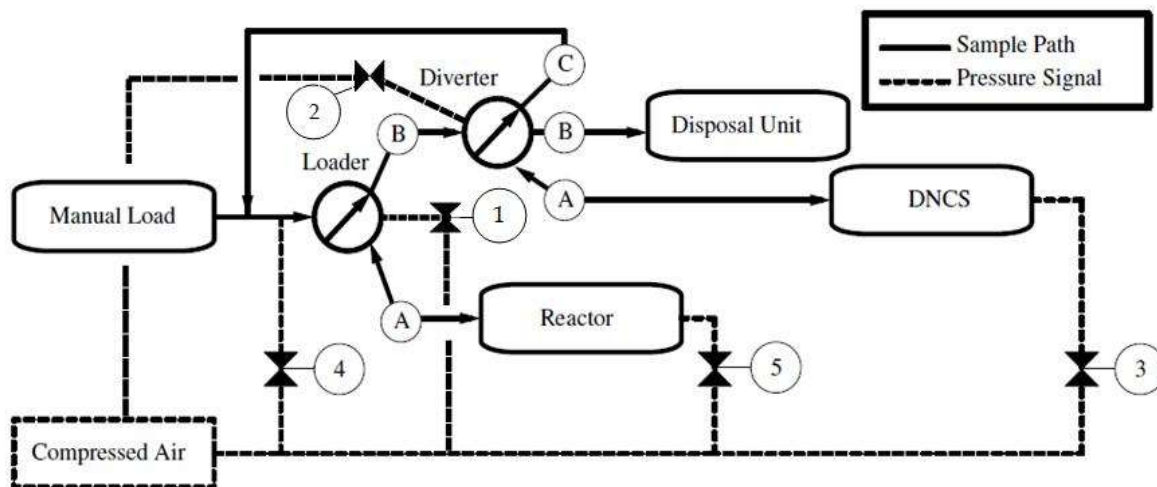


Figure 4-5: Possible Sample Pathways and Pressure Signals in the DNC System

Once the experimental parameters were input into the control executable, the sample was sent to the SLOWPOKE-2 reactor site 5 for the set irradiation duration. Once the irradiation time had elapsed, the sample was sent to the counter arrangement shown in Figure 4-3. A minimum delay of 2.9s between sample irradiation and counting is required to allow the sample time to travel and the nuclear instrumentation to begin counting. This delay is accounted for in the fissile analysis program, which assumes a default t_d of 2.9s unless otherwise specified during analysis. After the delay and/or decay time has expired the system begins recording the sample count rate in default 0.5s intervals for the specific count time. After the counting time has elapsed, the sample is sent to

the disposal unit also located in the SLOWPOKE-2 reactor room sufficiently far from the detector such that negligible background contributions occur.

The Determination of System Background

The background of the DNC system in the absence of fissile samples was determined by setting the system for an automatic 60s irradiation and subsequent 60s count time. Samples were not placed in the loader and the system proceeded to record the system neutron count rate of the reactor air pushed through the pneumatic tubing into the counter arrangement. To ensure the SLOWPOKE-2 neutron flux contribution was consistent this experiment was repeated several times over a period of months. Further data were collected with the reactor off to provide a comparison to natural background.

Many polyethylene vials were prepared in a manner similar to that of uranium analysis typical use to examine the contribution of the polyethylene vials used to transfer the fissile samples through the DNC system. Each sample was then irradiated for 60s with the SLOWPOKE-2 reactor operating at half power. The neutron count rate was recorded after the sample was irradiated. Twenty four vials were prepared with varying total mass of polyethylene to examine the possibility of the activation of impurities in the polyethylene. Eight vials were left empty, eight contained two inner 1.5 mL vials, and the remaining eight were filled with pieces of additional polyethylene (produced by cutting the vials into small pieces). The total polyethylene mass ranged from 3.3 to 6.6 g.

The original DNC system site (5) was temporarily switched to another inner irradiation site in the SLOWPOKE-2 (site 3) to examine any possible effects the site location may have on the polyethylene vial contribution. Twenty new vials were prepared in the previously described and irradiated for 60s in site 3. Further experimentation for varied irradiation times, 10s and 60s, was completed using two 7.0 mL polyethylene vials (each containing two smaller 1.5 mL vials).

Dead time Experimentation

Several sets of samples where the fissile content of s_x was equal to half of s_y were run through the delayed neutron counting procedure on different days to determine dead time. Each trial was run at SLOWPOKE-2 half power (with a nominal flux of 5.5×10^{11} neutrons $\text{cm}^{-2}\text{s}^{-1}$), an irradiation time of 60s, the default decay, and a count time of on 60s. D_b , the contribution of empty vials to the count, was determined by running empty polyethylene vials through the same experimental parameters and recording the total neutron count after 60s.

The Analysis of Fissile Samples

As mentioned previously a fissile analysis pre-test was conducted before samples containing any fissile content were analyzed by the DNC system. Typical operating conditions for fissile analysis in this work consisted of the SLOWPOKE-2 operating at half power creating a nominal flux of 5.5×10^{11} neutrons $\text{cm}^{-2} \text{s}^{-1}$ at site 5. Samples were irradiated for 60s and were subsequently counted for 60s after the 2.9s delay to account for sample transport to the counter arrangement and electronic system delays. After data were collected for each sample they were retrieved from the disposal unit and immediately placed in lead shielding for several days prior to being re-analyzed or handed to the Radiation Safety Officer for storage and disposal.

Chapter 5

Results & Discussion

This chapter provides an overview of all experimentation and analyses performed to validate the DNC system's SNM content determination through the examination of the delayed neutron count rate curve. A series of DNC system characteristics were determined in the early stages of development and are described in Sections 5.1 - 5.3. The system electronics were examined to find the ^3He detectors' counting plateaux and optimal distance from the delayed neutron source resulting in system count stability and a maximum efficiency respectively. The background of the DNC system was quantified and explanations of these backgrounds are provided in Section 5.2. A full understanding of the system's electrical performance particularly the quantification of delays and dead time in signal processing were required to measure system performance and efficiency. The delay in system processing was found to be consistent and a dead time value was determined using the two source method described in Section 5.3. An empirical dead time correction was found and compared to analytic models. The absolute efficiency of the DNC system was determined and compared to theoretical calculations using Eq. (3-12) as a final step in system characterization

Once the system was characterized, the capability of the fissile analysis program to model experimental results was examined in Section 5.4. The code used the empirical dead time correction, system delay and background data (determined in Sections 5.3) and Eqs. (3-12) and (3-14) to produce a theoretical model for delayed neutron behaviour in RMC's DNC system, which was subsequently compared to data collected by the system. The code was then used to quantify background contamination in the system in an attempt to improve the accuracy of ^{235}U determination. The reproducibility of DNC system results was examined by analyzing 64 samples containing natural uranium dissolved in nitric acid divided into eight sets, which were irradiated and

counted in the system over a period of several weeks. The effects of changes in sample volume and geometry were examined by varying the amount of nitric acid solution in several samples containing depleted uranium dissolved in nitric acid. The loading position of the samples into the DNC system was changed for several runs resulting in a displacement of 2.5 cm in the both the irradiation and counting positions.

The final section of this chapter discusses experimentation conducted using four different uranium solutions, varied in $^{235}\text{U}/^{238}\text{U}$ ratios and solution ^{235}U concentration. All samples were analyzed uninterrupted on the same day and the dead time, delay and efficiency values characterized in Sections 5.3 were used in the fissile analysis program to analyze the count rate curve and determine ^{235}U content in each solution. The data collected also analyzed reductions made in the background contribution through the removal of contamination in the system. Finally, the ^{235}U amounts determined by the DNC system were analyzed for both the natural and depleted uranium samples over a range which varied by three orders of magnitude from about 10 ng to almost 10 μg of fissile material.

5.1 Neutron Detector Optimization

To determine the optimal operating voltage of the ^3He detectors, a ^{252}Cf source was placed in direct contact with each ^3He detector and the counts were recorded for a one minute duration as a function of voltage. The optimal operating voltage of the six ^3He detectors used in the DNC system is shown in Figure 5-1 for the range of 0 to 1500 V. It was determined that slight variations in the operating voltage would least affect the system detection at 1300 V. Each of the six detectors increased in detector efficiency to a plateau around 1100-1350 V. The operating voltage is well below the maximum operating voltage of 2200 V specified by the manufacturer [58]. The selected voltage is also in good agreement with the plateau specified by the manufacturer.

The required thickness of paraffin to sufficiently de-energize the neutrons to levels of higher detection efficiencies was also determined using two ^{252}Cf sources. The total count as a function of paraffin thickness was recorded. The ideal thickness of paraffin was determined to be 3.8 ± 0.1 cm

as shown in Table 5-1. This paraffin thickness is comparable to other systems, but somewhat lower than those found in literature average of $\sim 6\text{-}8$ cm [21, 20]. The number of ^3He detectors available for use in the DNC system was limited by the connectors, which could be wired in parallel for data collection. Thus, the six most efficient ^3He detectors were used and placed in a concentric circle, each 3.8 cm away from the source location in the counter apparatus.

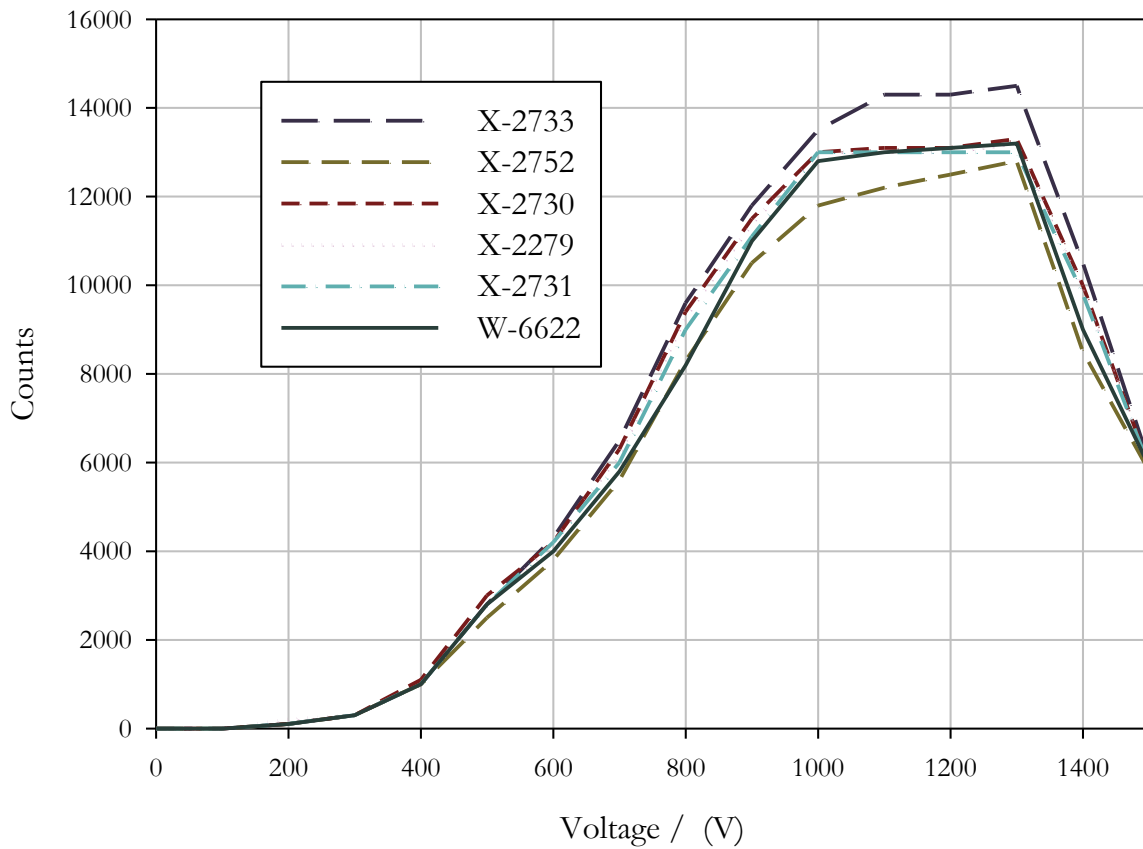


Figure 5-1: Helium-3 Detector Count Plateaux for Six Detectors used in Counter

Table 5-1: Moderator Thickness Effects on Neutron Count

Thickness (cm)	Count Source 1	Counts Source 2
0	198	693
1 ± 0.1	206	726
2.5 ± 0.1	216	803
3.5 ± 0.1	279	852
3.8 ± 0.1	291	1024
4.8 ± 0.1	251	933

5.2 Additional Contributions to Overall Count Rate

When minimizing the detection limit of DNC systems the background contributions must be properly characterized. This section discusses the extensive analysis of the background contributions to the overall count rate. The contribution of the SLOWPOKE-2 flux, presence of the polyethylene vials used to transport the samples through the system, gamma interferences and possible fast neutron reactions were all examined.

SLOWPOKE-2 Flux Contribution to System Background

The background counts in the system with the SLOWPOKE-2 at half power were measured eight times over a period of several days as shown in Figure 5-2. The air inside irradiation site 5 was sent to the counter and the background counts of the system showed no dependence on count time as shown in Figure 5-3. The independence of the count time (which begins once the irradiation and decay times have elapsed) indicated the radionuclides that may have been present in the gas stream coming from the SLOWPOKE-2 were not contributing to the overall delayed neutron count. The system background in the absence of a vial was determined to be 3.8 ± 0.4 counts per second when the SLOWPOKE-2 operates at half power (the average and 2σ uncertainties are denoted by the horizontal lines in Figure 5-2).

Background counts were also collected with the SLOWPOKE-2 at half power with no air transferred from the irradiation site to the counter. These results were statistically equivalent to previous experimentation further indicating radionuclides in the gas were not contributors to background. The background counts were dependent on the power of the SLOWPOKE-2 indicating this is the main source of background in the absence of vials.

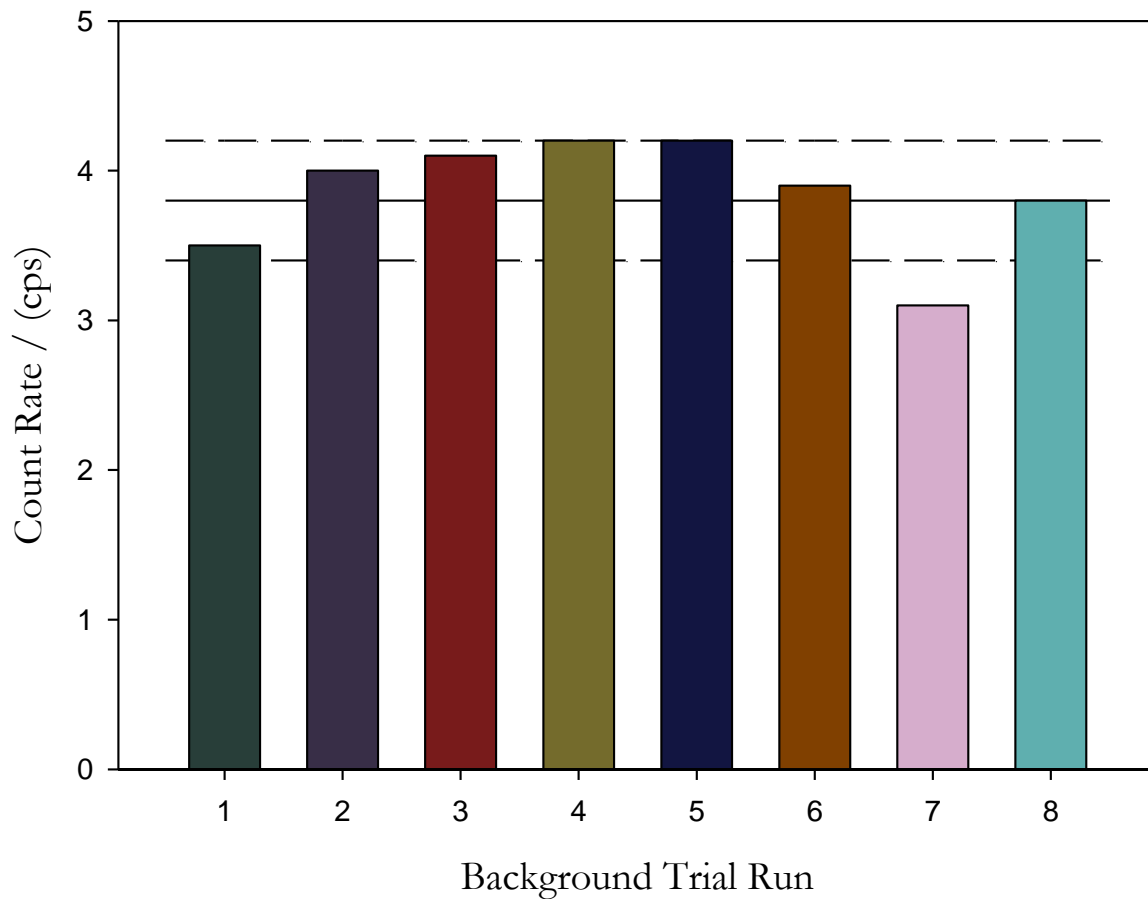


Figure 5-2: System Background in the Absence of Vials at SLOWPOKE-2 Site 5

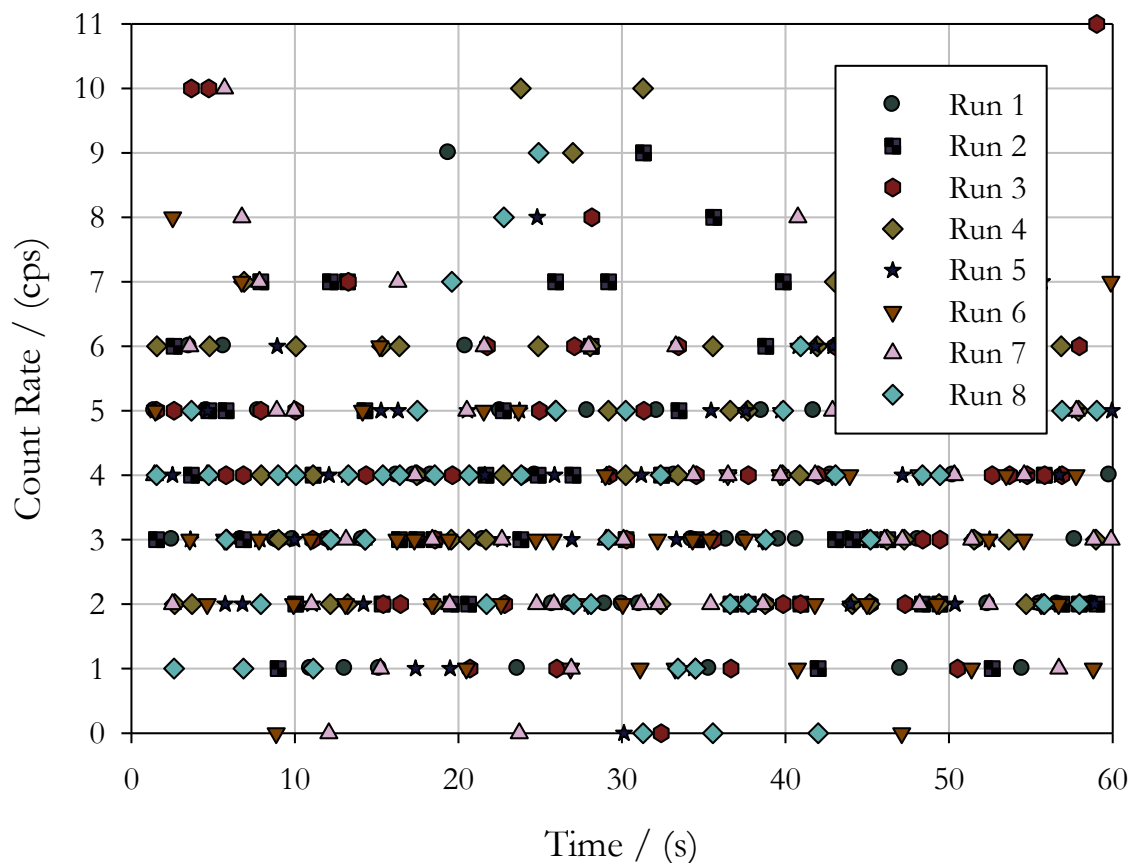


Figure 5-3: System Background Independence of Count Time

Sample Vial Contributions to DNC System Neutron Count Rate

Figure 5-4 shows the count rates as a function of elapsed count time for eight trial runs with empty polyethylene vials each with a 60s irradiation at half power and a decay time of 2.9s. The decay of 2.9s is the minimum time that can be employed at RMC's DNC system as it is the time for the sample to travel from the irradiation site to the counting site and for the control software to begin collecting data from the multichannel analyzer. A decay time of 2.9s also significantly reduces the contribution of uncertainties in timings to the overall error in the DNC system.

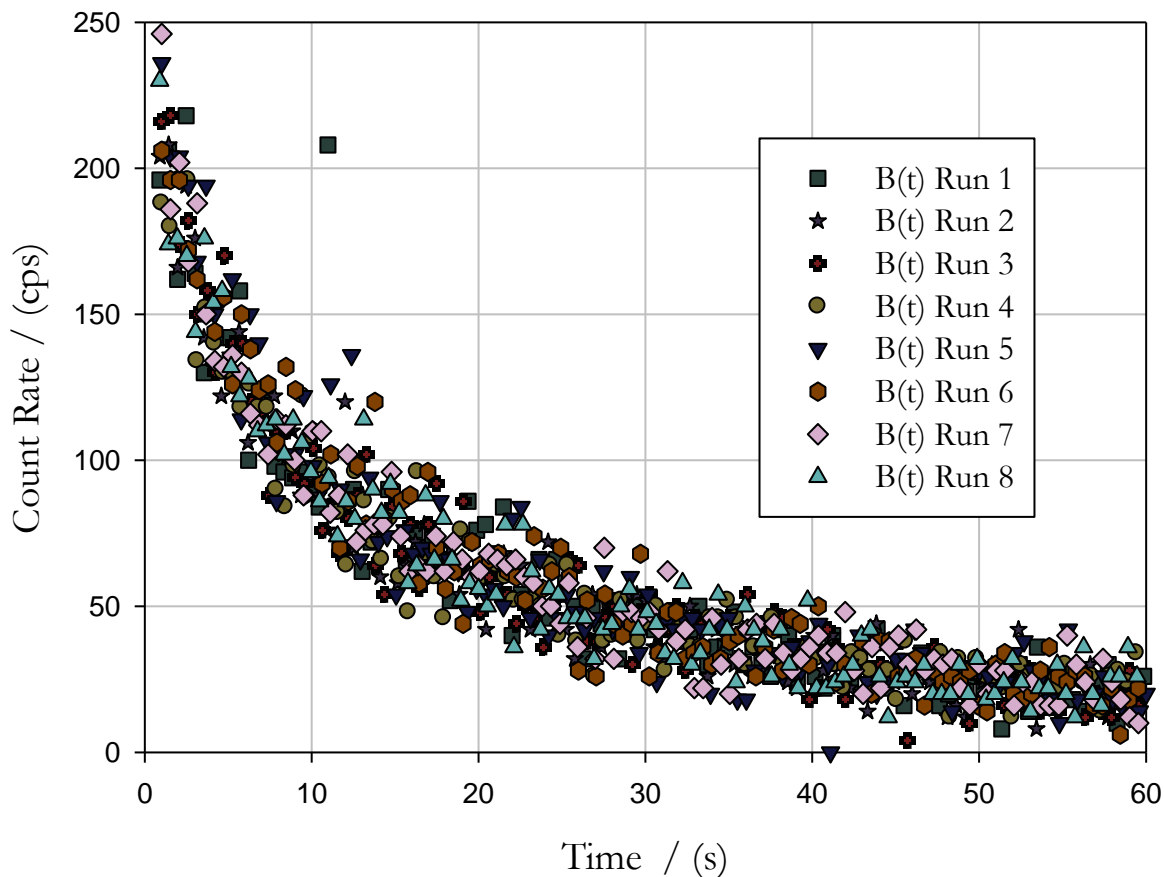


Figure 5-4: Consistency of Vial Counts, $B(t)$, Over Several Runs

The background resultant from the presence of the vial, $B(t)$, remained statistically consistent for each individual vial and over a period of several days as shown in Figure 5-4. A comparison of the background count rate (3.8 ± 0.4 cps), Figure 5-2, and the vial count rates confirm a time dependent count rate resultant from the presence of the vials. $B(t)$ was found to be independent of total polyethylene mass, Figure 5-5, indicating the source of delayed neutrons may be dependent on the surface area of the capsules and not the polyethylene mass. The repeated experimentation of the same vials confirmed the polyethylene vials used to transport DNC system samples can withstand many irradiation and counting cycles.

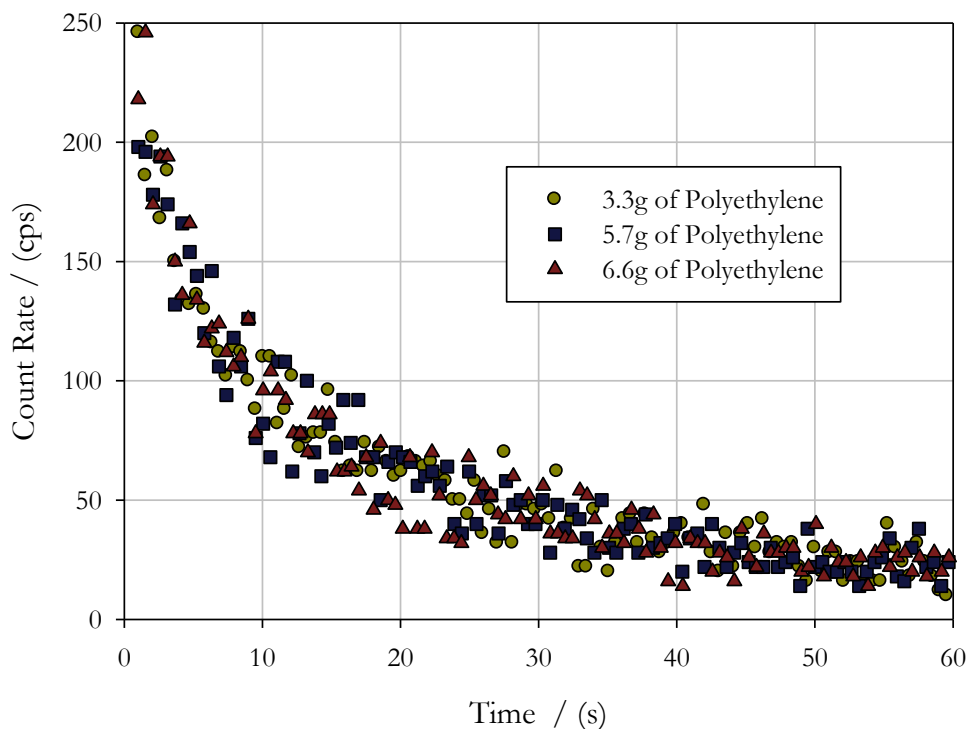


Figure 5-5: Selected Data Showing $B(t)$ Independence of Total Vial Mass

The background count rate in another SLOWPOKE-2 inner irradiation site not used for delayed neutron counting (site 3) was recorded for comparison purposes. The DNC system tubing leading from the manual loader was removed from site 5 and transferred to site 3, thus all DNC parts were used in an identical manner to regular operation. Twenty four polyethylene vials were prepared with total polyethylene mass ranging from 3.3g to 6.6g and were irradiated in site 3 and counted. All vials irradiated in site 3 had an equivalent count rate to the background count rate in site 3, 3.8 ± 0.4 vs. 3.7 ± 0.3 counts per second. Figure 5-6 illustrates the comparison of SLOWPOKE-2 sites 3 and 5 for the background, 3.3 g PE vial and 6.6 g PE vial count rates. The background contributions in site 3 in the presence and absence of the polyethylene vials were identical, indicating the vial dependent background contribution $B(t)$ was isolated to the site used for the DNC system. A ^{235}U sample (not shown in Figure 5-6) was also analyzed in site 3 to ensure that the electronics of the DNC were functioning in a manner that was consistent between the two sites.

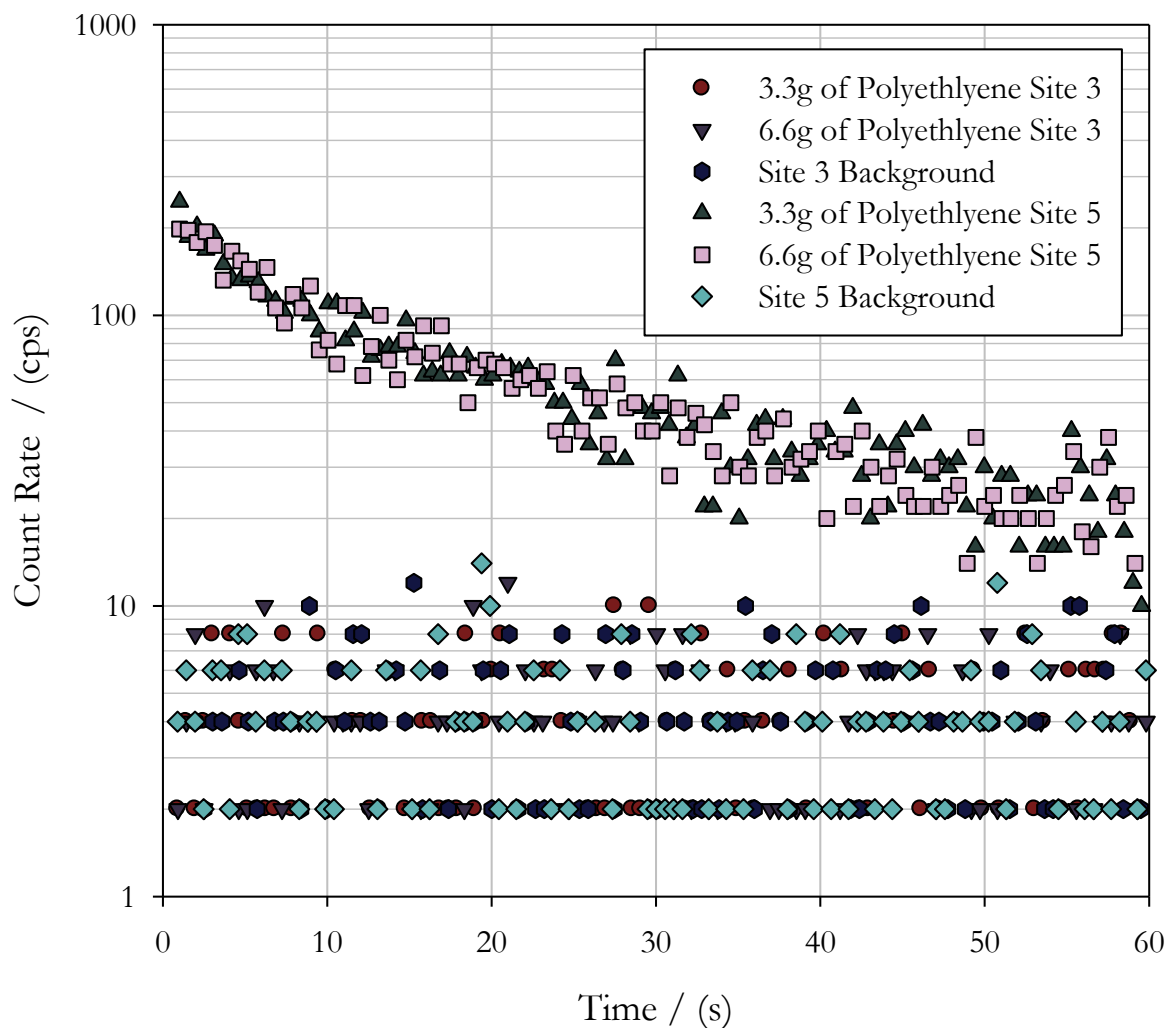


Figure 5-6: $B(t)$ Site Dependence

$B(t)$'s independence of total polyethylene mass and site 5 isolation indicated that the vials may be coming into contact with some form of contaminant during their travels in the site 5 irradiation tubing, which contributes to the overall neutron count rate. A similarity between the shape of $B(t)$ and that of the count rate of small amounts of ^{235}U was observed and were compared as shown in Figure 5-7. The vial and background contribution to count rates in Eq. (3-13) were subtracted and the resulting $S(t)$ was compared to $B(t)$. As illustrated in Figure 5-7, the similar trend in the $B(t)$ curve, indicates that the source of contamination was ~ 100 ng of ^{235}U for this particular

run. The amount of contamination deposited on the PE vials during their transport was found to vary over the period of experimentation reaching maximum levels equivalent to ~ 120 ng of ^{235}U .

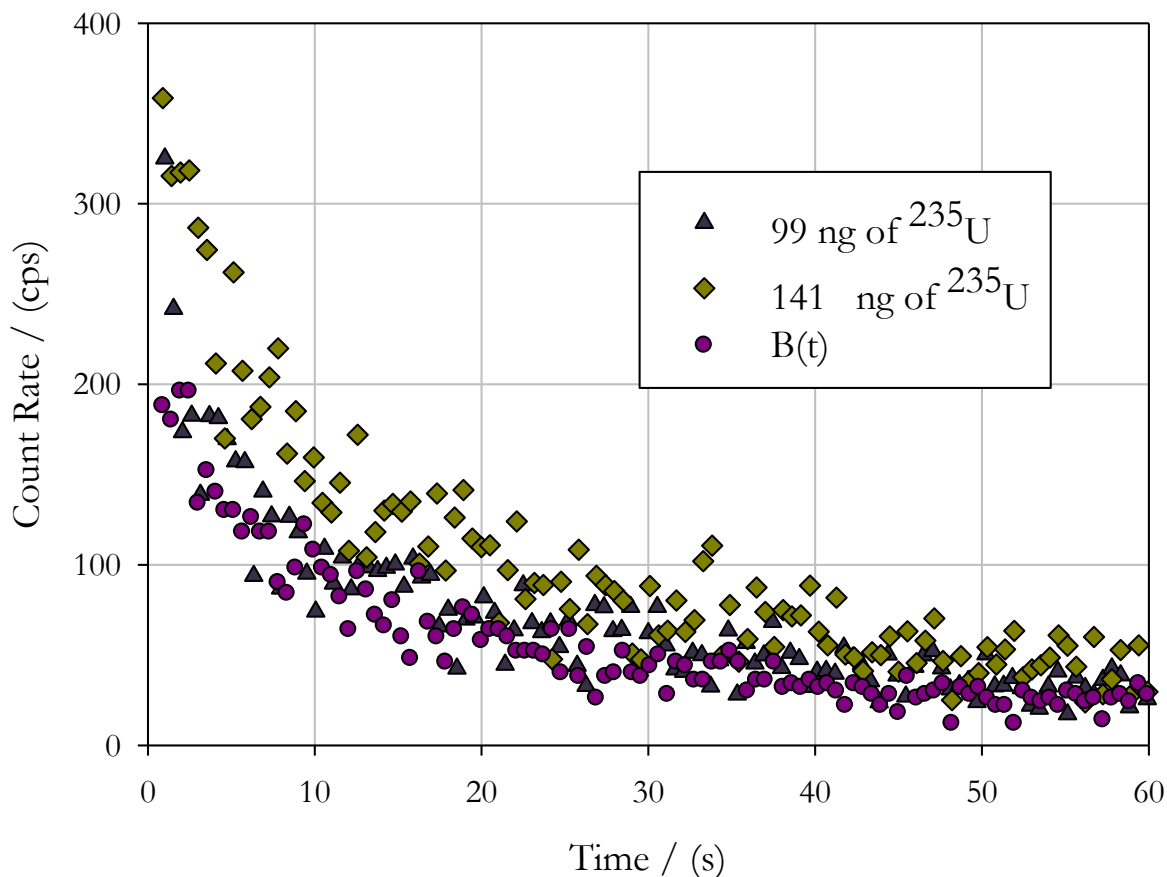


Figure 5-7: $B(t)$ Comparison to ^{235}U Experiments

Several experiments were completed with varying irradiation times to examine their effect on $B(t)$. Figure 5-8 shows selected data sets and the theoretical behaviour of ~ 100 ng of ^{235}U after a 10s and 60s irradiation duration. This comparison of theoretical and experimental values further indicated ^{235}U was indeed the source of contamination and was deposited on the vials during their transport. Considering the source of ^{235}U , contamination post-irradiation can be excluded since this material would not contribute to fissioned ^{235}U . A time dependence of the background contamination is observed. Any uranium located within the irradiation site would reach a secular equilibrium between fission and daughter decay. Since, it may be reasonably assumed that residence time within the irradiation site is irrelevant to the amount of ^{235}U that could be physically transferred

from irradiation site to vial, physical transfer of ^{235}U at irradiation site does not occur. Consequently, two mechanisms can be postulated. A body of ^{235}U may be resident at the irradiation site. Fission and subsequent daughter recoils would embed delayed neutron precursors in the vials in a time dependant manner. Alternatively, uranium transfer to the vial pre-irradiation (e.g., during sample transport) would add to the total fissile mass and undergo fission and delayed neutron production in an equivalent manner to ^{235}U within the sample. These mechanisms may only distinguished by further experimentation, specifically the determination, or absence, of surface uranium contamination.

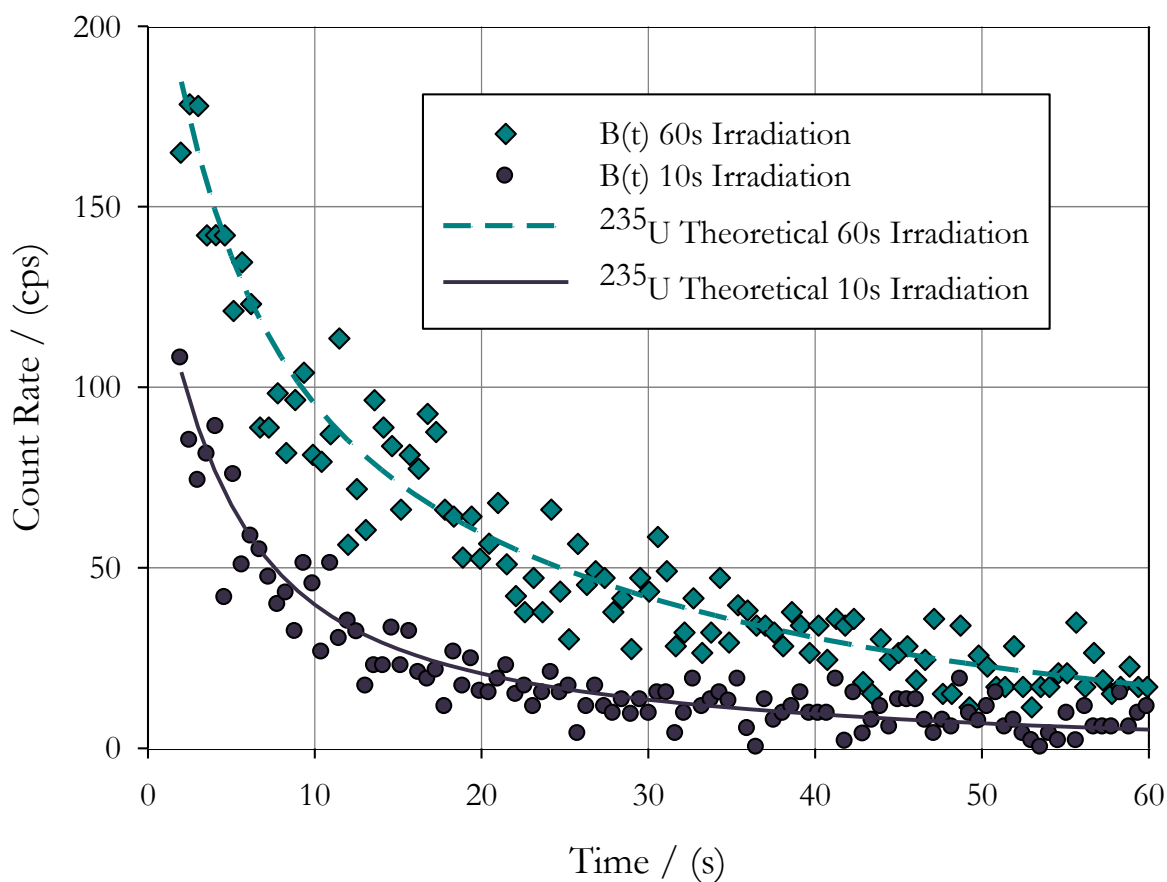


Figure 5-8: The Effects of Irradiation Time on $B(t)$

Contamination Quantification through the Fissile Analysis Program

The excess ^{235}U in the system transport system discussed in Section 5.2 contributes a significant background to the overall delayed neutron count rate. This contribution can be quantified by the fissile analysis program. The contamination on each vial was determined by irradiating blank vials under typical DNC system settings and recording the delayed neutron count rates. These count rates were then analyzed by the fissile material analysis program, which quantified the amount of ^{235}U present on the vials when they entered the counting arrangement. Figure 5-9 shows the consistency of the background contributions from the PE vials and the fissile analysis program's theoretical fit. The polyethylene vials in this particular trial were determined to be contaminated with 120 ± 3 ng of ^{235}U after each blank was analyzed in the fissile analysis program for the trial runs in Figure 5-9.

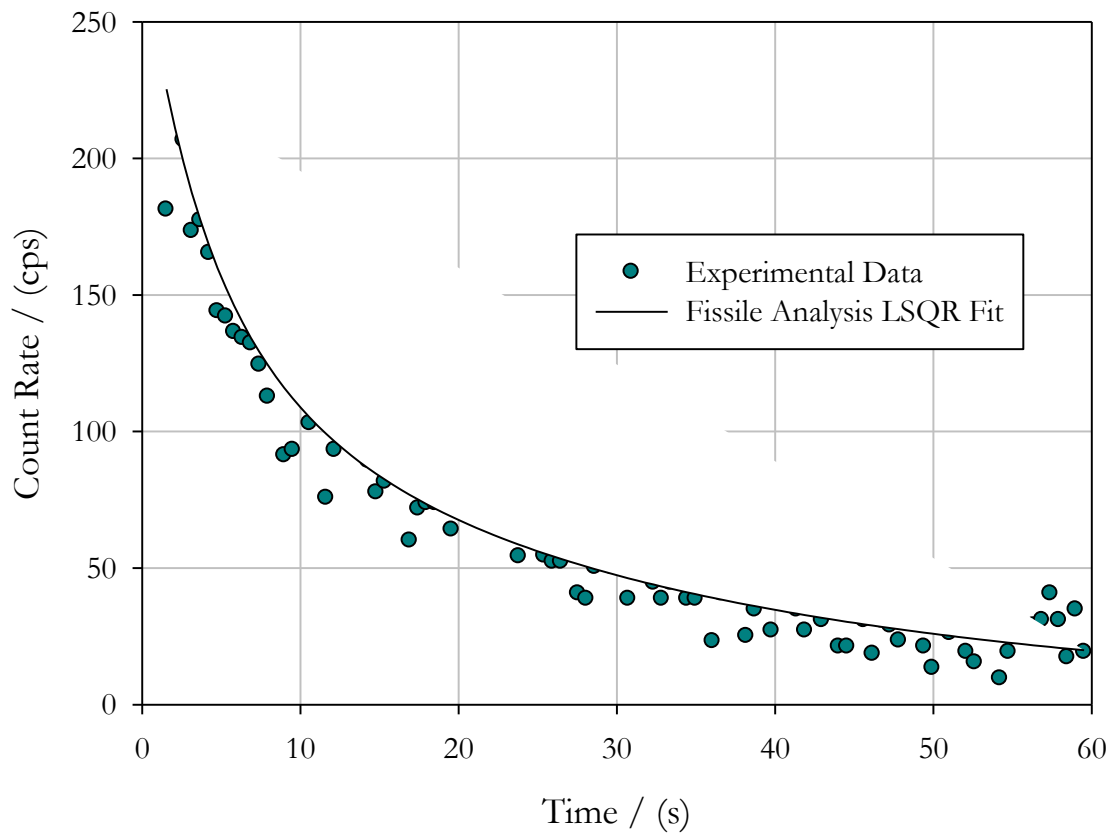


Figure 5-9: The Fissile Analysis Program Least Squares (LSQR) Fit to $B(t)$

While the consistency of the background uranium contamination did not vary over a period of a run consisting of eight to sixteen samples; it was found to steadily decrease over time. This discovery highlighted the requirement for a blank run for each ^{235}U determination in the system for accurate results. Samples which were analyzed with an unknown or inaccurate background contribution were found to display a mass-dependent bias. For example, the fissile analysis of the experimental count rate in the presence of higher background contamination were found to overestimate the total ^{235}U content in smaller samples. Additional measures should also be taken to ensure that there is minimal uranium contamination. These should include proper sealing of samples, resealing of samples if new data must be collected, and confirmation of the structural integrity of vials before samples are placed into the manual loader.

System Background Reduction Verification

In an attempt to reduce the magnitude of $B(t)$ in hope of lowering the detection limit of the DNC, system site 5 was cleaned and a significant amount of contaminant was removed. There was a disturbance to electrical equipment during this work, which affected the efficiency of the pre-amplifier connection. This was confirmed by the calibration set, which was as expected independent of ^{235}U content. It should also be noted that some of the electrical equipment in the DNC system, particularly the pre-amplifier and multi-channel analyzer instruments, are quite outdated and their replacement would likely reduce dead time effects and inconsistencies in data collection. As previously mentioned several blank polyethylene vials were examined in this trial to observe any effects from the cleaning of the inner lining of site 5 on $B(t)$. Figure 5-10 shows data collected before and after site 5 was cleaned.

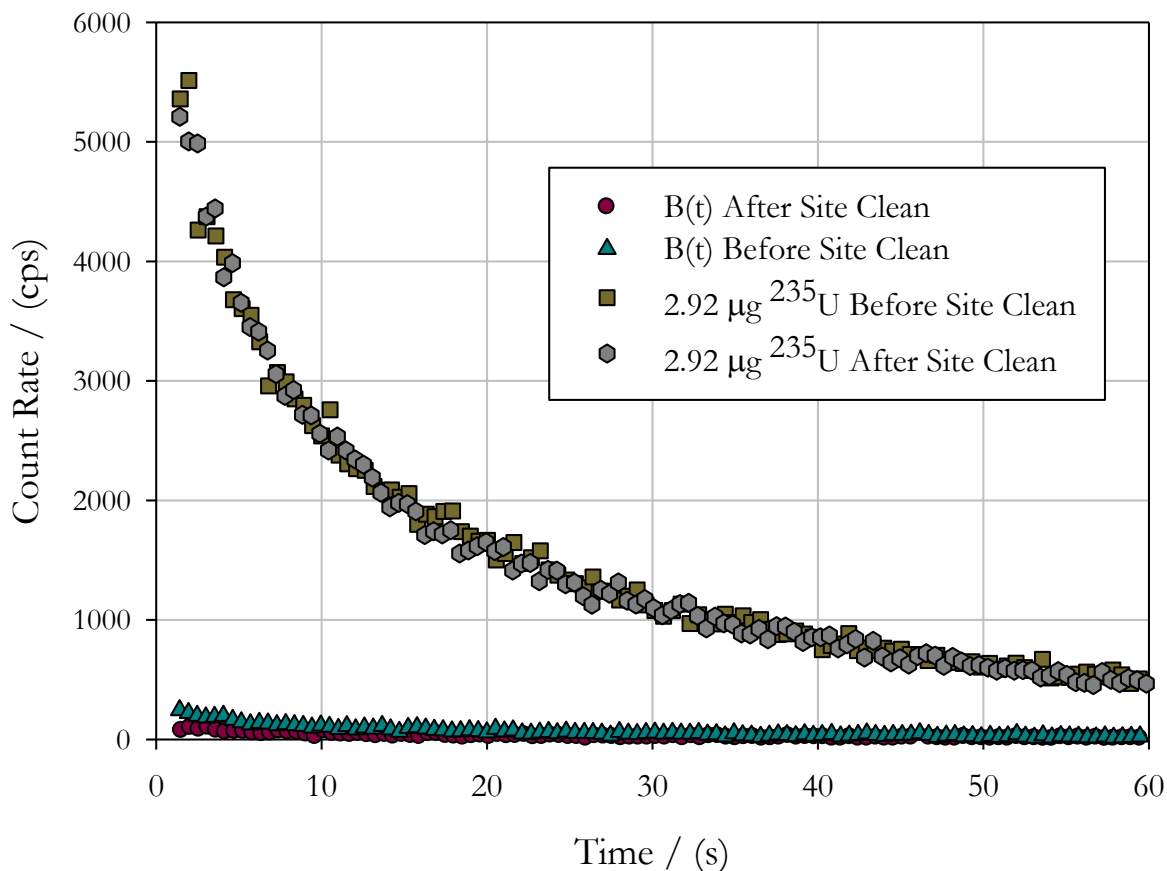


Figure 5-10: Comparison of 2.92 µg ²³⁵U in Site 5 before and After Cleaning

The data collected after site clean up have been normalized to account for the very slight differences in system efficiency. Two samples containing 2.92 µg of ²³⁵U prepared from the same solution were analyzed before and after the site cleaning to confirm the consistent behaviour of the system electronics. $B(t)$ was subtracted from each standard and the magnitudes were compared and normalized. This normalization was applied to $B(t)$ as well. The vial contributions, $B(t)$ are shown in more detail in Figure 5-11 and imply that cleaning site 5 had a significant effect on the magnitude of uranium contamination. $B(t)$ was quantified using the fissile analysis program to be approximately 50 ng of ²³⁵U, a significant reduction from previous maximum levels ~120 ng.

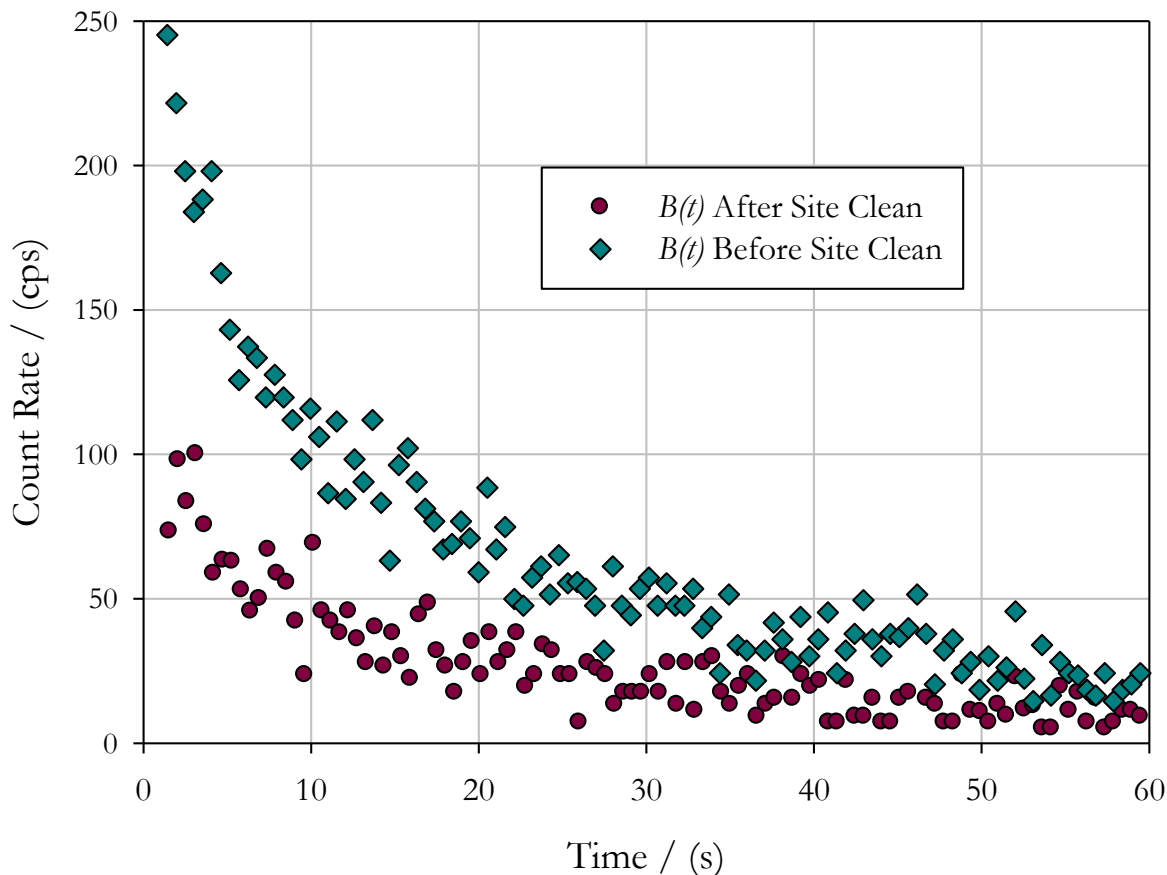


Figure 5-11: Comparison of Contamination in Site 5 before and After Cleaning

Additional Background Considerations

Experimentation using a 37 kBq multiple radionuclide gamma ray spectrometry source (Eckert and Ziegler) in direct contact with a ^3He detector used in the DNC system resulted in a background count rate of 4.7 ± 0.3 counts per second, which was indistinguishable from the immediately recorded background in the absence of the source of 4.9 ± 0.5 counts per second. The higher than normal background count rate can be attributed to the removal of the detector from the paraffin arrangement. The lack of paraffin moderator and the external metal container likely exposed the detectors to a higher background contribution. Multiple comparisons of irradiated empty polyethylene vials, vials filled with 2% nitric acid solution and those filled with sucrose displayed no

significant differences indicating that the possible interferences from the fast neutron reaction $^{17}\text{O}(n,p)^{17}\text{N}$ is minimal for samples containing small amounts of oxygen.

5.3 Characterizing the DNC System

Proper characterization of a delayed neutron counting system entails determining the efficiency of the system, the behaviour of the system dead time, and whether the dead time has significant effects on the experimental data collected by the apparatus. This section discusses the process by which dead time effects were quantified using the two source method and subsequently validated with experimental DNC data. The dead time correction was then used to determine the system efficiency, and the results were compared to a theoretical model.

DNC System Dead Time Determination

Experimentation using the two-source method was performed with samples containing ^{235}U and therefore recorded delayed neutron activity with a short half life. The mass of each sample and the dead time determined from the two source method, Eq. (3-11), are summarized in Table 5-2. Recall from Section 3.3, for the two source method s_x has half the mass of ^{235}U as s_y . The background was determined by counting a blank vial under identical experimental conditions. The dead time was determined to be $40 \pm 1 \mu\text{s}$ and individual dead time behaviour was found to be independent of the mass of samples. A dead time of $40 \pm 1 \mu\text{s}$ is comparable to other delayed neutron counting systems [59, 60] and will result in significant effects at count rates higher than 500 cps as shown in Figure 5-12. It should be noted that ideal neutron sources for the two source method dead time determination should have a long half life. However, no appropriate long lived neutron sources were available at RMC for dead time determination.

Figure 5-12 assumes a non-paralyzable model with a dead time of $40 \mu\text{s}$ as this model is most commonly assigned to similar systems, values are displayed with $\pm 2\sigma$ uncertainties, for a 95% confidence level. The solid black line shows an ideal detection system with no dead time. The non-

paralyzable model is shown and it begins to deviate from ideal behaviour as count rates approach 500 cps. For example, when the system interacts with 10^4 counts per second (true count rate) it would only record ~ 7000 of the counts as shown in Figure 5-12. At 10^4 cps the detectors would be occupied $\sim 30\%$ of the time which is shown by the dashed dead time losses line also in Figure 5-12.

Table 5-2: Sample Results for Dead Time Determination (2σ uncertainties)

Set	^{235}U Mass (μg)	Total Counts	τ (μs)
Ay	4.27 ± 0.02	118619	
Ax	2.13 ± 0.02	64694	41
By	4.28 ± 0.02	120368	
Bx	2.14 ± 0.02	65053	39
	Average		40 ± 1

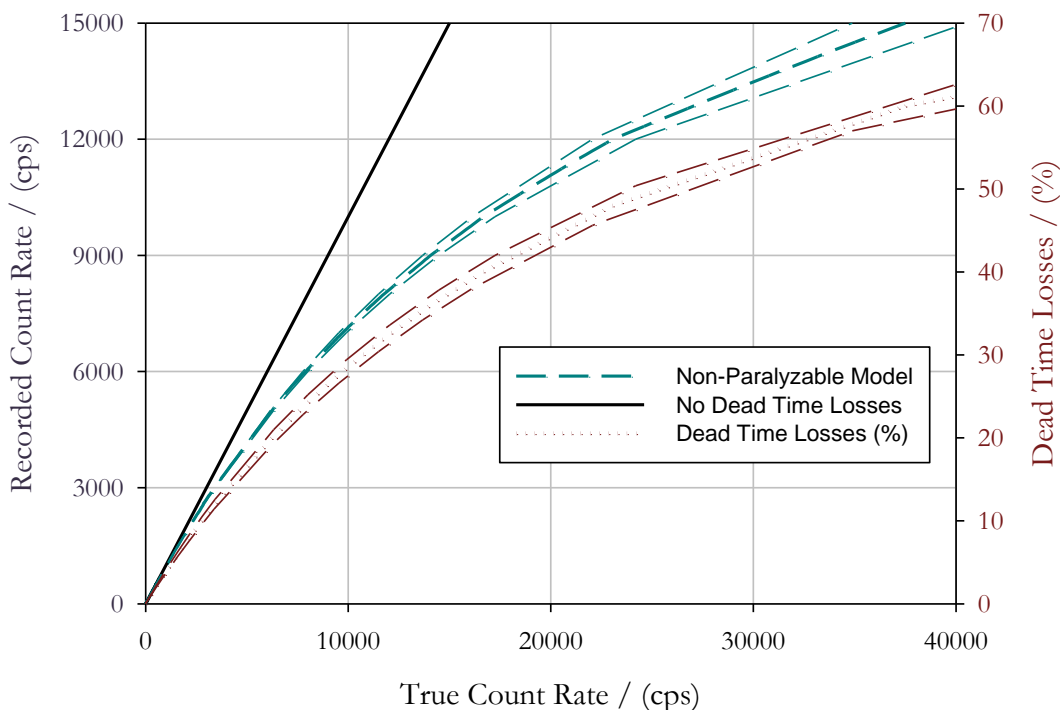


Figure 5-12: Recorded Count Rates and Dead Time for Non-paralyzable System

Efficiency Determination

A simple Monte Carlo N-Particle (MCNP5) [61] model was created to approximate the geometric efficiency of the DNC system and can be found in Appendix C. This model assumed an isotropic neutron source and modelled just the surface of one detector. The code was very straightforward and assumed no medium between the neutron source and detector surface. It recorded the fraction of original neutrons that interacted with the detector surface. This number was then multiplied by the number of detectors in the DNC counter arrangement to determine a maximum geometric efficiency of $\sim 57\%$. This, of course, is an estimate as it does not account for the scattering and absorption processes of the neutrons in the medium separating the detectors in addition to other physical effects. As previously mentioned an intrinsic efficiency is expected to be in the range of 50 - 80% for the ^3He detectors in this system. Therefore, an absolute *maximum* efficiency in the range of 29 - 46% was calculated using Eq. (3-5) for the DNC system detector arrangement used in this work.

The efficiency of the system was determined experimentally by analyzing samples containing known amounts of ^{235}U and using the dead time values found in the previous section. The non-paralyzable dead time model was used to correct experimental count rates. Only count rates less than 1000 cps were analyzed as the counts lost contributed only 4.1% of the total counts and any deficiencies in the non-paralyzable correction would be small. Eight samples of known ^{235}U content were analyzed to determine a system efficiency of $34.2 \pm 0.4 \%$, which was found to be independent of fissile mass as shown in Figure 5-13. The actual uncertainty in system efficiency is dependent on uncertainties in thermal neutron flux, sample mass, timings, and the least squares method determination and therefore an overall system efficiency value of $34 \pm 5 \%$ is more accurate. This efficiency was consistent with the one estimated by the MCNP5 model and manufacturer specifications. Since background contributions were neglected at this time, the identified efficiency probably contains a small, but systematic, overestimation.

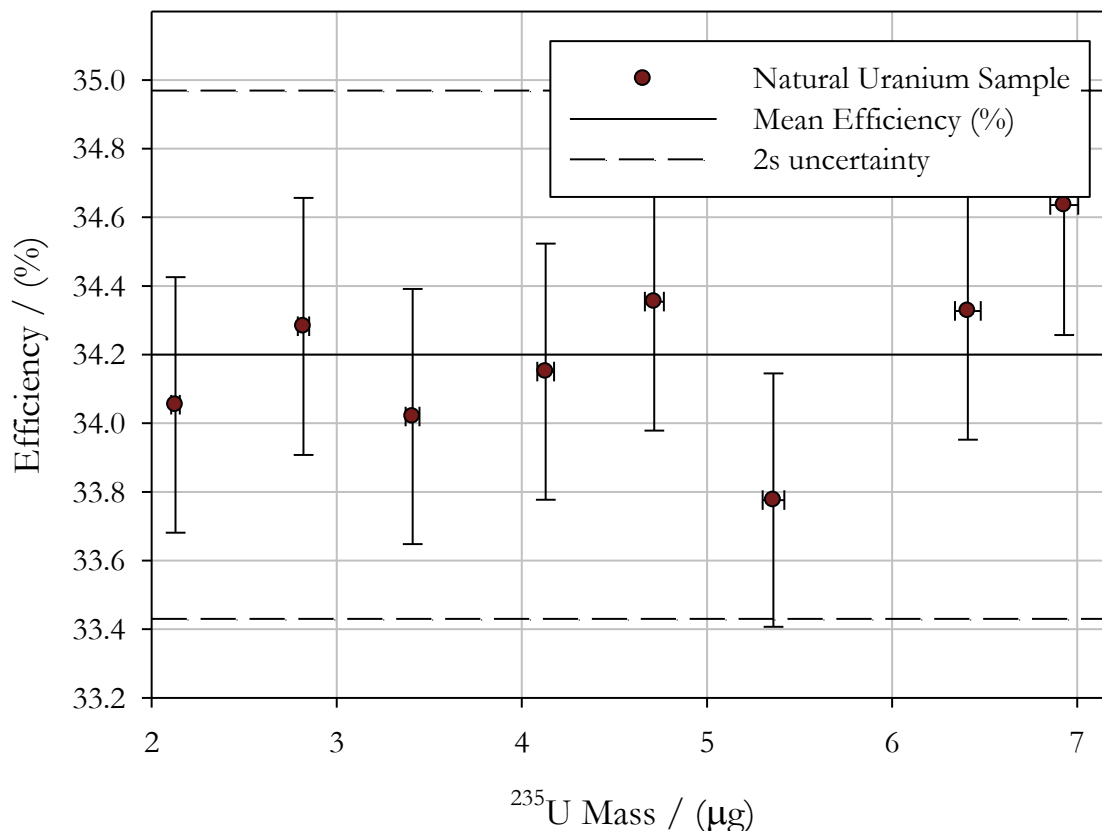


Figure 5-13: Efficiency Independence of ^{235}U Mass with 2σ Uncertainties

A Comparison of Theoretical & System Count Rates

The background and vial contributions to the overall count rate, system efficiency and electrical dead time values determined in Section 5.3 were used alongside Eq. (3-12) for comparison purposes. An analytical dead time correction using Eq. (3-14) and the determined dead time value of $40\ \mu\text{s}$, was found to be inadequate at higher system count rates as shown in Figure 5-14, and in semi-log format in Figure 5-15. An empirical dead time correction, Eq. (5-1) was determined from the experimental data of eight samples ranging from 1.5 to $6.8\ \mu\text{g}$ of ^{235}U . The empirical fit compared experimental and theoretical results, determined a parabolic fit, and is also shown in Figure 5-14 and Figure 5-15. The theoretical count rate (true) is also shown in the following Figures and denoted as the black curve. The empirical fit shown in Eq. (5-1) corresponds to a non-paralyzable dead time of

$\sim 33 \mu\text{s}$. When this dead time constant is compared to the experimentally determined $40 \mu\text{s}$ it is a better fit to the theoretical count rate for each sample, further indicating a longer lived neutron source should have been used in the two source method. The fissile analysis program uses the empirical fit for dead time corrections to experimental data to achieve the most accurate true count rates possible.

$$C(t)_{true} = (3.3 \pm 0.6) \times 10^{-5} C(t)_{actual}^2 + (1.03 \pm 0.03) C(t)_{actual} \quad (5-1)$$

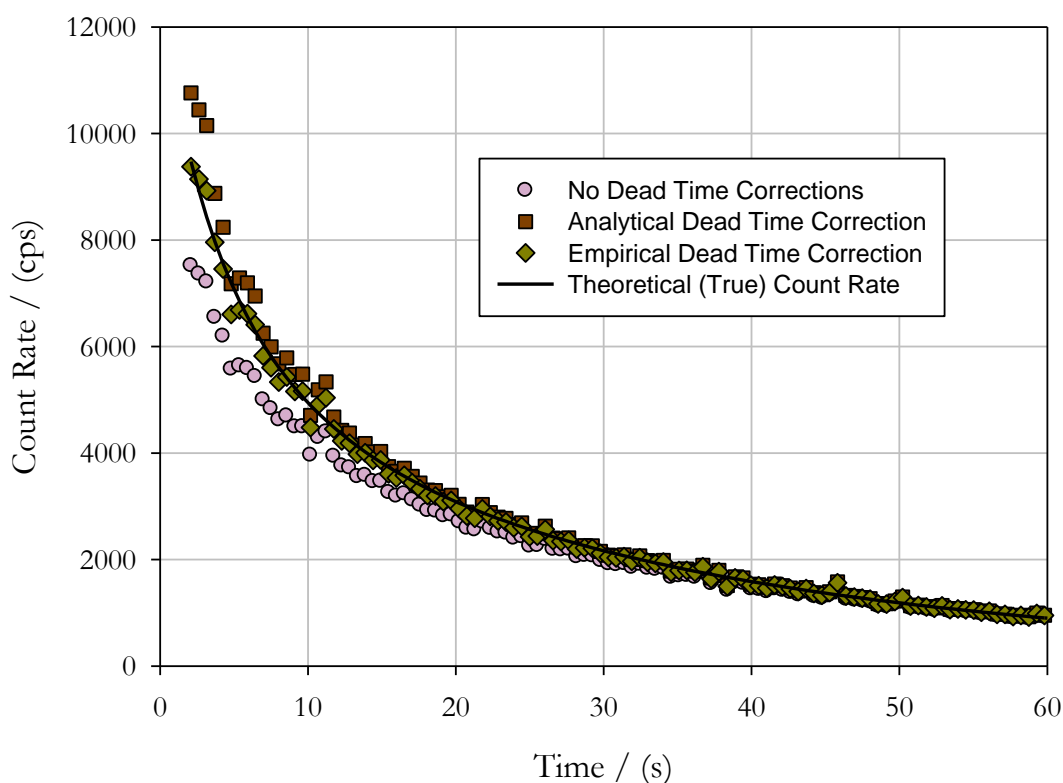


Figure 5-14: A Comparison of Analytical ($40 \mu\text{s}$, non-paralyzable), Empirical and No Dead Time Models

The example in Figure 5-14 shows that for higher count rates the analytical model determined by the two source method (orange squares) tends to overestimate the true values at higher count rates. As previously discussed, when dead time losses are great it is difficult to model them analytically. The empirical correction in Eq. (5-1) appears to accurately predict true count rates over a large range. Figure 5-16 shows that the empirical fit is an accurate and unbiased model even

as true count rates approach 10^4 cps as the ratio of the empirical fit and true count is close to one (1) for a range of counting rates.

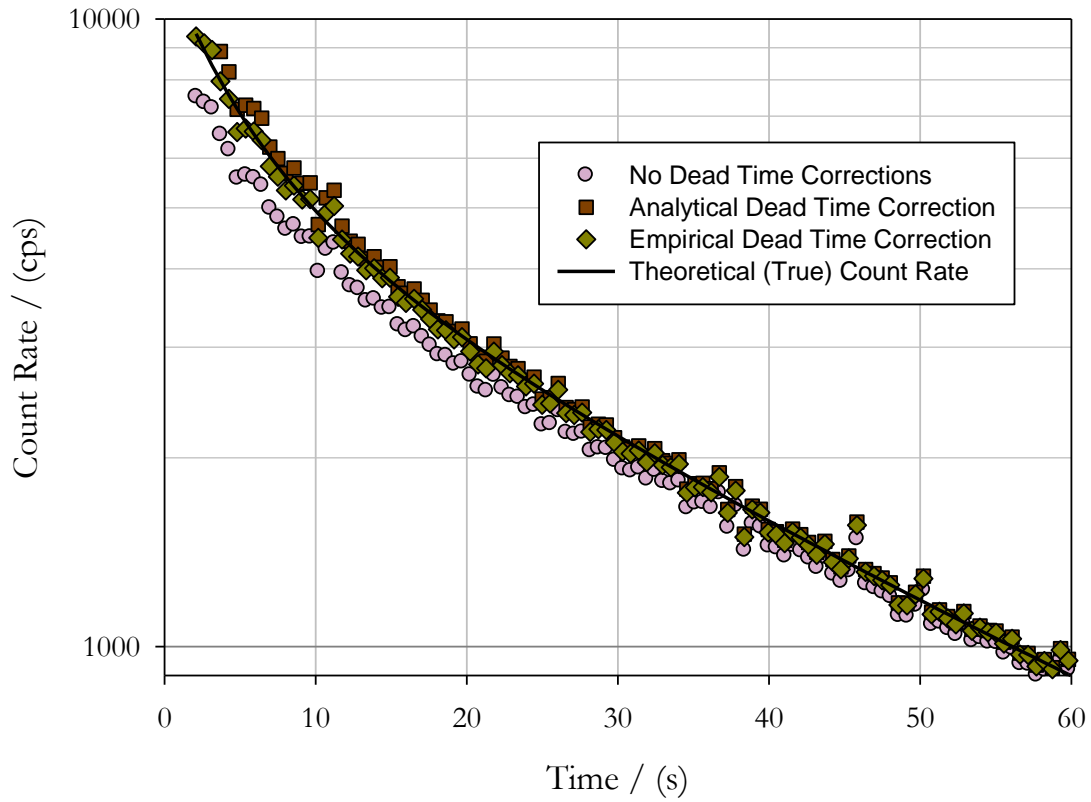


Figure 5-15: A Semi-log plot comparing dead time corrections.

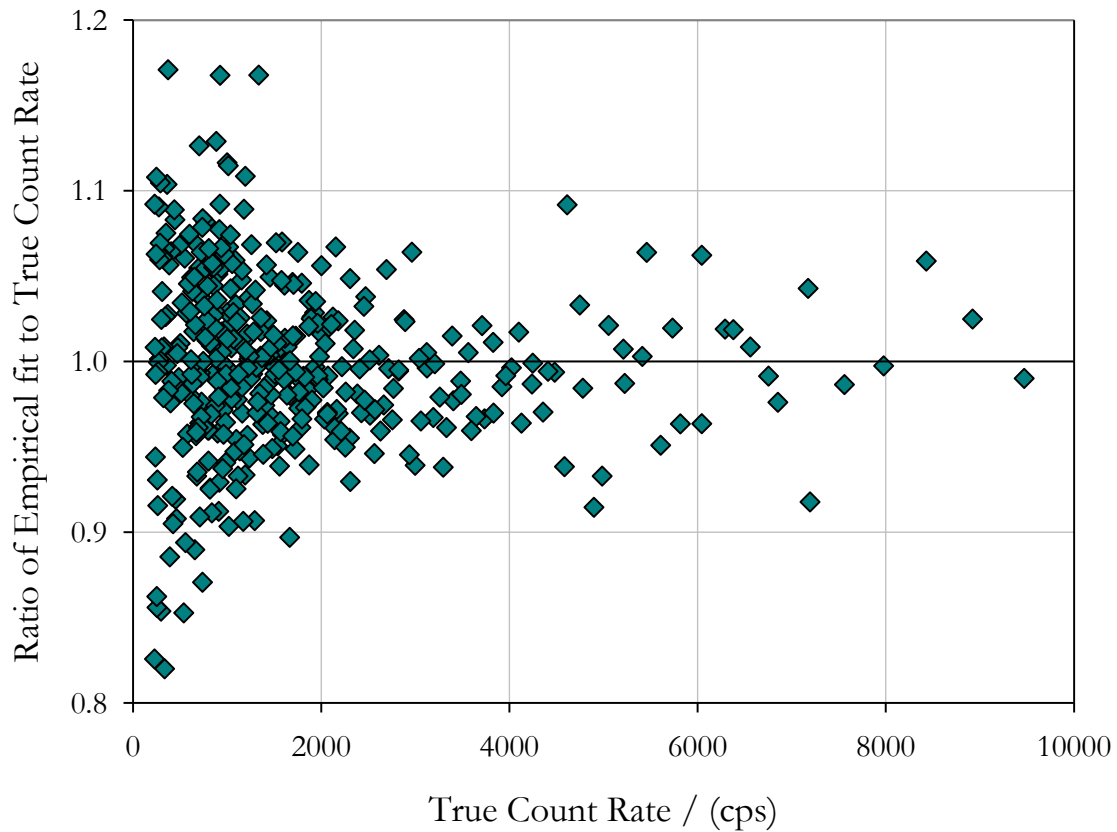


Figure 5-16: The Ratio of Empirical Fit to True Count Rate for Nat. U Samples

5.4 Validating the Fissile Analysis Program and DNC System

Fissile Analysis Program Fit to Experimental Data

The most important aspect of the fissile analysis program is its ability to determine fissile content using the time dependent count rate, Eq. (3-12) as this will be necessary when analyzing samples containing two or more of ^{239}Pu , ^{235}U or ^{233}U . After the DNC system efficiency and dead time were characterized as shown in Section 5.3, they were input into the system structure shown in Figure 4-4. The fissile analysis program then used the variable parameters including irradiation and decay timings and thermal neutron flux, which were either supplied by the user at the time of analysis or

hard coded into the program. Two examples of the least squares fit to the modified raw data from the DNC executable output and Eq. (3-12) are shown below in Figure 5-17.

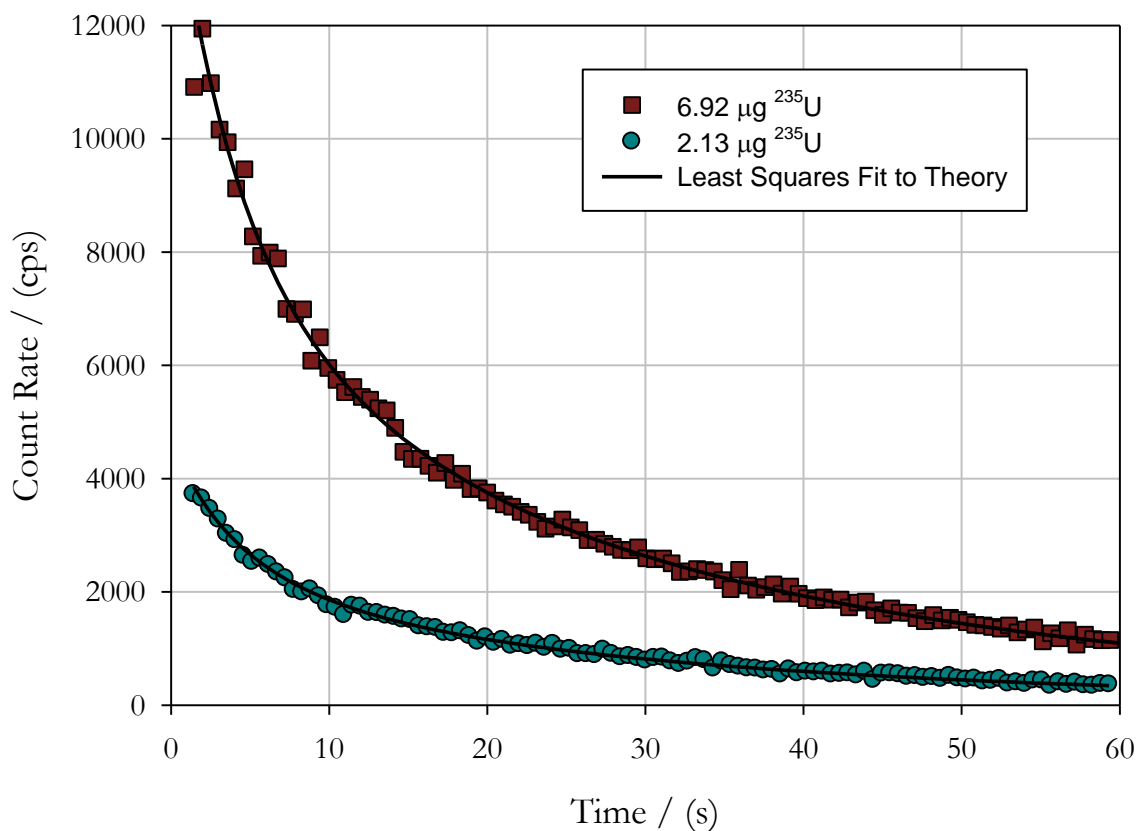


Figure 5-17: The Fissile Analysis Program Least Squares fit to Experimental Data

The precision of the data presented in Figure 5-17 are representative of all data analyzed from this set of 8 samples. All experimental data analyzed with the fissile analysis program were found to have a high degree of precision indicating the dead time experienced by the electronics and the system is efficiency and effectively characterized.

Validating the Reproducibility of the Results

The consistency of the DNC system output was compared to actual ²³⁵U mass using eight sets of eight samples containing natural uranium dissolved in a nitric acid/distilled water solution.

The efficiency determined in Section 5.3 was used in the analysis of additional sets of as shown in Figure 5-18. This figure shows the relationship between actual ^{235}U mass and DNC output with 2σ uncertainties on both the actual fissile mass amount and the DNC system output. The relationship between actual ^{235}U amounts and DNC system output was found to be highly reproducible as shown in Table 5-3. The reproducible slope of one implies that the technique is accurate.

The outlier with an actual mass $\sim 4.7 \mu\text{g}$ and a DNC determined mass of $\sim 3.8 \mu\text{g}$ shown in Figure 5-18 could be the possible source of contamination previously discussed in Section 5.2. After this DNC system was found to underestimate grossly the total ^{235}U content present in this sample it was visually confirmed that the solution was not the nominal 1 ml quantity originally prepared. It is very likely this solution leaked in the SLOWPOKE-2 irradiation site 5 and is the source of ^{235}U contamination. This hypothesis was further supported when the outlier passed the rejection quotient discussed in Appendix D.

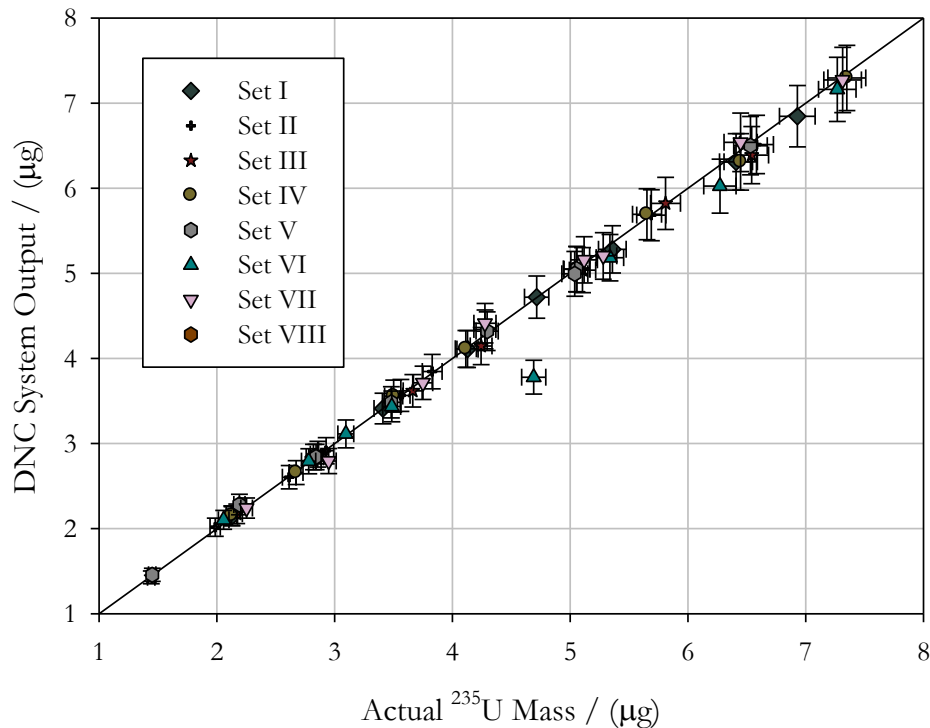
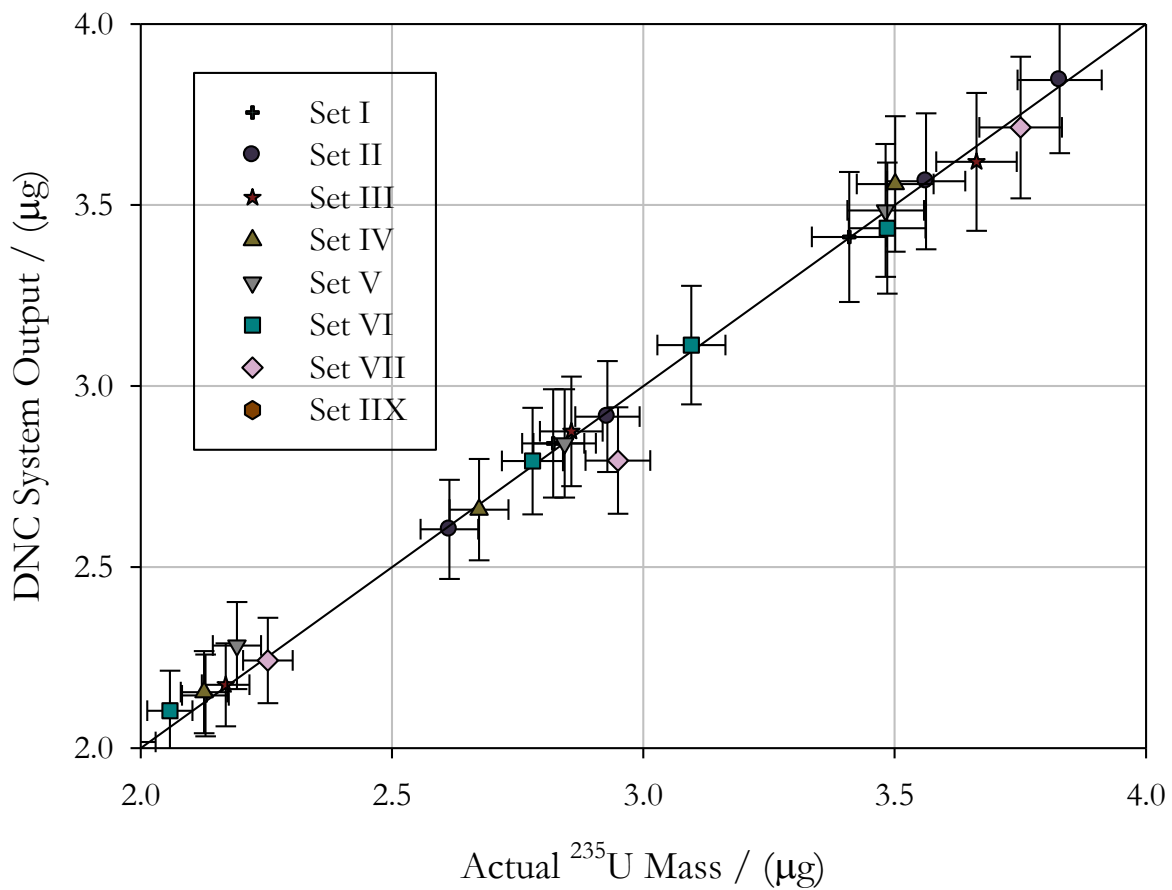


Figure 5-18: Comparison of Count Consistency for Eight Sets

Table 5-3: Consistency of DNC System Output

Set	Slope (2σ uncertainty)	Y-Intercept (μg) (2σ uncertainty)
I	0.98 ± 0.01	0.08 ± 0.04
II	0.96 ± 0.08	0.1 ± 0.4
III	1.00 ± 0.02	-0.02 ± 0.06
IV	1.0 ± 0.1	0.04 ± 0.06
V	0.98 ± 0.01	0.08 ± 0.04
VI	0.96 ± 0.08	0.1 ± 0.3
VII	1.00 ± 0.02	0.0 ± 0.1
IIX	0.99 ± 0.01	0.04 ± 0.06

**Figure 5-19: Detailed Comparison of Count Consistency for Eight Sets**

Verifying the Calibration with Depleted Uranium

The calibration data from the natural uranium samples were used to determine the ^{235}U content of depleted uranium samples as shown in Table 5-4. The amount of ^{235}U determined by the fissile analysis program and DNC system was a consistent underestimation. The error is such that individual results may not be considered statistically different from the target value. However, in the context of the overall dataset, it is evident that the measured values are systematically lower than those expected. Although several sources of this systematic error are possible, it is plausible that one of the largest sources of uncertainty in the ^{235}U determination is from the preparation and dilution of the CRM (certified reference material) samples. Concerns relating to the possibility of epithermal ^{238}U fissioning contributing to the overall delayed neutron count are also addressed by a comparison of the relative errors in Table 5-4. If ^{238}U delayed neutron production were happening in significant quantities this would result in an overestimation of ^{235}U in depleted uranium (DU) samples as the DU sample's ratio of $^{238}\text{U}/^{235}\text{U}$ is higher than natural uranium. Another large source of error is the contribution of $B(t)$ to the overall count rate, if the background contribution is improperly characterized it will result in inaccuracies, particularly for samples with small amounts of fissile material.

Table 5-4: Challenging DNC Calibration with Depleted Uranium (2σ Uncertainty)

Sample	Actual ^{235}U	DNC System ^{235}U	Relative Error
	Mass (μg)	Determination (μg)	
1	5.52 ± 0.06	5.3 ± 0.4	-3.45%
2	5.56 ± 0.06	5.3 ± 0.4	-5.35%
3	5.50 ± 0.06	5.3 ± 0.4	-3.01%
4	5.56 ± 0.06	5.3 ± 0.4	-4.32%
5	5.53 ± 0.06	5.3 ± 0.4	-4.78%
6	5.62 ± 0.06	5.4 ± 0.4	-4.45%
7	5.59 ± 0.06	5.4 ± 0.4	-4.24%
8	5.53 ± 0.06	5.3 ± 0.4	-4.47%

The Effects of Sample Volume and Geometry

The effects of sample volume and positioning in the SLOWPOKE-2 irradiation site and counter were examined using depleted uranium samples. The DU samples containing approximately 1.48 – 1.60 μg of ^{235}U were further diluted with varying amounts of HNO_3 and distilled water as shown in Table 5-5. The total solution mass was found to have no effect on the DNC system's ^{235}U determination. This suggests the DNC system may be capable of determining fissile content in a variety of matrices and this could be observed through further experimentation.

Table 5-5: Solution Volume Effects on ^{235}U Determination (2σ uncertainties)

Actual ^{235}U mass (μg)	Total Solution Mass (g)	Experimental Mass (g)	Relative Error (%)
1.54 \pm 0.04	0.290 \pm 0.003	1.5 \pm 0.1	-3.2
1.54 \pm 0.04	0.379 \pm 0.003	1.5 \pm 0.1	-3.2
1.54 \pm 0.04	0.568 \pm 0.003	1.5 \pm 0.1	-2.6
1.55 \pm 0.04	0.660 \pm 0.003	1.6 \pm 0.1	-0.6
1.53 \pm 0.04	0.819 \pm 0.003	1.5 \pm 0.1	-3.9
1.46 \pm 0.04	0.738 \pm 0.003	1.5 \pm 0.1	-1.4
1.59 \pm 0.04	0.943 \pm 0.003	1.5 \pm 0.1	-3.8

The default sample geometry was disturbed by placing sample vials in the DNC manual loader upside down. Loading the sample in this manner results in a displacement of approximately 2.5 cm in both the irradiation site and the neutron detection arrangement. Several samples were analyzed in their default position followed by a run in which they were loaded upside down. Figure 5-20 shows the neutron count rate for one sample as a function of time for four individual runs, two in the default position and two with the solution displaced. Each run was conducted on different days and were found to be independent of vial displacement. The relative differences at the commencement of the counting period result from timing uncertainties having a greater effect. The relative differences also increase as overall counts decrease and therefore smaller fluctuations have a significant effect. The indifference of experiments conducted with the samples displaced agrees with

work done by Andrews [51] who found the upper and lower portion of irradiation site 5 to be statistically identical.

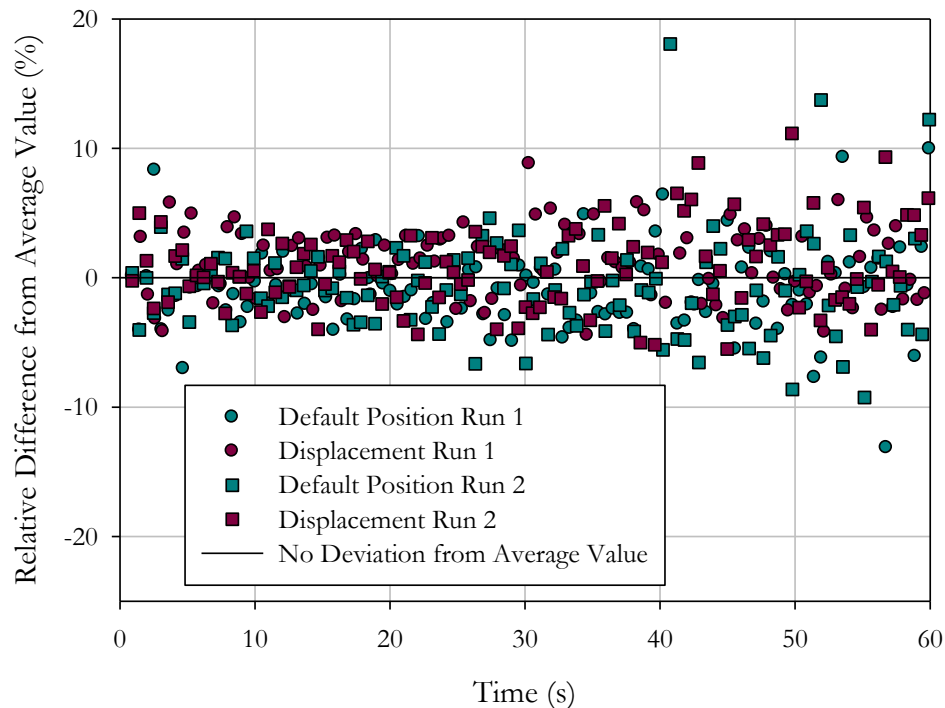


Figure 5-20: A Comparison of Displacement and Default Position Runs

5.5 The Experimental Determination of ^{235}U Content

After the characterization of the DNC system and its validation, four solutions containing different concentrations of ^{235}U were analyzed. The first solution contained 7.32 ppm ^{235}U was further diluted and used for calibration purposes to values ranging from $\sim 1\ \mu\text{g}$ to $7\ \mu\text{g}$ of fissile content. This was required to confirm the efficiency of the system and quantify dead time effects. There was a disturbance to the electrical equipment before these experiments, which was found to slightly affect the efficiency. The preamplifier appeared to be highly sensitive to changes in apparatus orientations.

After the background vial contribution was determined by the DNC and the new efficiency values found, several additional sets of samples prepared from different solutions were analyzed by the DNC system and the fissile analysis program. Figure 5-21 shows the DNC system output for all

samples with ^{235}U content ranging almost three orders of magnitude. The natural uranium solution was used as a calibration and is depicted in plot as squares. These samples were used to determine an efficiency value and dead time behaviour which was subsequently used in the ^{235}U determination of all other samples, including those with just nanogram quantities of ^{235}U .

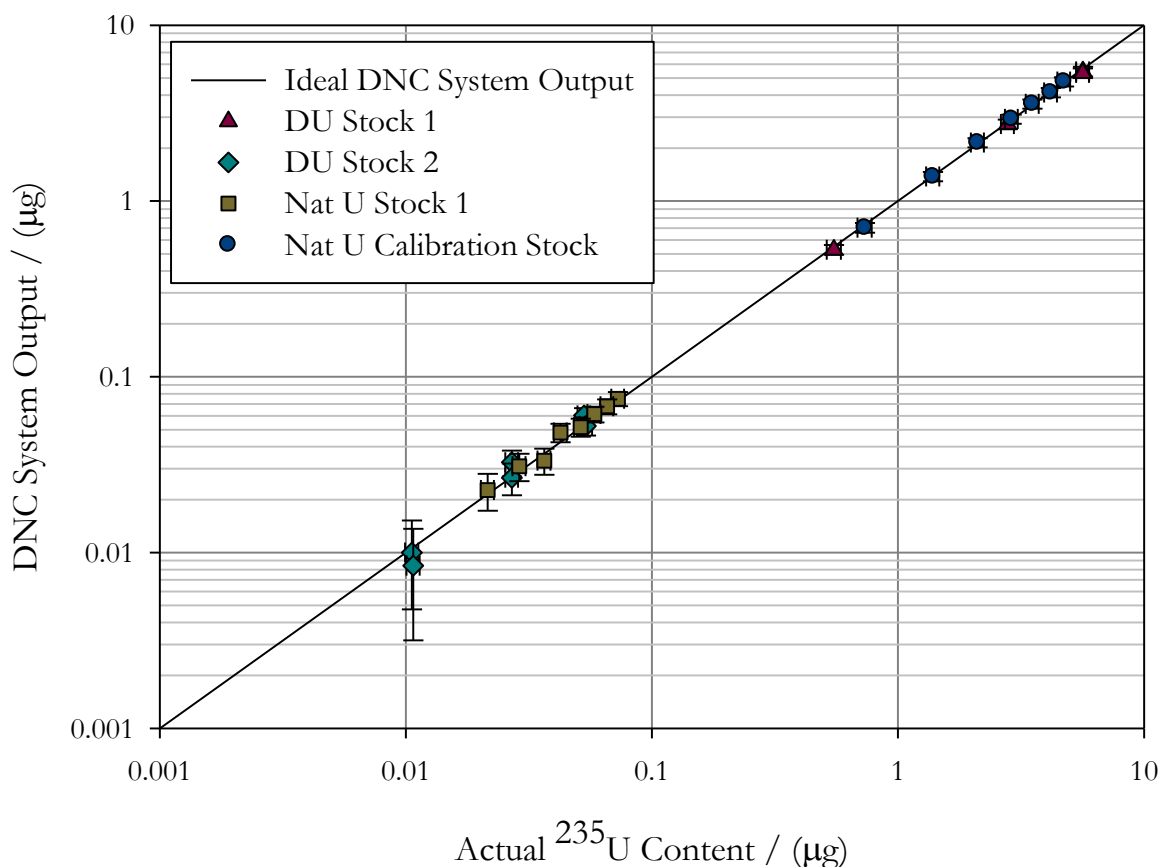


Figure 5-21: A Comparison of DNC Output for Natural and Depleted U Samples

The black line in Figure 5-21 shows ideal DNC system output and most sample ^{235}U determinations are within experimental uncertainty of this line. Figure 5-22 shows a close up of samples containing microgram quantities of ^{235}U . The DNC output for the depleted uranium samples in 5.4 ppm ^{235}U quantities are all within uncertainty of the actual values but are all have a slightly negative relative error. This is likely because of uncertainties in the ^{235}U content of the samples used for either the calibration or the depleted uranium samples as previously discussed. The average relative error for the 5.4 ppm depleted uranium samples was found to be -3.6% and

independent of total ^{235}U mass. This is consistent with previous experimentation with samples prepared from the same solution stock.

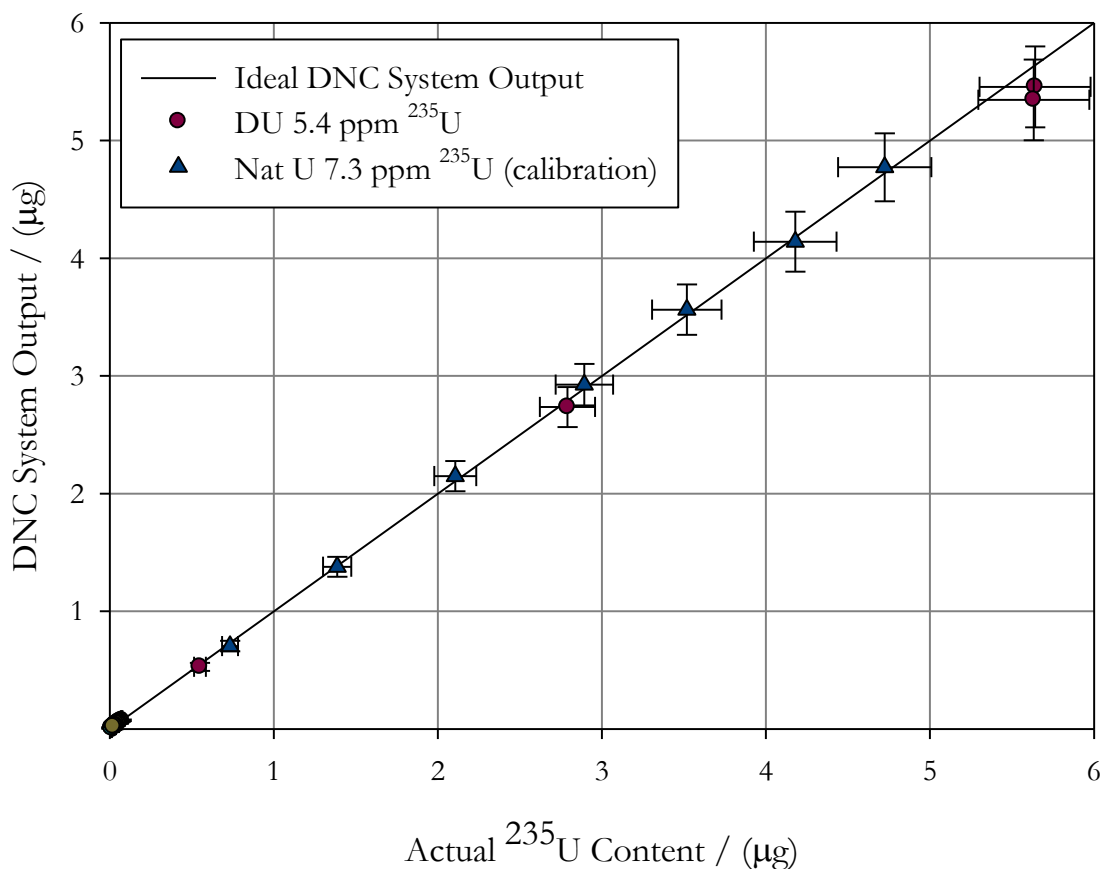


Figure 5-22: A Comparison of DNC Output μg Quantities of ^{235}U

Figure 5-23 shows the DNC system output for the final two sets of solutions containing depleted and natural uranium in 54 and 73 ppb quantities respectively. At such small ^{235}U amounts it is essential to properly quantify the background, $B(t)$, as this is a significant contribution to the overall count rate. Most ^{235}U values determined by the DNC system in the nanogram amounts were accurate indicating that calibrations performed with much greater amounts of ^{235}U are sufficient for the detection and quantification of small amounts of ^{235}U . The detection limit of the DNC system at RMC is 5 ± 1 ng of ^{235}U , the derivation of which can be found in Appendix D. It is expected the

detection limit and accuracy of the system could be significantly improved with a reduction the background signal, $B(t)$.

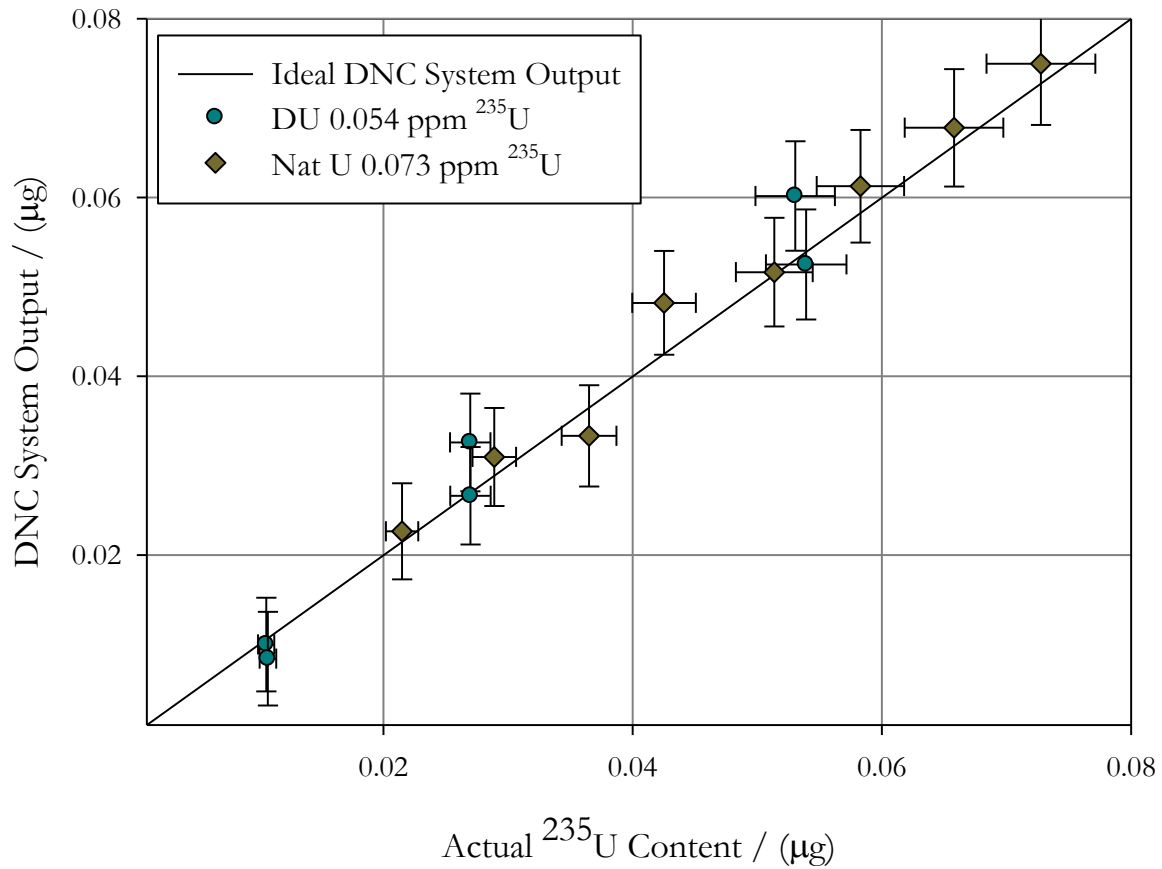


Figure 5-23: A Comparison of DU and Nat U in nanogram quantities

Chapter 6

Conclusions & Recommendations

6.1 Conclusions

The required software and hardware has been designed and installed to accommodate a DNC system for the analysis of SNM at RMC. This included a custom LabVIEW™ program that readily allows the modification of experimental parameters and efficient control of the system hardware and electronics. The DNC system hardware has been proven to be reliable and robust. It is able send samples to the SLOWPOKE-2 reactor and subsequently records their delayed neutron count rates as a function of time. These count rates are recorded for each sample and are read by another custom code, which is capable of accurately determining ^{235}U mass under variable experimental conditions.

Samples have been shown to withstand several irradiation/counting cycles with no visible degradation and have produced consistent count rates. The dead time effects of the system were quantified both by the two-source method and a comparison of theoretical count rate and non-paralyzable effects. The dead time has been accounted for in the analysis code by an empirical function, which has been proven to be an accurate model for count rates as high as 10^4 cps. The efficiency of the system has been determined by comparing the theoretical model with dead time modifications to recorded count rates and was determined to be 34 ± 5 %. This efficiency is consistent with a predicted maximum system efficiency in the range of 29 – 46 % based on predicted geometric efficiencies determined by a small MCNP5 program and intrinsic efficiencies for similar detectors.

The DNC system has been established as a rapid and accurate analytical tool for the analysis of samples containing ^{235}U . The count rate curve has been analyzed and provided accurate ^{235}U determinations over a range of three orders of magnitude with a detection threshold of 5 ± 1 ng. The capability of the system to determine fissile content is independent of small changes in total analyte volume and geometry. The DNC system was also used to identify the uranium contamination on the inner lining of the SLOWPOKE-2 site 5. It is expected that the DNC system could analyze the fissile isotopes ^{233}U and ^{239}Pu with similar degrees of accuracy.

6.2 Recommendations

^{235}U masses have been determined using the DNC system count rate method for a range of sample masses, volumes and geometries. It is recommended that experimentation with the DNC system is expanded to include the analysis of ^{233}U and ^{239}Pu by this same method and establish the system's capability to detect and accurately determine the concentrations of these isotopes. Once the unique signatures for each fissile isotope for RMC's DNC system have been ascertained, mixtures of two or more fissile isotopes could be examined. It is the intention of RMC that the system and associated hardware will be capable of deconvolving the signatures of mixtures of ^{235}U , ^{233}U and ^{239}Pu .

In order to have a more consistent system output, it is recommended that significant upgrades to the system equipment be made. The pre-amplifier in particular has shown great sensitivity to slight changes in system set up resulting in inconsistent data collection and the necessity to recalibrate the system after such incidents. The multichannel analyzer is another outdated piece of equipment that, if replaced, would likely result in significant reductions in dead time effects. To further increase the efficiency of the system it is possible the remaining three neutron detectors available at RMC be added to the detector arrangement. The detection limit of the DNC system can be reduced by further cleaning of site 5 or by changing the system site placement in the SLOWPOKE-2 arrangement. The background count of the DNC system could also be further reduced through shielding the counter apparatus. Standards containing known amounts of fissile material in addition to empty polyethylene vials should be irradiated and counted during each experimental set to ensure expected system behaviour.

A greater understanding of the DNC system behaviour can be developed by modelling the system in MCNP. The preliminary model in Section 5.3 could be expanded to include all detectors, the moderator material and the source material. The model output could be confirmed through a variety of experiments using the fissile isotopes ^{235}U , ^{233}U and ^{239}Pu distributed in a wide variety of matrices. Modelling the DNC system in MCNP would require the proper characterization of the epithermal and thermal flux at site 5, parameters that can be determined experimentally. The full characterization of DNC system behaviour through MCNP would significantly reduce uncertainties in system efficiency and fissile mass determination.

References

- [1] K.J. Moody, I.D. Hutcheon, P.M. Grant, *Nuclear Forensic Analysis*, Taylor & Francis, Boca Raton, FL, (2005).
- [2] Joint Working Group of the American Physical Society and the American Association for the Advancement of Science “Nuclear Forensics, Role, State of the Art, Program Needs”, website: <http://www.aps.org/policy/reports/upload/Nuclear-Forensics-Report-FINAL.pdf>, (2009).
- [3] International Atomic Energy Agency, “Nuclear Forensics Support” IAEA Nuclear Security Series No. 2, Vienna (2006).
- [4] International Atomic Energy Agency “Treaty on the Non-Proliferation of Nuclear Weapons” INFCIRC/140 Vienna, (1970).
- [5] C.L. Larsson, D.S. Haslip, Consolidated Canada Results to the HEU Round Robin Exercise: Performed under the Auspices of the Nuclear Smuggling International Technical Working Group (ITWG), DRDC Ottawa TM 2004-192, Defence Research and Development Canada, November 2004.
- [6] United States Nuclear Regulatory Commission, “Special Nuclear Material” website: <http://www.nrc.gov/materials/sp-nucmaterials.html> (2011).
- [7] A. Nilsson, *IAEA Illicit Trafficking Database*. Vienna : International Atomic Energy Agency, 2008. Fact Sheet.

- [8] D.K. Smith, “Recent Activities of the International Atomic Energy Agency to Combat Illicit Trafficking of Nuclear and Other Radioactive Material” website: <http://www.jaea.go.jp/04/np/activity/2010-10-05/2010-10-05-12.pdf> (2010).
- [9] M.J.A. Armelin, M.B.A. Vasconcellos, “An Evaluation of the Delayed Neutron Counting Method for Simultaneous Analysis of Uranium and Thorium and for $^{235}\text{U}/^{238}\text{U}$ Isotopic Ratio Determination” *Journal of Radioanalytical and Nuclear Chemistry*, 100 1 (1986) 37 – 47.
- [10] A. El-Jaby, *A Model for Predicting Coolant Activity Behaviour for Fuel-Failure Monitoring Analysis*, PhD Thesis, Royal Military College of Canada (2009).
- [11] R. Sher, S. Untermyer II, *The Detection of Fissionable Materials by Non-destructive Means*, American Nuclear Society, Illinois, 1980.
- [12] Lenntech, “Plutonium-Pu”, website: <http://www.lenntech.com/periodic/elements.pu.htm> (2010).
- [13] H. Gabelmann, M. Lerch, K.L. Kratz, W. Rudolph, “Determination of uranium in urine samples of fuel element fabrication workers by beta-delayed neutron counting” *Journal of Nuclear Instruments and Methods in Physics Research*, 223 2-3 (1984) 544 – 548.
- [14] P. M. Rinard, “Accountability Quality Shuffler Measurements on Pits,” *Los Alamos National Laboratory report LA-13757-MS, October 2000*.
- [15] W. Rosenstock, T. Köble, M. Risse, W. Berky, “Detection of Concealed Fissionable Material by Delayed Neutron Counting”, website: http://www-pub.iaea.org/MTCD/publications/PDF/P1433_CD/datasets/presentations/SM-EN-09.pdf Accessed Jan 2011 (2009).
- [16] R. Benzing, N.M. Baghini, B.A. Bennett, S.J. Parry, “Apparent neutron emissions from polyethylene capsules during neutron activation and delayed neutron counting” *Journal of Radioanalytical and Nuclear Chemistry*, 244 2 (2000) 447-451.

- [17] S. Amiel, M. Peisach, "Oxygen-18 Determination by Counting Delayed Neutrons of Nitrogen-17" *Journal of Analytical Chemistry*, 35 3 (1963) 323-327.
- [18] J. H. Moon, S. H. Kim, Y.S. Chung, J.M. Lim, G.H. Ahn, M.S. Koh "U determination in environmental samples by delayed neutron activation analysis in Korea" *Journal of Radioanalytical and Nuclear Chemistry*, 282 (2009) 33-35.
- [19] M.T. Sellers, D.G. Kelly, E.C. Corcoran, "An Investigation of the Time-Dependent Background Counts in the Delayed Neutron Counting System at the Royal Military College of Canada" *Proceedings of the 36th Annual Canadian Nuclear Society Student Conference, Niagara, Ontario, June 7, 2011.*
- [20] X. Li, R. Henkelmann, F. Baumgärtner, "Rapid Determination of Uranium and Plutonium Content in Mixtures through the measurement of the Intensity-time Curve of Delayed Neutrons", *Journal of Nuclear Instruments and Methods in Physics Research B*. 215 (2003) 246-251.
- [21] M.J.M. Duke, "Geochemistry of the Exshaw Shale of Alberta – An Application of Neutron Activation Analysis and Related Techniques" *University of Alberta, MSc Thesis, (1983).*
- [22] R.J. Rosenberg, V. Pitkänen, A. Sorsa, "An Automatic Uranium Analyzer Based on Delayed Neutron Counting" *Journal of Radioanalytical Chemistry*, 37 (1977) 169-179.
- [23] H. Kunzendorf, L. Løvborg, E.M. Christiansen, "Automated Uranium Analysis by Delayed Neutron Counting", *Risø R 429, Risø National Laboratory, October 1980.*
- [24] M.M. Minor, W.K. Hensley, M.M. Denton, S.P. Garcia, "An Automated Activation Analysis System" *Journal of Radioanalytical Chemistry*, 70 1 (1982) 459 -471.
- [25] P.C. Ernst, E.L. Hoffman, "Development of Automated Analytical Systems for Large Throughput" *Journal of Radioanalytical and Nuclear Chemistry*, 70 1-2 (1982) 527 – 537.

- [26] R. M. Lindstorm, D.C. Glasgow, R.G. Downing, “Trace Fissile Measurement by Delayed Neutron Activation Analysis at NIST” Proceedings of: American Chemistry Society Meeting, San Francisco, September 10 – 14, 2006.
- [27] D.C. Glasgow, “Delayed Neutron Activation Analysis for Safeguards” *Journal of Radioanalytical and Nuclear Chemistry*. 276 1 (2008) 207 – 211.
- [28] M. Leventhal. “Deuterium Formation Hypothesis for the Diffuse Gamma-ray Excess at 1 MeV”, *Nature*, 246 (1973) 136-138.
- [29] G. Choppin, J.O Liljenzin, J. Rydberg, *Radiochemistry and Nuclear Chemistry* 3rd Edition, Butter-Heinemann, Massachusetts, 2002.
- [30] J.R. Lamarsh, A.J. Baratta, *Introduction to Nuclear Engineering*, 3rd Edition, Prentice-Hall, New Jersey, 2001.
- [31] L.G.I. Bennett, B.J. Lewis, “Phys 491: The Physics of Nuclear Reactors” Department of Physics, Queen’s University (2008).
- [32] W. E. Burgham, *Nuclear Physics: An Introduction*, William Clowes and Sons, London, 1963.
- [33] International Atomic Energy Agency, “Evaluated Nuclear Data File ENDF”, website: <http://nds-iaea.org/exfor/endl.htm> (2011).
- [34] T.S. Belanova “Evaluation of Thermal Neutron Cross Sections and Resonance Integrals of Protactinium, Americium, Curium, and Berkelium Isotopes” INDC (CCP) – 391 International Atomic Energy Agency, December 1994.
- [35] G. Friedlander, J.W. Kennedy, E.S. Macias, J.M. Miller, *Nuclear and Radiochemistry* 3rd Edition, John Wiley & Sons, New York, 1981.

- [36] S. A. Badikov, C. Zhenpeng, A.D. Carlson, E.V. Gai, G.M. Hale et al. “International Evaluation of Neutron Cross Section Standards”, 90-0-100807-4, International Atomic Energy, November 2007.
- [37] A. Lunden “On the Decay of Bromine Isotopes ^{86}Br and ^{87}Br ” Z. Physik 236 (1976) 403-409.
- [38] Table of Radioactive Isotopes, “ ^{87}Br ” website:
<http://ie.lbl.gov/toi/nuclide.asp?iZA=350087> (2011).
- [39] R.W. Waldo, R.A. Karam, R.A. Meyer, “Delayed neutron yields: Time dependent measurements and a predictive model” Physical Review, 23 3 (1981) 1113 – 1127.
- [40] International Atomic Energy Agency, “IAEA Handbook for Nuclear Data for Safeguards”, website: <http://www-nds.iaea.org/sgnucdat/> (2009).
- [41] E.M. Baum, H.D. Knox, T.R. Miller, Nuclides and Isotopes, Sixteenth Edition, Knolls Atomic Power Laboratory, 2002.
- [42] E.M.A. Hussein, Handbook on Radiation Probing, Gauging, Imaging and Analysis, Kluwer Academic Publishers, Dordrecht, The Netherlands, 2003.
- [43] S.E. Binney, R. I. Schepelz, “A Review of the Delayed Fission Neutron Technique” Nuclear Instruments and Methods 154 (1978) 413 – 431.
- [44] G.F. Knoll, Radiation Detection and Measurement, 3rd ed. John Wiley & Sons, New Jersey, 2000.
- [45] LabVIEW Version 2009, National Instruments, Austin, TX .
- [46] M.E. Wise, R.E. Kay, “Description and Safety Analysis for the SLOWPOKE-2 Reactor” CPR-26, Rev. 1, Atomic Energy of Canada Limited, September 1983.

- [47] J.R.M. Pierre, Low Enrichment Uranium (LEU)-Fueled SLOWPOKE-2 Nuclear Reactor Simulation with the Monte-Carlo Based MCNP 4A Code, MASC Thesis, Royal Military College of Canada, (1996).
- [48] A.D. Smith, B.M. Townes, “Description and Safety Analysis for the SLOWPOKE-2 Reactor with LEU Oxide Fuel”, Atomic Energy of Canada Limited, Ottawa, Canada (1985).
- [49] H.W. Bonin, M. Pierre, “Monte Carlo Simulation of the LEU-Fueled SLOWPOKE-2 Reactor with MCNP4A”, website: <http://www.rmc.ca/aca/cce-cgc/gsr-esr/ens-esn/mcslfsnr-smmcrnsc-eng.asp> (2011).
- [50] L.R. Cosby, “SLOWPOKE Integrated Reactor Control and Instrumentation Software (SIRCIS)” Proceedings of the 26th Annual Canadian Nuclear Society Student Conference, Toronto, Ontario, June 2001.
- [51] W.S. Andrews, Thermal Neutron Flux Mapping Around the Reactor Core of the SLOWPOKE-2 at RMC, MASC Thesis, Royal Military College of Canada, (1989).
- [52] T.W. Crane, M.P. Baker. Neutron detectors, Chap. 13, Passive Nondestructive Assay of Nuclear Materials, ed. Reilly. D. et al., Technical Report NUREG/CR-5550; LA-UR-90-732, Los Alamos National Laboratory, NM, USA. 1991.
- [53] R2008b, Mathworks, Natick, MA.
- [54] D.G. Kelly, L.G.I. Bennett, M.M. Fill, K.M. Mattson, K.S. Nielsen, S.D. White, J.F. Allen, “Analytical Methods for the environmental quantification of uranium isotopes: Method of validation and environmental application” Journal of Radioanalytical and Nuclear Chemistry 278 3 (2008) 807-811.
- [55] M.T. Sellers, D.G. Kelly, E.C. Corcoran “An Automated Delayed Neutron Counting System for the Mass Determination of Fissile Isotopes” Journal of Radioanalytical and Nuclear Chemistry 291 2 (2012) 281-285 .

- [56] Personal communication. K.S. Nielsen, E-mail message. Director of the SLOWPOKE-2 at the Royal Military College of Canada 24 Feb, 2011.
- [57] Atomic Energy of Canada Limited, “Reactor Manual for the SLOWPOKE-2 Facility at RMC” April 2007.
- [58] GE Energy, RS-P4-1613-202 “He-3 Neutron Detector- Proportional Counter”, Private Document.
- [59] D.J. Loaize, “High-efficiency ^3He proportional counters for the detection of delayed neutrons”, Nuclear Instruments and Methods in Physics Research A, 422 (1999) 43-46.
- [60] G. Rudstam, E. Lund, “Delayed-neutron activities produced in fission: Mass range 79-98”, Physical Review C 13 1 (1976) 321-330
- [61] Los Alamos National Laboratory, “A General Monte Carlo N-Particle Transport Code – Version 5” website: <http://mcnp-green.lanl.gov/> (2004).
- [62] D.B. Rorabacher, “Statistical Treatment for the Rejection of Deviant Data” Analytical Chemistry, 63 (1991) 139 – 144.
- [63] G.D. Christian, Analytical Chemistry, 6th Edition, John Wiley & Sons, New Jersey, 2004.
- [64] M.T. Sellers, E.C. Corcoran, D.G. Kelly, “An Automated Delayed Neutron Counter for the Analysis of Special Nuclear Materials” Proceedings of the 35th Annual Canadian Nuclear Society Student Conference, Montreal Quebec, June 2010.
- [65] National Instruments “Industrial Digital I/O Device for USB – 60 V Channel- to-Channel Isolated” website: http://www.ni.com/pdf/products/us/cat_usb6525.pdf (2009).

Appendices

Appendix A

Supplemental Theory & Background

Additional Nuclear Data

As mentioned in Section 3.1 the fission cross section of ^{238}U is orders of magnitude lower than that of special nuclear materials in the thermal to epithermal range, this is illustrated in Figure A-1. In a reactor with only thermal neutrons the fission of ^{238}U is negligible when compared to ^{235}U as their cross sections are 582.6 b and 1.68×10^{-5} b respectively [33]. The differences in production ratios for various fissile isotopes are highlighted in Table A-1 and Table A-2, which contain delayed neutron data for ^{233}U and ^{239}Pu , respectively. A tabulated list of delayed neutron precursors is presented in Table A-3; P_n is defined as the fraction of decays of the isotope AZ which result in a delayed neutron.

Table A-1: Delayed Neutron Data for Thermal Fission in ^{233}U [30]

Group	$t_{1/2}$ [s]	λ [s^{-1}]	$\beta_i = \nu_i/\nu_a$	$\alpha_i = \nu_i/\nu_t$
1	55.6	0.014267	0.0797 ± 0.0036	0.0214 ± 0.0015
2	24.5	0.028292	0.1670 ± 0.0035	0.0448 ± 0.0024
3	16.3	0.042524	0.1500 ± 0.0030	0.0402 ± 0.0022
4	5.21	0.133042	0.200 ± 0.040	0.054 ± 0.012
5	2.37	0.292467	0.298 ± 0.022	0.0799 ± 0.0071
6	1.04	0.666488	0.0388 ± 0.0008	0.01040 ± 0.00055
7	0.424	1.634781	0.056 ± 0.025	0.015 ± 0.0068
8	0.198	3.554600	0.0105 ± 0.0002	0.00281 ± 0.00015

Table A-2: Delayed Neutron Data for Thermal Fission in ^{239}Pu [30]

Group	$t_{1/2}$ [s]	λ [s^{-1}]	$\beta_i = \nu_i/\nu_d$	$\alpha_i = \nu_i/\nu_t$
1	55.6	0.014267	0.032 ± 0.012	0.0072 ± 0.0028
2	24.5	0.028292	0.237 ± 0.034	0.0533 ± 0.0081
3	16.3	0.042524	0.0826 ± 0.0016	0.01859 ± 0.00098
4	5.21	0.133042	0.182 ± 0.052	0.041 ± 0.012
5	2.37	0.292467	0.294 ± 0.029	0.0662 ± 0.0073
6	1.04	0.666488	0.0816 ± 0.0016	0.01836 ± 0.00097
7	0.424	1.634781	0.072 ± 0.031	0.0162 ± 0.0071
8	0.198	3.554600	0.0185 ± 0.0004	0.00416 ± 0.00023

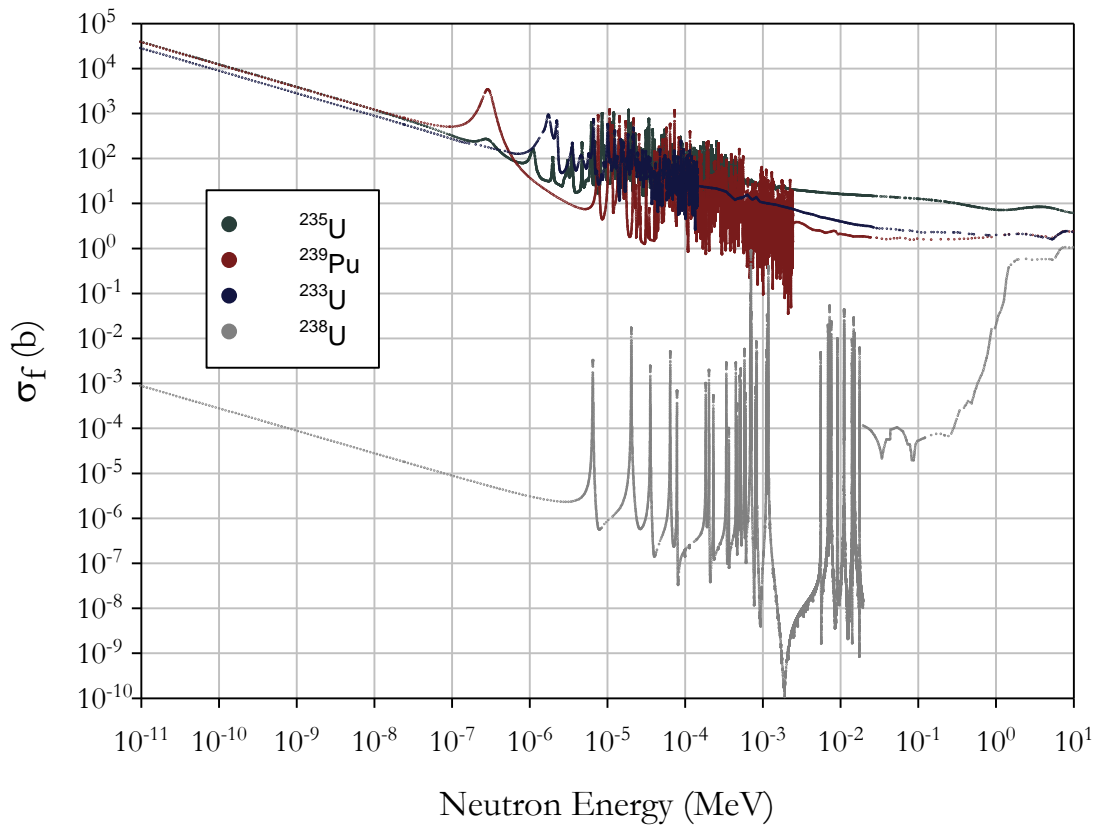


Figure A-1: A Comparison of ^{238}U σ_f to SNM [33]

Table A-3: A List of Delayed Neutron Precursors [39]

Precursor			Half-Life	Precursor			Half-Life	Precursor			Half-Life
Z	A	P _n (%)	(s)	Z	A	P _n (%)	(s)	Z	A	P _n (%)	(s)
35	87	2.38	55.6	39	98	3.4	2.0	33	87	44.00	0.73
55	137	6.6	24.9	43	109	1.7	2.0	57	150	0.94	0.648
53	137	6.6	24.4	35	90	21.2	1.92	31	82	21.90	0.6
52	136	0.9	17.5	32	83	0.17	1.9	53	140	23.00	0.6
35	88	6.7	16.0	42	110	1.3	1.892	38	99	3.40	0.6
41	103	0.13	15.669	36	92	0.033	1.85	55	145	13.3	0.585
51	134	0.108	10.4	41	105	2.9	1.8	49	130	1.38	0.58
56	147	5.2	10.0	56	150	0.24	1.798	40	105	1.40	0.559
53	138	5.3	6.53	55	143	1.68	1.78	34	90	11.00	0.555
37	93	1.39	5.85	54	141	0.044	1.73	35	91	10.9	0.542
33	84	0.090	5.6	55	142	0.091	1.71	41	106	5.5	0.535
34	87	0.190	5.6	51	135	15.6	1.71	36	95	9.5	0.5
37	92	0.012	4.5	31	80	0.8	1.66	56	148	23.9	0.5
35	89	13.5	4.38	34	88	0.6	1.52	53	141	39	0.47
40	104	0.11	3.783	47	122	1.4	1.5	38	97	0.27	0.43
39	97	0.06	3.7	50	133	0.02	1.47	51	137	20	0.284
57	149	0.81	2.864	52	138	6.3	1.4	49	131	1.73	0.28
31	79	0.094	2.86	39	99	1.2	1.4	34	91	21	0.27
52	137	2.50	2.8	36	93	1.96	1.29	32	86	22	0.259
37	94	10.4	2.76	54	142	0.42	1.24	32	85	20	0.234
30	79	1.1	2.74	31	81	11.9	1.23	55	147	25.4	0.21
49	129	3.5	2.5	32	84	10	1.20	36	94	5.7	0.208
53	139	9.42	2.38	38	100	5	1.046	37	96	14.2	0.201
56	147	5.2	2.23	50	134	17	1.04	35	93	41	0.201
41	104	0.71	1.0	52	139	6.3	0.424	53	142	16	0.196
54	144	0.73	1.0	34	89	5	0.41	37	97	28	0.17
56	149	0.03	0.917	47	123	4.6	0.39	49	132	4.3	0.13
33	86	12.00	0.9	37	95	8.8	0.384	37	98	16	0.119
49	128	0.057	0.84	35	92	22	0.362	37	99	15	0.076
43	110	0.10	0.83	55	146	13.2	0.335	39	100	5.50	0.756
48	128	0.11	0.83	53	143	18	0.328	54	143	1.2	0.30
51	136	23.00	0.82	31	83	56	0.31	50	135	8.6	0.291
68	98	0.36	0.8								

Dead Time Calculations

The following is the derivation of the two source method formula outlined in Chapter 3. The non-paralyzable relationship between actual and real counts is presented in Eq. A.1.

$$R = \frac{D}{1 - D\tau} \quad (\text{A.1})$$

Applying the binomial expansion to the denominator

$$(1 - D\tau)^{-1} \quad (\text{A.2})$$

if k is any real number and $|x| < 1$, then one has:

$$(1 + x)^k = 1 + kx + \frac{k(k-1)x^2}{2!} + \dots \quad (\text{A.3})$$

Therefore:

$$(1 - D\tau)^{-1} = 1 + (-1)(-D\tau) + \frac{(-1)(-1-1)(-D\tau)^2}{2!} + \dots \quad (\text{A.4})$$

$$(1 - D\tau)^{-1} = 1 + D\tau - (D\tau)^2 + (D\tau)^3 \dots \quad (\text{A.5})$$

In these types of experiments dead time effects are small and $m\tau \ll 1$ thus the above equation can be approximated as:

$$(1 - D\tau)^{-1} \approx 1 + D\tau \quad (\text{A.6})$$

Substituting Eq. A.6. into Eq. A.1. yields:

$$R = D(1 + D\tau) \quad (\text{A.7})$$

Therefore if there are two sources:

$$R_1 + R_2 = R_{12} + R_b \quad (\text{A.8})$$

Substituting Eq. A.7. into the above equation and assuming $R_b = D_b$ as background contributions are normally small and dead time effects therefore negligible.

$$D_1(1 + D_1\tau) + D_2(1 + D_2\tau) = D_{12}(1 + D_{12}\tau) + D_b \quad (\text{A.9})$$

and isolating for τ , one obtains:

$$\tau = \frac{D_1 + D_2 - D_{12} - D_b}{D_{12}^2 - D_1^2 - D_2^2} \quad (\text{A.10})$$

Appendix B

The Fissile Analysis Program

B.1 An Example of Fissile Data Analysis

The following is an example of the fissile data analysis of a sample, Q1, containing depleted uranium dissolved in a HNO₃/distilled water solution. The sample was analyzed under typical operating conditions which included the SLOWPOKE-2 reactor at its half power setting, an irradiation time of 60s, followed by the default 2.9s decay time and a 60s counting time during which the counts were recorded in approximately half second intervals. Q1 was the only sample run in this sequence (sample # 1) and it was run through the DNC system just once (J-cycle = 1), during the count time 79306 counts were recorded by the apparatus. Table B-1 shows the raw data recorded by the DNC system at RMC for sample Q1. These tables are imported into Matlab™ and usually saved in the format of “samplename.date” so they are easy to recall for further analysis.

Table B-1: Raw DNC System Data for Sample Q1

SLOWPOKE Test Data				
11/04/2011	11:47:49 AM			
Sample a Standard: YES				
Sample #	J-Cycles	Time	Counts	Cumulative Count
1	1	1.015625	1863	79306
1	1	1.546875	1821	79306
1	1	2.0625	1759	79306
1	1	2.59375	1691	79306
1	1	3.125	1673	79306
1	1	3.640625	1642	79306

1	1	4.171875	1582	79306
1	1	4.703125	1514	79306
1	1	5.234375	1509	79306
1	1	5.75	1459	79306
1	1	6.28125	1401	79306
1	1	6.796875	1373	79306
1	1	7.328125	1353	79306
1	1	7.859375	1277	79306
1	1	8.390625	1233	79306
1	1	8.90625	1284	79306
1	1	9.4375	1256	79306
1	1	9.96875	1237	79306
1	1	10.48437	-1172	79306
1	1	11.01562	1129	79306
1	1	11.54687	1070	79306
1	1	12.0625	1063	79306
1	1	12.59375	1034	79306
1	1	13.125	1020	79306
1	1	13.65625	1024	79306
1	1	14.1875	974	79306
1	1	14.70312	977	79306
1	1	15.23437	944	79306
1	1	15.76562	946	79306
1	1	16.29687	910	79306
1	1	16.8125	895	79306
1	1	17.34375	951	79306
1	1	17.73437	1272	79306
1	1	18.5625	931	79306
1	1	19.125	913	79306
1	1	19.6875	890	79306
1	1	20.21875	809	79306
1	1	20.75	826	79306
1	1	21.28125	743	79306
1	1	21.8125	734	79306
1	1	22.34375	707	79306
1	1	22.875	737	79306
1	1	23.40625	687	79306
1	1	23.9375	702	79306
1	1	24.46875	690	79306
1	1	25	698	79306
1	1	25.54687	696	79306
1	1	26.07812	737	79306

1	1	26.60937	638	79306
1	1	27.14062	620	79306
1	1	27.67187	625	79306
1	1	28.20312	644	79306
1	1	28.73437	669	79306
1	1	29.26562	643	79306
1	1	29.79687	604	79306
1	1	30.32812	590	79306
1	1	30.85937	578	79306
1	1	31.39062	561	79306
1	1	31.92187	580	79306
1	1	32.45312	559	79306
1	1	32.98437	558	79306
1	1	33.51562	532	79306
1	1	34.04687	563	79306
1	1	34.57812	521	79306
1	1	35.10937	484	79306
1	1	35.64062	500	79306
1	1	36.17187	470	79306
1	1	36.71875	473	79306
1	1	37.25	506	79306
1	1	37.78125	459	79306
1	1	38.3125	443	79306
1	1	38.84375	449	79306
1	1	39.375	464	79306
1	1	39.90625	438	79306
1	1	40.4375	450	79306
1	1	40.96875	425	79306
1	1	41.5	420	79306
1	1	42.03125	432	79306
1	1	42.5625	431	79306
1	1	43.09375	479	79306
1	1	43.625	435	79306
1	1	44.15625	439	79306
1	1	44.73437	424	79306
1	1	45.26562	413	79306
1	1	45.79687	408	79306
1	1	46.32812	395	79306
1	1	46.85937	393	79306
1	1	47.40625	399	79306
1	1	47.9375	370	79306
1	1	48.46875	384	79306
1	1	49	372	79306

1	1	49.53125	400	79306
1	1	50.0625	375	79306
1	1	50.59375	331	79306
1	1	51.125	347	79306
1	1	51.65625	310	79306
1	1	52.1875	379	79306
1	1	52.71875	331	79306
1	1	53.25	342	79306
1	1	53.78125	354	79306
1	1	54.3125	341	79306
1	1	54.84375	321	79306
1	1	55.39062	289	79306
1	1	55.92187	271	79306
1	1	56.45312	277	79306
1	1	56.98437	308	79306
1	1	57.51562	286	79306
1	1	58.04687	292	79306
1	1	58.59375	308	79306
1	1	59.125	297	79306
1	1	59.65625	278	79306
1	1	60.0625	165	79306

Once this table has been imported into Matlab it is saved as “Q1april11” and is easily recalled using the command window, Figure B-1.



Figure B-1: Retrieving Data in the Matlab Command Prompt

As previously mentioned there are two versions of the fissile analysis code written, one which prompts the user to enter experimental parameters including reactor flux, irradiation duration and the decay time, the other has these hardcoded in so the default values can be recalled easily. The fissile analysis code is also retrieved using the command window shown below in Figure B-2.

```
>>
>>
>>
>>
>>
>>
>>
fx >> fissileanalysis|
```

Figure B-2: Calling the Fissile Analysis Program

Once the fissile analysis code has been recalled it performs the procedure outlined in the preceding section and displays the ²³⁵U amount in the sample as determined by the DNC system at RMC, in µg, Figure B-3. In addition to displaying the experimentally determined ²³⁵U content in the sample analyzed, the fissile analysis program outputs a plot showing the fitted calibration curve to the experimental data, shown in Figure B-4 and Figure B-5.

```
U235Amount =
|
5.4228
fx >> |
```

Figure B-3: The Fissile Analysis Program Display of ²³⁵U amounts

An instant view of how the experimental data fits that of the calibration curve allows the user to deduce quickly if the electronics were functioning improperly, as was the case in Figure B-5.

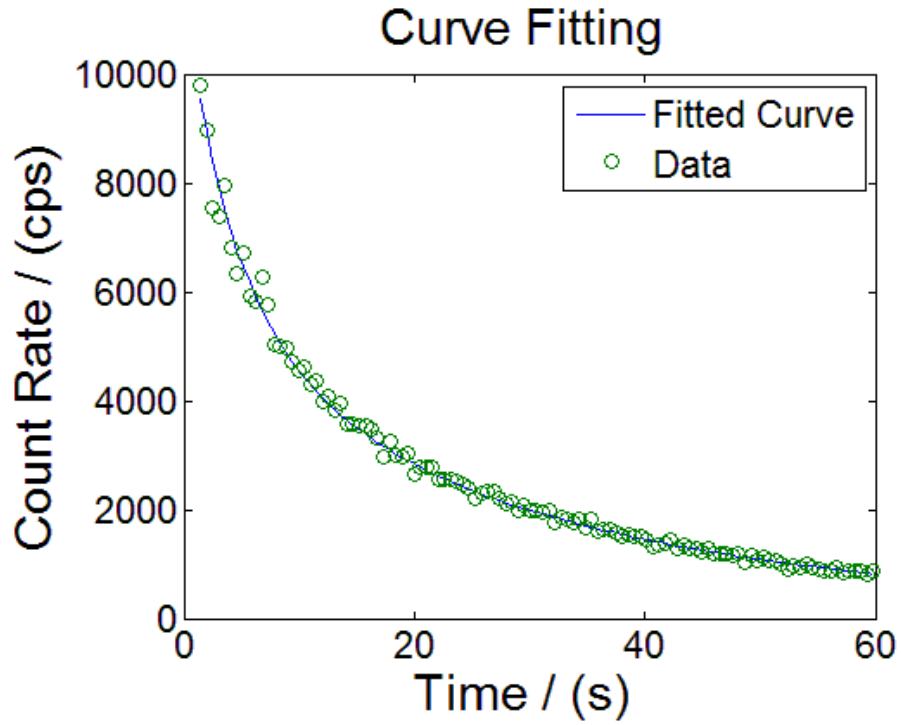


Figure B-4: The Fissile Analysis Program Curve Fit to Experimental Data

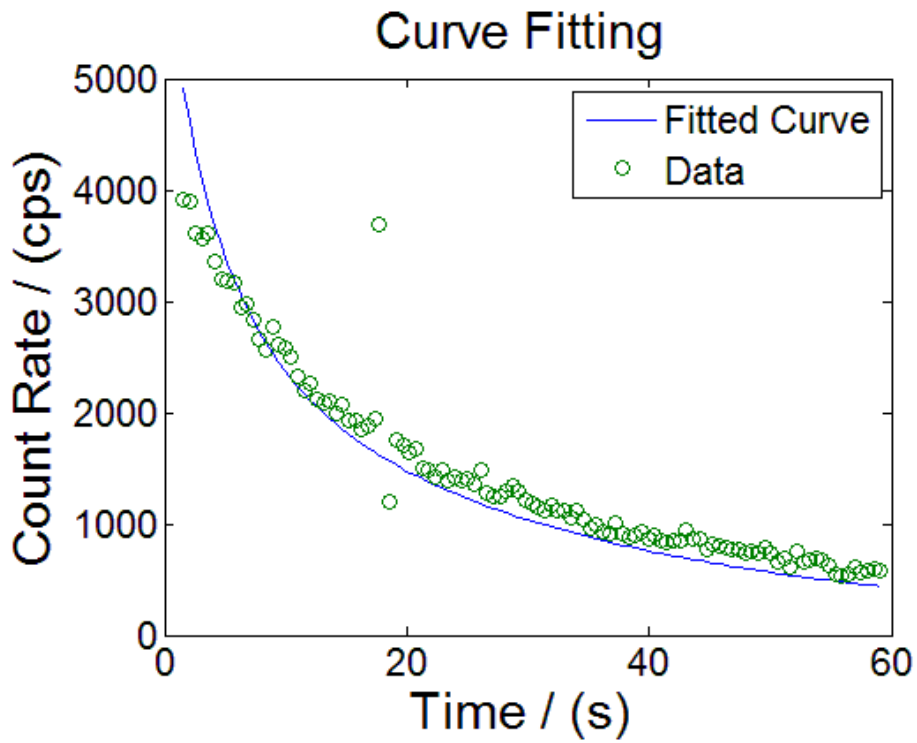


Figure B-5: Fissile Analysis Curve Fitting to Improperly Functioning Electronics

B.2 The Fissile Analysis Program Code

```
% DNCS Fissile Analysis Code
```

```
% M. Sellers Feb. 2 2011
```

```
%This code imports the data produced by LabVIEW
```

```
%This section takes the LabView excel file and manipulates the relevant
```

```
%data (time and counts), it will delete any unnecessary cells.
```

```
%manipulation of the import data
```

```
[datam,datan]=size(data);
```

```
%saves information relevant to the user, if for example the user wished to
```

```
%know how many cycles each sample went through they would type
```

```
%"numberofsamples" into the command window
```

```
numberofsamples=max(data(1:datam,1));
```

```
numberofcycles=max(data(1:datam,2));
```

```
numberofruns=max(data(1:datam,3));
```

```
%eliminating non numerical values from table
```

```
%finds cells in first column where the sample numbering begins
```

```
v=[find(data(1:datam,1)>0)];
```

```
%eliminates non data rows and redefining size of matrix
```

```
Z=data(min(v):datam,1:datan);
```

```
[Zm,Zn]=size(Z);
```

```
%determines the number of data per sample
```

```
datapersample=Zm/numberofsamples/numberofcycles;
```

```
%At this point all misc information (dates, invalid cells) has been
```

```
%deleted, matrix contains solely sample number, run number neutron
```

```
%counts and timings
```

```
%the for loop will run for each cycle of each run (jend)
```

```
jend=Zm/datapersample;
```

```

for j = 1:jend;
    %makes a new matrix for each sample
    A=Z(1+(j-1)*datapertsample:(j-1)*datapertsample+datapertsample,1:Zn);
    [Am,An]=size(A);

    %finding count vector, B is all counts for all times for all
    %samples, the rows are sample #, run #, time (s) and counts (i.e.
    %A(1:Am,4))
    b=A(1:Am,4);
    B(1:Am,j)=abs(b);

    %finding time vector (T), time should be the same (or very close!) for
    %each sample run
    t=A(1:Am,3);
    T(1:Am,j)=t;
    [tm,tn]=size(t);
end

```

```

%-----

```

```

%This portion of the code produces theoretical matrix using values from the
%time vector (T)
%matrix values

```

```

%Experimental Parameters

```

```

%Efficiency

```

```

efficiency=0.342;

```

```

%Irradiation Time [s]

```

```

tb=60;

```

```

%Decay Time [s]

```

```

tc=2.9;

```

```

%Neutron Flux of SLOWPOKE-2[s]

```

```
flux=5.5e11;
```

%U235 Properties

```
%Number of Neutrons in a Fission of Uranium-235
```

```
numberofneutronsperfissionU235=0.0162;
```

```
%Molar Mass of Uranium-235
```

```
MU235=235.0439299;
```

```
%Thermal Neutron Cross Section of Uranium-235
```

```
fissioncrosssectionU235=584.4e-24;
```

```
%Delayed Neutron Fractions
```

```
BU235=[0.0328; 0.1539; 0.091; 0.1971; 0.3308; 0.0902; 0.0812; 0.0229];
```

```
%Lifetime of Delayed Neutron Groups
```

```
lambdaU235=[0.012467; 0.028292; 0.042524; 0.133042; 0.292467; 0.666488; 1.634784;  
3.5546];
```

```
avagadrosnumber=6.02214*(10^23);
```

%Uranium-235

```
%coefficients of counts
```

```
CU235=1e-
```

```
6*efficiency*numberofneutronsperfissionU235*avagadrosnumber*fissioncrosssectionU235*  
flux/MU235;
```

```
CountsU235=ones(tm,tn); %initializing count vectors
```

```
U235=ones(tm,tn); %U235 count coefficients initialization
```

```
%takes each time value and the delayed neutron values relevant to
```

```
%U235 and creates the theoretical vector for U235
```

```
for k=1:tm %determining total counts for each time value
```

```
tcount=t(k,1); %initializing tcount to LabView values
```

```
for i=1:8 %summing up values for each delayed neutron group of U235
```

```
CountsU235(i,1)=CU235*BU235(i,1)*(1-exp(-lambdaU235(i,1)*tb))*(exp(-  
lambdaU235(i,1)*tc))*((exp(-lambdaU235(i,1)*tcount)));
```

```
end
```

```
SU235=CountsU235(1,1)+CountsU235(2,1)+CountsU235(3,1)+CountsU235(4,1)+Counts  
U235(5,1)+CountsU235(6,1)+CountsU235(7,1)+CountsU235(8,1);
```

```
%creating final count coefficient vector for U-235
```

```
U235(k,1)=SU235;
```

```
end
```

```
a=size(U235);
```

```
%normalizing to cps
```

```
for m=2:tm
```

```
    d(m,1)=B(m,1)/(t(m,1)-t(m-1,1)) ;
```

```
end
```

```
[D,E]=size(d);
```

```
%deleting first time interval
```

```
t1=t(2:D+1,1);
```

```
%correcting for dead time effects (empirical fit) and noise from
```

```
%SLOWPOKE-2 reactor
```

```
for n=1:D
```

```
    b(n,1)=d(n,1)*d(n,1)*0.0000325+1.03*d(n,1)-4
```

```
end
```

```
[x,flag,relres,iter]=lsqr(U235(2:a-1),b(1:a-2))
```

```
U235Amount=x
```

Appendix C

Further Results & Discussion Analysis

C.1 Linear Least Squares to DNC System Output for Calibration

The calibration relationship determined for the DNC system at RMC and presented in Table 5-3 was determined by fitting a linear least squares fit to the experimental data. This fit was chosen as it is the statistically best linear fit to a series of experimental points [63]. The sum of the squares is shown below:

$$S = \sum (y_i - y_1)^2 \quad (\text{C.1})$$

Where S is the sum of the squares, y_i the experimental output of interest (DNC system output), y_1 is the corresponding fit's output for the same x value (actual ^{235}U mass). Eq. D.1. can also be defined as shown below:

$$S = \sum (y_i - (mx_i + b))^2 \quad (\text{C.2})$$

Where m and b are the slope and y-intercept of the fitted line respectively. The uncertainty quoted in Table 5-3 does not account for uncertainties in the actual ^{235}U mass, x_i , as the purpose of the section

was determined the consistency and precision of the technique, rather than the accuracy. The accuracy of the calibration was challenged in Table 5-4 which used a different CRM solution to compare the DNC calibration with natural to that of depleted uranium.

C.2 The Q-Test for Data Rejection

As discussed in Section 5.4 there was one significant outlier presented in Figure 5-4. This outlier was further examined by the Q test described below. In the case of this Q test, the relative error from all 64 calibration data points were sorted by increasing value and they ranged from 0.006% to 19.3% for the particular data point of interest. In a Q test, the quantity between the suspect point (diamond) and that of its closest neighbour (square), a , in Figure C-1, is compared with the total range, w . The Q value is presented in Eq. D.5.

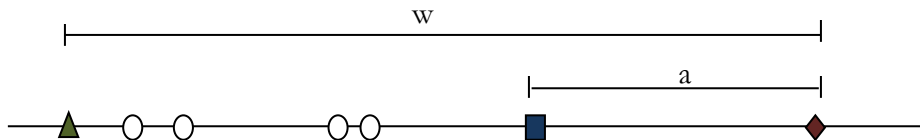


Figure C-1: An Example of the Q-Test for Data Rejection [63]

$$Q = \frac{a}{w} \quad (\text{C.3})$$

In the case of this data set, the next closest point was 10.6%, resulting in a and w values of 8.68 and 19.28 respectively. This gave a Q value of 0.450 which meets the requirement for rejection [63]. The rejection quotient indicates the data can be rejected with >99% confidence there was an error in this measurement as for a data set with only 20 points, Q values greater than 2.8 indicate there was an error in the measurement [62].

C.3 Detection Limit Calculations

The detection limit is commonly denoted as the minimum concentration of analyte which produces a signal greater than 3σ than that of the blank signal [63]. The detection limit of the DNC system at RMC was determined by running several blanks and standards through the typical DNC system experimental parameters. The total counts for a sixty second irradiation and count from each blank sample and the determined standard deviation of the blank contribution is listed below in Table C-2. The standard deviation was determined the below equation [63]:

$$s = \sqrt{\frac{\sum(x_i - \bar{x})^2}{N - 1}} \quad (\text{C.4})$$

where s is the standard deviation of a finite set of data, x_i the individual data point, \bar{x} is the mean value of all measurements and N is the number of measurements.

Table C-1: Blank Signal Counts, Mean and Standard Deviation

Blank	Counts	$(x_i - \bar{x})^2$
Q1	1047	1616
Q2	1073	202
Q3	1148	3697
Q4	1089	3
Q5	1079	67
\bar{x}	1087	
s	37.4	

The mean blank signal count was determined to be 1087 ± 37 counts. The 3σ limit was therefore determined to be 112 counts (3×37.4). Therefore a signal of at least 1199 (the mean blank signal plus 3 standard deviations) is required for detection using the DNC system.

The standards used to determine the detection limit contained small amounts of ^{235}U to reduce any dead time effects on the sample counts recorded by the apparatus. The detection limit for each sample was calculated by determining the number of counts associated with that amount of ^{235}U . For example, if 53 ng of ^{235}U had 2553 counts associated with it, the number of counts per ng of ^{235}U would be $(2553-1087)/53$ or 27.6 counts ng^{-1} of ^{235}U . Therefore, the detection limit of 112 counts would correspond to 4.0 ng for this example. Considering the results of six low-level analyses, the detection limit of the DNC system was determined to be 5 ± 1 ng.

Table C-2: Standard Counts & Detection Limit Determination

Standard	^{235}U (ng)	Total Counts	Net Reading	Counts per 1 ng	Calculated Detection Limit (ng)
<i>1</i>	53	2553	1466	27.6	4.0
<i>2</i>	54	2117	1030	19	5.9
<i>3</i>	27	1824	737	27.3	4.1
<i>4</i>	27	1632	545	20.2	5.6
<i>5</i>	11	1281	194	17.6	6.4
<i>6</i>	11	1392	305	27.7	4.0
<i>Mean value</i>				23.2	5 ± 1

Appendix D

DNC System Technical Specifications

Figure D-2 shows a schematic of RMC's DNC system apparatus and is also displayed on the GUI's secondary panel [64]. The individual components shown in the diagram are described in the following sections.

D.1 Mechanical Components

Enclosure Box

Most of the DNC system is housed inside a large gray enclosure box measuring approximately 88 x 72 x 17 cm (height x width x depth) which is mounted on the Northwest corner of the SLOWPOKE-2 reactor room. The contents of this box include the system loader, diverter, relays (6), piston valves (2), terminal box, air intake valves (2), and sample tubing. The enclosure box was obtained from NEDCO.

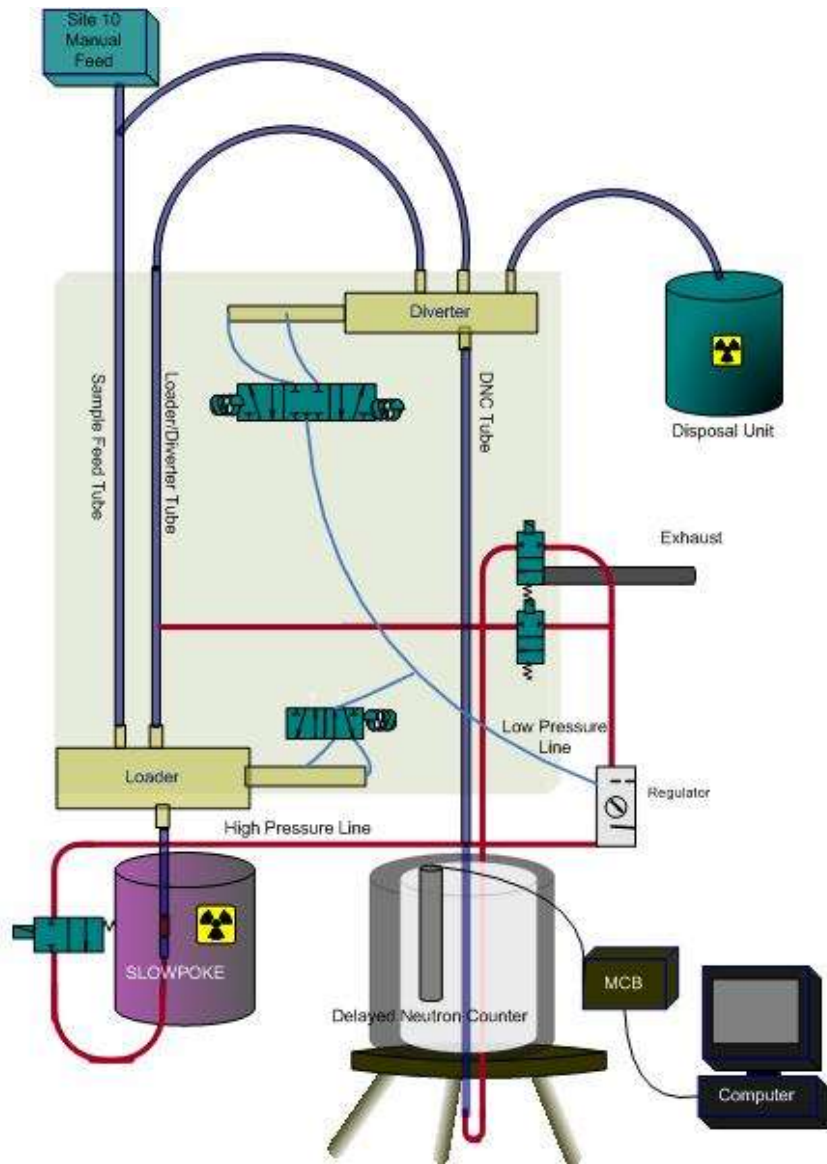


Figure D-2: The DNC System at RMC Schematic [64]

Loader and Diverter

The DNC loader was manufactured from aluminum at RMC and is mounted to the bottom left of the enclosure box. The enclosure box has two tubing attachments at its top and one at the bottom through which the sample will travel. The top left tube is the sample feed from site 5 and is adjacent to the sample tube leading to and from the diverter. The loader bottom leads to and from

the SLOWPOKE-2 site 5 irradiation site. Once a sample is fed into the loader, the sample position will be shifted by the accompanying piston to a position over top site 5. Compressed air can then push the sample to the site and back up through the loader to the diverter.

The DNC diverter is located at the top of the enclosure case and is shown in Figure D-2. The diverter has three top positions referred to as loader, cyclic and disposal. The loader position sends and receives the samples to and from the SLOWPOKE-2 irradiation site. The cyclic position sends the sample to the back of a line of samples and the disposal sends the sample to a safe place for retrieval by the Radiation Safety Officer. The diverter positions are controlled by the left and right hand sides of valve 2 shown in Figure 4-5. The diverter piston is supplied by a constant air supply on its right air intake side making its default position loader. To change the position of the diverter to cyclic, air must be received from the left side of valve 2. To change the position of the diverter to the dump, air must be received from the right side of valve 2. The air pressure from valve 2 must be greater than the default air.

Air Supply Valves

The air supply valves 3 and 4, shown in Figure 4-5 supply air to the DNC eject air and diverter/loader tube, respectively. The large air supply valves are labeled valves 3 and 4. Valve 3 is mounted in the top right side of the enclosure box and has a constant in air supply in line with valve 4. Valve 3 controls the air that is fed to the bottom of the delayed neutron counter which pushes samples out and into the diverter. While in its default position, all input air is vented through the exhaust. Valve 4 is the bottom right valve in the apparatus. Identical in design to valve 3, it has a constant air supply. When given a signal, valve 4 sends air into the diverter/loader tube. The purpose of this air is to push the sample from the loaded into the SLOWPOKE.

Loader and Diverter Control Valves

Valve 1 is located in the bottom left corner of the apparatus. It controls the movement of the sample loader, with its default position allowing air to flow from the top of the component to

the bottom right hand side of the valve. When given a signal, valve 1 pushes air through the left side. Valve 2 is located near the middle of the apparatus; it controls the 3 position diverter. Air is constantly supplied to valve 2 and when it is in its default position, no air is passed through the valve. When a signal is sent to the right side of the valve 2, air will be sent through the top of the right hand side, also into the diverter position.

Sample Disposal/Storage

The sample sits in the SLOWPOKE's site 5 position where it is irradiated for a user-specified amount of time. Once this time has expired the sample is shot back up through the diverter/loader tube using air from the SLOWPOKE-2 site 5. The sample now travels through the diverter/loader tubing into the diverter which is in a position such that the sample travels straight through into the delayed neutron counter. The sample is sent to the disposal unit when the user has finished irradiating and counting the sample. For the sample to go to the disposal unit, it must be in the DNC and diverter in the rightmost position. Air is sent from valve 3 to send the sample up and valve 2 to position diverter correctly.

D.2 Electrical Components

The input/output board selected for the DNC is model USB 6525 from National Instruments. NI USB 6525 contains eight 60 VDC/30 V_{RMS}, 500 mA solid state relays in addition to eight +/- 60 VDC digital input. Further board specifications can be found at the National Instrument's website [65]. The NI pin board supplies 5 V to each of the several relays previously described who in turn are wired to valves. The first side of the relay receives a 5 V signal which allows 120 V to pass through the other side.

- [1] K.J. Moody, I.D. Hutcheon, P.M. Grant, Nuclear Forensic Analysis, Taylor & Francis, Boca Raton, FL, (2005).
- [2] Joint Working Group of the American Physical Society and the American Association for the Advancement of Science “Nuclear Forensics, Role, State of the Art, Program Needs”, website: <http://www.aps.org/policy/reports/upload/Nuclear-Forensics-Report-FINAL.pdf>, (2009).
- [3] International Atomic Energy Agency, “Nuclear Forensics Support” IAEA Nuclear Security Series No. 2, Vienna (2006).
- [4] International Atomic Energy Agency “Treaty on the Non-Proliferation of Nuclear Weapons” INFCIRC/140 Vienna, (1970).
- [5] C.L. Larsson, D.S. Haslip, Consolidated Canada Results to the HEU Round Robin Exercise: Performed under the Auspices of the Nuclear Smuggling International Technical Working Group (ITWG), DRDC Ottawa TM 2004-192, Defence Research and Development Canada, November 2004.
- [6] United States Nuclear Regulatory Commission, “Special Nuclear Material” website: <http://www.nrc.gov/materials/sp-nucmaterials.html> (2011).
- [7] A. Nilsson, *IAEA Illicit Trafficking Database*. Vienna: International Atomic Energy Agency, 2008. Fact Sheet.
- [8] D.K. Smith, “Recent Activities of the International Atomic Energy Agency to Combat Illicit Trafficking of Nuclear and Other Radioactive Material” website: <http://www.jaea.go.jp/04/np/activity/2010-10-05/2010-10-05-12.pdf> (2010).

- [9] M.J.A. Armelin, M.B.A. Vasconcellos, “An Evaluation of the Delayed Neutron Counting Method for Simultaneous Analysis of Uranium and Thorium and for $^{235}\text{U}/^{238}\text{U}$ Isotopic Ratio Determination” *Journal of Radioanalytical and Nuclear Chemistry*, 100 1 (1986) 37 – 47.
- [10] A. El-Jaby, A Model for Predicting Coolant Activity Behaviour for Fuel-Failure Monitoring Analysis, PhD Thesis, Royal Military College of Canada (2009).
- [11] R. Sher, S. Untermyer II, The Detection of Fissionable Materials by Non-destructive Means, American Nuclear Society, Illinois, 1980.
- [12] Lenntech, “Plutonium-Pu”, website:
<http://www.lenntech.com/periodic/elements.pu.htm> (2010).
- [13] H. Gabelmann, M. Lerch, K.L. Kratz, W. Rudolph, “Determination of uranium in urine samples of fuel element fabrication workers by beta-delayed neutron counting” *Journal of Nuclear Instruments and Methods in Physics Research*, 223 2-3 (1984) 544 – 548.
- [14] P. M. Rinard, “Accountability Quality Shuffler Measurements on Pits,” *Los Alamos National. Laboratory report LA-13757-MS, October 2000*.
- [15] W. Rosenstock, T. Köble, M. Risse, W. Berky, “Detection of Concealed Fissionable Material by Delayed Neutron Counting”, website: http://www-pub.iaea.org/MTCD/publications/PDF/P1433_CD/datasets/presentations/SM-EN-09.pdf Accessed Jan 2011 (2009).
- [16] R. Benzing, N.M. Baghini, B.A. Bennett, S.J. Parry, “Apparent neutron emissions from polyethylene capsules during neutron activation and delayed neutron counting” *Journal of Radioanalytical and Nuclear Chemistry*, 244 2 (2000) 447-451.

- [17] S. Amiel, M. Peisach, "Oxygen-18 Determination by Counting Delayed Neutrons of Nitrogen-17" *Journal of Analytical Chemistry*, 35 3 (1963) 323-327.
- [18] J. H. Moon, S. H. Kim, Y.S. Chung, J.M. Lim, G.H. Ahn, M.S. Koh "U determination in environmental samples by delayed neutron activation analysis in Korea" *Journal of Radioanalytical and Nuclear Chemistry*, 282 (2009) 33-35.
- [19] M.T. Sellers, D.G. Kelly, E.C. Corcoran, "An Investigation of the Time-Dependent Background Counts in the Delayed Neutron Counting System at the Royal Military College of Canada" *Proceedings of the 36th Annual Canadian Nuclear Society Student Conference, Niagara, Ontario, June 7, 2011.*
- [20] X. Li, R. Henkelmann, F. Baumgärtner, "Rapid Determination of Uranium and Plutonium Content in Mixtures through the measurement of the Intensity-time Curve of Delayed Neutrons", *Journal of Nuclear Instruments and Methods in Physics Research B*. 215 (2003) 246-251.
- [21] M.J.M. Duke, "Geochemistry of the Exshaw Shale of Alberta – An Application of Neutron Activation Analysis and Related Techniques" *University of Alberta, MASC Thesis, (1983).*
- [22] R.J. Rosenberg, V. Pitkänen, A. Sorsa, "An Automatic Uranium Analyzer Based on Delayed Neutron Counting" *Journal of Radioanalytical Chemistry*, 37 (1977) 169-179.
- [23] H. Kunzendorf, L. Løvborg, E.M. Christiansen, "Automated Uranium Analysis by Delayed Neutron Counting", *Risø R 429, Risø National Laboratory, October 1980.*
- [24] M.M. Minor, W.K. Hensley, M.M. Denton, S.P. Garcia, "An Automated Activation Analysis System" *Journal of Radioanalytical Chemistry*, 70 1 (1982) 459 -471.
- [25] P.C. Ernst, E.L. Hoffman, "Development of Automated Analytical Systems for Large Throughput" *Journal of Radioanalytical and Nuclear Chemistry*, 70 1-2 (1982) 527 – 537.

- [26] R. M. Lindstorm, D.C. Glasgow, R.G. Downing, “Trace Fissile Measurement by Delayed Neutron Activation Analysis at NIST” Proceedings of: American Chemistry Society Meeting, San Francisco, September 10 – 14, 2006.
- [27] D.C. Glasgow, “Delayed Neutron Activation Analysis for Safeguards” Journal of Radioanalytical and Nuclear Chemistry. 276 1 (2008) 207 – 211.
- [28] M. Leventhal. “Deuterium Formation Hypothesis for the Diffuse Gamma-ray Excess at 1 MeV”, Nature, 246 (1973) 136-138.
- [29] G. Choppin, J.O Liljenzin, J. Rydberg, Radiochemistry and Nuclear Chemistry 3rd Edition, Butter-Heinemann, Massachusetts, 2002.
- [30] J.R. Lamarsh, A.J. Baratta, Introduction to Nuclear Engineering, 3rd Edition, Prentice-Hall, New Jersey, 2001.
- [31] L.G.I. Bennett, B.J. Lewis, “Phys 491: The Physics of Nuclear Reactors” Department of Physics, Queen’s University (2008).
- [32] W. E. Burgham, Nuclear Physics: An Introduction, William Clowes and Sons, London, 1963.
- [33] International Atomic Energy Agency, “Evaluated Nuclear Data File ENDF”, website: <http://nds-iaea.org/exfor/endl.htm> (2011).
- [34] T.S. Belanova “Evaluation of Thermal Neutron Cross Sections and Resonance Integrals of Protactinium, Americium, Curium, and Berkelium Isotopes” INDC (CCP) – 391 International Atomic Energy Agency, December 1994.

[35] G. Friedlander, J.W. Kennedy, E.S. Macias, J.M. Miller, Nuclear and Radiochemistry 3rd Edition, John Wiley & Sons, New York, 1981.

[36] S. A. Badikov, C. Zhenpeng, A.D. Carlson, E.V. Gai, G.M. Hale et al. “International Evaluation of Neutron Cross Section Standards”, 90-0-100807-4, International Atomic Energy, November 2007.

[37] A. Lundon “On the Decay of Bromine Isotopes ⁸⁶Br and ⁸⁷Br” Z. Physik 236 (1976) 403-409.

[38] Table of Radioactive Isotopes, “⁸⁷Br” website:
<http://ie.lbl.gov/toi/nuclide.asp?iZA=350087> (2011).

[39] R.W. Waldo, R.A. Karam, R.A. Meyer, “Delayed neutron yields: Time dependent measurements and a predictive model” Physical Review, 23 3 (1981) 1113 – 1127.

[40] International Atomic Energy Agency, “IAEA Handbook for Nuclear Data for Safeguards”, website: <http://www-nds.iaea.org/sgnucdat/> (2009).

[41] E.M. Baum, H.D. Knox, T.R. Miller, Nuclides and Isotopes, Sixteenth Edition, Knolls Atomic Power Laboratory, 2002.

[42] E.M.A. Hussein, Handbook on Radiation Probing, Gauging, Imaging and Analysis, Kuver Academic Publishers, Dordrecht, The Netherlands, 2003.

[43] S.E. Binney, R. I. Schepelz, “A Review of the Delayed Fission Neutron Technique” Nuclear Instruments and Methods 154 (1978) 413 – 431.

[44] G.F. Knoll, Radiation Detection and Measurement, 3rd ed. John Wiley & Sons, New Jersey, 2000.

[45] LabVIEW Version 2009, National Instruments, Austin, TX .

- [46] M.E. Wise, R.E. Kay, "Description and Safety Analysis for the SLOWPOKE-2 Reactor" CPR-26, Rev. 1, Atomic Energy of Canada Limited, September 1983.
- [47] J.R.M. Pierre, Low Enrichment Uranium (LEU)-Fueled SLOWPOKE-2 Nuclear Reactor Simulation with the Monte-Carlo Based MCNP 4A Code, MASC Thesis, Royal Military College of Canada, (1996).
- [48] A.D. Smith, B.M. Townes, "Description and Safety Analysis for the SLOWPOKE-2 Reactor with LEU Oxide Fuel", Atomic Energy of Canada Limited, Ottawa, Canada (1985).
- [49] H.W. Bonin, M. Pierre, "Monte Carlo Simulation of the LEU-Fueled SLOWPOKE-2 Reactor with MCNP4A", website: <http://www.rmc.ca/aca/cce-cgc/gsr-esr/ens-esn/mcslfsnr-smmcrnsc-eng.asp> (2011).
- [50] L.R. Cosby, "SLOWPOKE Integrated Reactor Control and Instrumentation Software (SIRCIS)" Proceedings of the 26th Annual Canadian Nuclear Society Student Conference, Toronto, Ontario, June 2001.
- [51] W.S. Andrews, Thermal Neutron Flux Mapping Around the Reactor Core of the SLOWPOKE-2 at RMC, MASC Thesis, Royal Military College of Canada, (1989).
- [52] T.W. Crane, M.P. Baker. Neutron detectors, Chap. 13, Passive Nondestructive Assay of Nuclear Materials, ed. Reilly. D. et al., Technical Report NUREG/CR-5550; LA-UR-90-732, Los Alamos National Laboratory, NM, USA. 1991.
- [53] R2008b, Mathworks, Natick, MA.
- [54] D.G. Kelly, L.G.I. Bennett, M.M. Fill, K.M. Mattson, K.S. Nielsen, S.D. White, J.F. Allen, "Analytical Methods for the environmental quantification of uranium isotopes:

Method of validation and environmental application” Journal of Radioanalytical and Nuclear Chemistry 278 3 (2008) 807-811.

[55] M.T. Sellers, D.G. Kelly, E.C. Corcoran “An Automated Delayed Neutron Counting System for the Mass Determination of Fissile Isotopes” Journal of Radioanalytical and Nuclear Chemistry 291 2 (2012) 281-285 .

[56] Personal communication. K.S. Nielsen, E-mail message. Director of the SLOWPOKE-2 at the Royal Military College of Canada 24 Feb, 2011.

[57] Atomic Energy of Canada Limited, “Reactor Manual for the SLOWPOKE-2 Facility at RMC” April 2007.

[58] GE Energy, RS-P4-1613-202 “He-3 Neutron Detector- Proportional Counter”, Private Document.

[59] D.J. Loaize, “High-efficiency ^3He proportional counters for the detection of delayed neutrons”, Nuclear Instruments and Methods in Physics Research A, 422 (1999) 43-46.

[60] G. Rudstam, E. Lund, “Delayed-neutron activities produced in fission: Mass range 79-98”, Physical Review C 13 1 (1976) 321-330

[61] Los Alamos National Laboratory, “A General Monte Carlo N-Particle Transport Code – Version 5” website: <http://mcnp-green.lanl.gov/> (2004).

[62] D.B. Rorabacher, “Statistical Treatment for the Rejection of Deviant Data” Analytical Chemistry, 63 (1991) 139 – 144.

[63] G.D. Christian, Analytical Chemistry, 6th Edition, John Wiley & Sons, New Jersey, 2004.

[64] M.T. Sellers, E.C. Corcoran, D.G. Kelly, “An Automated Delayed Neutron Counter for the Analysis of Special Nuclear Materials” Proceedings of the 35th Annual Canadian Nuclear Society Student Conference, Montreal Quebec, June 2010.

[65] National Instruments “Industrial Digital I/O Device for USB – 60 V Channel- to-Channel Isolated” website: http://www.ni.com/pdf/products/us/cat_usb6525.pdf (2009).